



1 The circulation and water mass (trans)formations in the Arctic Mediterranean Sea and their impact
2 on the ocean deep circulation: a review.

3

4

5

6

7 Bert Rudels¹ and Eddy Carmack²

8

9

10

11

12

13 ¹Research Professor Emeritus, Finnish Meteorological Institute, Helsinki, Finland

14 (bert.rudels@kitnet.fi)

15 Corresponding author

16

17 ²Senior Research Scientist Emeritus, Fisheries and Oceans Canada, Sidney, BC, Canada

18 (eddy.carmack@gmail.com)

19

20



21 Abstract

22 The Arctic Mediterranean is rapidly changing, a statement that is often made, but the follow-up
23 statements: changing from what and towards what are often omitted. Hence its role in the global
24 climate system, particularly regarding the Atlantic Meridional Overturning Circulations remains
25 poorly constrained. This review of the oceanography of the Arctic Mediterranean Sea develops an
26 unified perspective of how interacting components of the system evolve in space and time, and the
27 processes that determine their evolution. To set the stage a succinct overview of the geographic
28 setting and early explorations is given. We then follow the pathways of the principal water masses to
29 describe inflows, inter-basin circulations, water mass transformations, and outflows of heat and salt
30 to the bordering subpolar gyre and the global ocean. The fundamental connection to the global
31 ocean, the Atlantic water, is traced along its route into and through the Arctic Mediterranean. Its
32 transformations, driven by cooling, and by the freezing and melting of sea ice, lead to the creation of
33 both denser and less dense waters that form and maintain the water column structures within the
34 Arctic Mediterranean; the so-called double estuary. A second advective component to the Arctic, the
35 low salinity water carried by the Pacific inflow, is concentrated into the Amerasian Basin and acts
36 there to further isolate the denser waters derived from the Atlantic inflow. Hence, the waters return
37 to the North Atlantic either as dense overflows or buoyant outflows. The water masses within
38 diverse regions of the Arctic Mediterranean have changed over the past few decades, and this
39 influences their exchanges with the world ocean across the Greenland-Scotland Ridge. That the
40 water mass transformations in the Arctic Mediterranean take place beyond a ridge allows for the
41 build-up of significant density differences that, through entrainment, can increase the impact of the
42 Arctic Mediterranean on global overturning circulation.

43

44

45

46 Summary

47 This review traces the pathways and transformations of water masses within the Arctic
48 Mediterranean Sea, and elucidates how waters leaving this domain differ from those entering.
49 Processes constraining sea ice formation and melting due to both atmospheric interaction and heat
50 and salt exchanges with the underlying ocean are central to understanding the present and future
51 Arctic Ocean. The focus is on the Atlantic water, how its northward circulation affects the Arctic
52 conditions, and how returning, transformed water impacts the global circulation.

53



54 Section 1 Introduction

55 The mean surface temperature of the earth is rising and how this may influence the circulation of the
56 atmosphere and in the oceans is largely unknown. The observed temperature increase is strongest in
57 the high northern latitudes, which primarily are covered by ocean and one question is: Does the
58 presence of an ocean accelerates or mitigates the observed changes? To address this and related
59 questions we review in section 2 the global radiation balance and how the high north responds to the
60 radiative and mechanical forcing generated by the sun and by the atmosphere. The focus is on the
61 Arctic Mediterranean Sea, which comprises the Arctic Ocean and the Nordic Seas. We also describe
62 the physical and geographical settings and the bathymetric features of the Arctic Mediterranean Sea
63 and its connections to and communications with lower latitudes in the ocean and in the atmosphere.

64 Section 3 describes how our knowledge of the Arctic has evolved during the 500 years
65 that has elapsed since the exploration of the northern latitudes started. The section also reviews the
66 circulation and the water mass (trans)formations taking place in the Arctic Mediterranean, and how
67 our understanding has evolved during the about 150 years that oceanographic observations and
68 studies have been conducted in the Arctic Mediterranean. It also discusses the early views of the
69 deep circulation in the world ocean and finally brings up the establishment of the Committee for the
70 Exploration of the Sea (ICES) in 1899 and its importance for the improvement of measurement
71 techniques and theoretical understanding of the ocean circulation.

72 Section 4 examines the different inflows to the Arctic Mediterranean, the Pacific
73 inflow through Bering Strait and the North Atlantic circulation from the subtropical gyre to the
74 subpolar gyre and into the Nordic Seas. The next sections concentrate on specific features, areas and
75 processes that are presently active and may become more (or less) important in a future warmer
76 climate. Section 5 focusses on sea ice, its physical properties and how its growth and melting
77 influence the underlying water column. Section 6 describes the two inflows from the Nordic Seas to
78 the Arctic Ocean, through Fram Strait and over the Barents Sea, and the interactions (freezing and
79 melting) between Atlantic water and sea ice. Section 7 concentrates on the transformations of the



80 Atlantic water as it moves eastward along the two inflow paths and on the subsequent meeting and
81 remerging of the two inflow branches at the continental slope north of the Kara Sea, Severnaya
82 Zemlya and the Laptev Sea. In this section the wind driven model proposed by Nøst and Isachsen
83 (2003) is also discussed.

84 Eastward of the Laptev Sea the influence of the Atlantic water diminishes and the
85 circulation becomes dominated by freshwater input, both as continental runoff from Siberia and as
86 the direct inflow of low salinity Pacific water through the shallow Bering Strait (section 8). The upper
87 ocean circulation and mixing are determined by wind and by the seasonal changes in thermohaline
88 forcing, while the deeper (Atlantic) layers become isolated and the observed changes appear due to
89 internal mixing processes such as double-diffusion and diffusive interfaces. In the Transpolar Drift the
90 Siberian branch transports runoff and sea ice from the Laptev Sea and the anticyclonic Beaufort Gyre
91 brings low salinity water towards Greenland. The convergence of the streams leads to exchanges
92 between the two gyres. The differences between the deep waters in the Amerasian and Eurasian
93 basins and their causes are also described and discussed.

94 In section 9 the exchanges through Fram Strait are described from two hydrographic
95 sections, one north of the strait and one along the sill. The different waters are identified and the
96 transports of volume, freshwater and heat through the strait are discussed based on the geostrophic
97 estimates obtained by Rudels et al. (2008).

98 The Nordic Seas, especially the Greenland Sea, are regions characterized by weak
99 stability and are areas for deep convection and deep water renewal and the convection in the
100 Greenland Sea is discussed in section 10. The water column in the Greenland Sea has exhibited large
101 changes during the last 50 years, indicating that the nature of the active convection process has
102 changed. This is perhaps the area, where the effects of a warming climate have been most evident.

103 The three overflows of dense water across the Greenland-Scotland Ridge, through the
104 Faroe Bank Channel, across the Iceland Faroe Ridge, and through Denmark Strait are examined in



105 section 11. The focus is on the Denmark Strait overflow, its possible sources, and the entrainment as
106 the overflow plumes descend into the deep North Atlantic.

107 The outflows in the upper layer occur through Fram Strait in the East Greenland
108 Current and through the channels in the Canadian Arctic Archipelago to Baffin Bay are discussed in
109 section 12. As the East Greenland Current passes Cape Farewell it turns north as the West Greenland
110 Current and also enters Baffin Bay. The outflows are modelled as geostrophic flows through control
111 sections with the coast at the righthand side (Werenskiold, 1935). The Canadian Arctic Archipelago
112 and Baffin Bay are considered as a connected and interacting system, where the transports are
113 estimated from geostrophic exchanges through the channels and the heat loss and ice formation that
114 determine the upper layer characteristics in Baffin Bay. Estimates of the freshwater storage in the
115 Arctic Ocean are also given and the effects of increased freshwater input from the Greenland icecap
116 are also discussed. Finally, the exchanges between the Arctic Mediterranean and the subpolar gyre
117 and the Labrador and Irminger seas are discussed in section 13, where also the impact of water mass
118 transformations taking place in a semi-isolated sea could have on the overturning circulation.

119 This review is written with focus on observation and their interpretation. Processes
120 are described and their possible importance discussed, occasionally by the use of conceptual models.
121 For further aspects of the oceanography of the Arctic Mediterranean we refer the readers to the
122 review articles by Coachman and Aagaard (1974), Timmermans and Marshall (2020), Rudels and
123 Carmack (2022), and the books by Lewis et al., (2000), Dickson et al. (2008), Mills (2009) and Rudels
124 (2021).

125



126 Section 2 The Setting

127 The earth receives its energy as shortwave radiation from the sun and its rapid rotation limits the
128 diurnal temperature differences between the sunlit and the dark hemispheres. Large temperature
129 differences arise, however, because of the spherical shape of the earth. The zenith angle of the sun
130 increases with latitude and higher latitudes receive less solar radiation per unit area. The energy
131 received on the luminated hemisphere is radiated back to space as longwave radiation from the
132 entire earth surface. The energy input and output are globally but not locally balanced and the net
133 heat input at lower latitudes is transported by the atmosphere and the oceans to higher latitudes,
134 where it is radiated back to space. The presence of an atmosphere that contains greenhouse gases
135 that absorb and reradiate longwave radiation leads to a higher mean temperature of the earth than
136 if no atmosphere were present.

137 The earth's rotation axis makes an angle of 23.5° to the ecliptic. This leads to large
138 seasonal variations in incoming solar radiation especially north and south of the polar circles ($>66.5^\circ$).
139 In summer the incoming radiation at the top of the atmosphere is larger at the poles than at the
140 equator, while in winter the sun is below the horizon and the long, dark polar night reigns. The
141 contrasts between the two polar regions are, however, large. In the south the entire ice covered
142 Antarctic continent is in direct contact with the circumpolar Southern Ocean, while in the north there
143 is a confined ocean, the Arctic Mediterranean Sea, with restricted communications to the world
144 ocean and with its northernmost part, the Arctic Ocean, partly covered by perennial sea ice.

145 The atmospheric poleward heat transport is carried by three distinct circulation cells,
146 the direct Hadley cell where warm air rises at the equator, cools and then sinks back to the surface at
147 20° to 25° N(S). Some of the sinking air returns towards the equator, creating the trade winds, while
148 the rest is transported poleward by the westerlies in the eddy dominated Ferrell cell. Over the polar
149 areas, in the direct Polar cell, the air is cooled and returns equatorward forcing the warmer air of the
150 Ferrel cell to rise.



151 At low latitudes the poleward oceanic heat transport is larger than the corresponding
152 atmospheric transport, but the transports become equal around 30°N(S). At higher latitudes the
153 ocean transport diminishes and beyond 65° only the heat transport in the North Atlantic is different
154 from zero. The Atlantic is different from the other oceans in that it carries heat across the equator
155 from the southern to the northern hemisphere. The warm water ultimately comes from the Indian
156 Ocean and it is carried by the South Atlantic circulation to and across the equator.

157 The atmospheric circulation transports not only heat but also water vapor from lower
158 to higher latitudes. In the south this builds up and sustains the glaciers on the Antarctic continent
159 and the freshwater returns as calving icebergs to the Southern Ocean. In the north the water
160 condensates, releasing latent heat and then precipitates, partly over the Arctic Mediterranean but
161 primarily on the continents surrounding the Arctic Ocean. The drainage area is twice as large as the
162 surface area of the Arctic Ocean and provides a large freshwater input, 10% of the entire global
163 continental runoff, to the Arctic Ocean.

164 In summer the net heat input from the sun is larger than the net outgoing longwave
165 radiation and the radiation balance is positive (more heat received than lost). However, the outgoing
166 longwave radiation and the downward reradiated longwave radiation are both larger than the
167 downward shortwave solar radiation. During the long winters with no local energy input from the
168 sun the heat advected from lower latitudes cannot balance the radiative heat loss to space and the
169 surface temperature decreases drastically.

170 The surface air temperature in the Arctic is above the melting temperature of sea
171 water in summer but much below in winter. This leads to phase changes. Sea ice is formed in winter
172 and melts again in summer. The latent heat released by freezing becomes a local heat source that
173 somewhat increases the surface temperature in winter. In summer the returning solar radiation
174 raises the surface temperature and eventually the ice cover starts to melt. The melting ice acts as a
175 thermostat that keeps the surface temperature close to melting temperature as long as ice is
176 present. Ice formed and melted does not contribute any net heat to the Arctic Ocean, but the

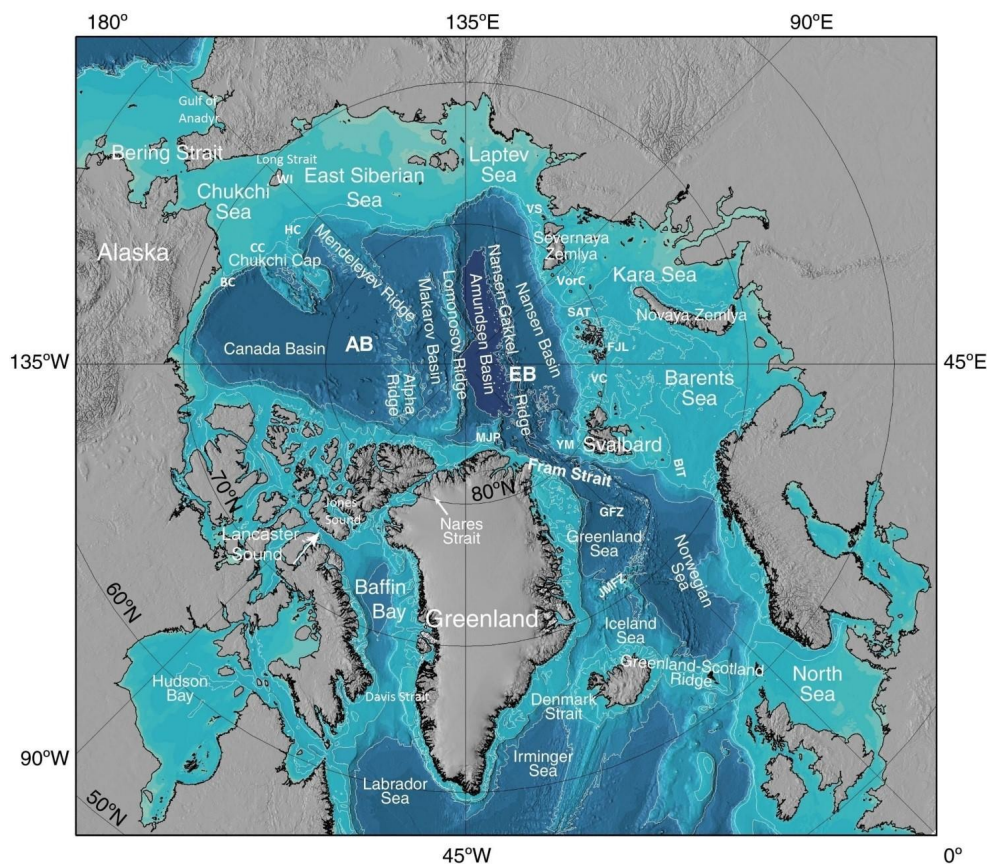


177 melting in summer stabilizes the water column and isolates the deeper layers from the surface
178 forcing both in summer and in winter. The ice not melted in summer is eventually exported by the
179 ocean currents southward and becomes a heat source to the Arctic.

180 The Arctic Mediterranean Sea is a part of the North Atlantic and comprises the Arctic
181 Ocean and the Nordic Seas; the Greenland, Iceland and Norwegian seas, that form an anteroom to
182 the larger Arctic Ocean. The Nordic Seas communicate to the south with the North Atlantic across
183 the Greenland-Scotland Ridge and are connected to the Arctic Ocean through Fram Strait and over
184 the Barents Sea in the north. There is also a direct connection between the Arctic Ocean and the
185 North Atlantic through the narrow straits in the Canadian Arctic Archipelago and then via Baffin Bay
186 and Davis Strait to the Labrador Sea. The Arctic Ocean is connected to the North Pacific through
187 Bering Strait. It is thus not a bay but a convoluted channel between the stagnant North Pacific and
188 the ventilated North Atlantic.

189 The Arctic Ocean is the smallest of the Earth's oceans ($9.5 \cdot 10^{12} \text{ m}^{12}$), if it could be
190 called an ocean, comprising only about 3% of the area and less than 1% of the volume of the global
191 ocean. More than half of the area of the Arctic Ocean consists of shallow shelf seas mainly located
192 north of the Eurasian continent. Farthest to the west is the Barents Sea, separated from the Kara Sea
193 by Novaya Zemlya and Franz Josef Land. The Kara Sea connects eastward to the Laptev Sea through
194 Vilkitsky Strait between Siberia and Severnaya Zemlya. The New Siberian Islands separate the Laptev
195 Sea from the East Siberian Sea, which communicates through Long Sound between the Siberian
196 mainland and Wrangel Island with the Chukchi Sea located north of Bering Strait. Eastward of Alaska
197 the coastline is different. Instead of shallow shelf seas and low lying coasts, it forms the mountainous
198 Canadian Arctic Archipelago, comprising several large islands creating a maze of channels. The most
199 important passages are Lancaster Sound, Jones Sound, and the Nares Strait between Ellesmere Island
200 and Greenland that all connect the Arctic Ocean to Baffin Bay (Figure 1).

201



202
203

204 Figure 1: Map of the Arctic Mediterranean Sea showing geographical and bathymetric features. The
205 bathymetry is from the IBCAO updated data base and the projection is Lambert Equal Area. The 200,
206 500, 2000 and 4000 m isobaths are shown. AB; Amerasian Basin, BIT; Bear Island Trough (Barents Sea
207 opening), BC; Barrow Canyon, CC; Central Channel, EB; Eurasian Basin, FJL; Franz Josef Land, GFZ;
208 Greenland Fracture Zone, HC; Herald Canyon, MJ; Morris Jessup Plateau, JMFZ; Jan Mayen Fracture
209 Zone, SAT; St. Anna Trough, YP; Yermak Plateau, VC; Victoria Channel, VorC; Voronin Canyon, VS;
210 Vilkiltskij Strait, WI Wrangel Island (Adapted from Rudels 2019, figure 1).

211

212 The deeper part of the Arctic Ocean consists of major two basins, the Amerasian and
213 the Eurasian Basin, separated by the narrow Lomonosov Ridge with an average sill depth around
214 1600 m. The Amerasian Basin is divided by the Alpha and Mendeleyev ridges into the large Canada
215 Basin and the smaller Makarov Basin, both with maximum depth of the abyssal plains around 4000
216 m. The Eurasian Basin also consists of two basins, the about 4000 m deep Nansen Basin between the



217 Eurasian continental slope and the Gakkel Ridge and the deeper, 4500 m, Amundsen Basin extending
218 from the Gakkel Ridge to the Lomonosov Ridge. The connection to the Nordic Seas through Fram
219 Strait is deep, sill depth 2600 m. The Greenland Sea comprises two basins, the Greenland Basin with
220 maximum depth about 3500 m and the northerly, smaller and shallower Boreas Basin. The
221 Norwegian Sea is separated into the Norwegian Basin and the Lofoten Basin both about 3000 m
222 deep, while the Iceland Sea is shallower, less than 2000 m deep.

223 Three deeper passages across the Greenland-Scotland Ridge connect the Nordic Seas
224 to the North Atlantic, the 640 m deep Denmark Strait between Greenland and Iceland, the 400 m to
225 500 m deep ridge between Iceland and the Faroes, and the channel between the Faroes and
226 Scotland, ending in the more than 800 m deep Faroe Bank Channel. West of Greenland the channels
227 from the Arctic Ocean to Baffin Bay are narrow and shallow. Nares Strait has a sill depth of 220 m
228 and Lancaster Sound and Jones Sound have sill depths between 100 m and 150 m. Baffin Bay is deep,
229 about 2600 m, and the sill depth in Davis Strait to the Labrador Sea is 630 m. Bering Strait between
230 the North Pacific to the Arctic Ocean is narrow, 85 km, and shallow, 45 m.

231



232 Section 3 Exploration

233 Section 3.1 voyages of discovery

234 It was after Bartolomeu Diaz rounded the Cape of Good Hope in 1488 and the discovery of a new
235 world by Christopher Columbus in 1492 that the exploration of the northern waters of the Atlantic
236 Ocean began in earnest. The papal meeting in Tordesillas in 1494 had divided the world into two
237 spheres of interest. The one east of 49°W should be explored and exploited by Portugal and the one
238 west of that longitude by Spain. The newly discovered American continents constituted a barrier for
239 a direct sailing to Cathay and the treaty excluded other nations such as England, France and Holland
240 from using the southern routes to India and China. This forced them to explore the east coast of the
241 North American continent to find a passage westward from the Atlantic. The Genua born John Cabot
242 made the first English sailing northward along the American coast already in 1497 but found no
243 passage. This was 16 years before Vasco de Balboa first looked upon the Southern (Pacific) Ocean
244 from the Mexican western shore and 25 years before Magellan sailed through the strait named after
245 him and discovered the southern passage to the Pacific Ocean and to China and India.

246 The efforts to find a northern route between the Atlantic and Pacific continued,
247 however, and the possibilities to find both a Northwest Passage north of North America and a
248 Northeast Passage north of the Eurasian continent were explored but with no success. The
249 expeditions were stopped by ice and many ended with the loss of ship and crew. It would take 300
250 years before both passages had been navigated by a single vessel, the Northeast Passage by *Vega*
251 1878-1880 and the Northwest Passage by *Gjøa* 1903-1905.

252 The Frenchman John Cartier explored the Gulf of St Lawrence and the St Lawrence
253 river in 1535, which proved to be an entrance for France to the interior of North America, but it was
254 no passage to the Pacific. The English search eventually concentrated on higher latitudes. Martin
255 Frobisher 1576 sailed west of Greenland and entered a passage that he thought might lead to the
256 Pacific, but it was just a bay, later named Frobisher Bay. John Davis made two voyages west of
257 Greenland and north of Frobisher Bay but on his return voyage he noticed a strait with strong current



258 that might lead to a passage west. In 1610 Henry Hudson was given the task to examine this passage,
259 but after passing through the strait, later named after him, and entering the large open water area
260 autumn was approaching and the ship became trapped in the ice and the expedition had to
261 overwinter. In spring when the ship came loose of the ice there was a mutiny and Hudson, his son
262 and seven members of the crew were put in a lifeboat facing a certain death.

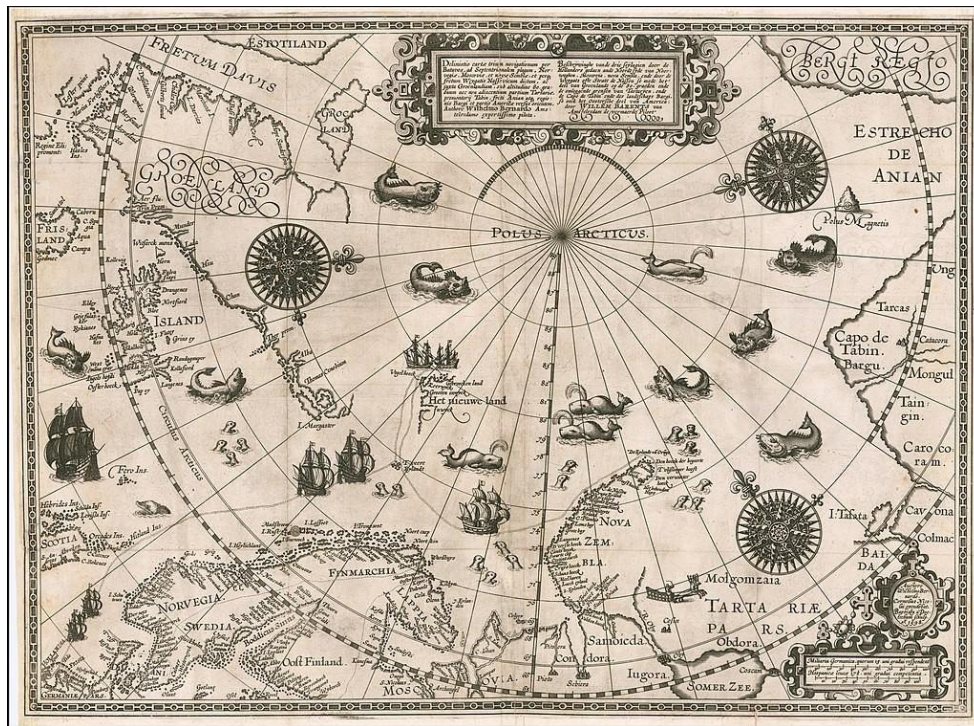
263 When the ship returned to London the crew presented Hudson's sailing notes and was
264 pardoned. Further expeditions showed that Hudson had sailed into a Bay, Hudson Bay, not into a
265 passage to the Pacific. In 1616 Robert Bylot, with William Baffin as pilot sailed as far north as they
266 could west of Greenland and discovered three possible passages, Smith Sound, Jones Sound and
267 Lancaster Sound but they judged that they were not leading to the Pacific. Baffin's sailing notes were,
268 unfortunately, never published and the expedition was all but forgotten.

269 The English efforts to find the Northwest Passage eventually led to the establishing of
270 one early successful commercial venture in the new world, the Hudson Bay company, and the search
271 for the Northeast Passage resulted in contacts with Russian traders at the river Dvina and to the
272 formation of the Muscovy company. This put an end to the English efforts to navigate the Northeast
273 passage but the search continued, now mainly sponsored by Dutch merchants. On three voyages in
274 1594, 1595 and 1596 with Willem Barents as pilot the Dutch reached Novaya Zemlya but could not
275 penetrate farther east. The 1596 expedition took a more northerly route and sighted Bear Island and
276 Spitsbergen before it turned east and reached the northern cape of Novaya Zemlya. Here the ship
277 was trapped in the ice and the expedition members overwintered on land. The following spring they
278 tried to reach the Kola peninsula in a small boat, but Barents died already in the beginning of the
279 sailing.

280 The discovery of the northern seas with their abundance of life, whales and walrus,
281 was found more rewarding than failed searches for an unknown Northeast Passage and an intensive
282 whaling industry was established, mainly by the Dutch, on Spitsbergen. Holland had now become



283 independent from Spain and Spain had given up its monopoly of the southern routes to Cathay. No
284 pressing need for the Dutch to find the Northeast Passage then remained (Figure 2).
285



286
287
288 Figure 2: A map of the Arctic Ocean by Willem Barents drawn around 1598 showing the then known
289 features of surrounding lands and islands. The ships north of Svalbard probably indicate open water,
290 the Whalers' Bay (from Häkli, 1992).

291

292 Russian explorers, however, continued to chart the northern Eurasian coastline. The
293 northernmost cape, Cape Chelyuskin was reached in the early 17th century and in 1648 Semen
294 Dezhnev sailed from the mouth of the Kolyma river in the Arctic Ocean to the Gulf of Anadyr in the
295 Pacific thus proving that the Northeast passage did exist, and that Eurasia was separated from North
296 America, almost a century before Vitus Bering sighted the Alaskan shore.



297 In the 18th century the initiative to finance expeditions to the northern seas shifted
298 from merchants and adventurers to governments, and the expeditions focused on discoveries and to
299 extend the influence of the home country. In 1730 Russia began its Great Northern Expedition led by
300 Vitus Bering, where different segments of the Northeast passage were charted separately. Vitus
301 Bering on his first expedition observed, and on his second expedition reached Alaska, but he then
302 died on the return voyage. Russia eventually established a permanent presence in Alaska, and this
303 Russian settlement reactivated the English efforts to find the mythical Strait of Anian (Fig. 2) and the
304 Northwest Passage, partly in concern that the Russians might be the first to discover the passage.
305 Bering had not completed the charting of the strait between Asia and North America. This was done
306 by James Cook on his last voyage in 1779, and a later expedition, 1791 to 1795, commanded by
307 George Vancouver finally proved that the Strait of Anian did not exist. Any ship sailing into the Arctic
308 Ocean from the North Atlantic to the North Pacific had to exit through Bering Strait.

309 About the same time the possibility to sail directly across the Arctic Ocean to Bering
310 Strait was considered. One early, but failed, attempt to cross the Arctic Ocean had been made by
311 Henry Hudson already in 1608. In spite of the fact that all previous expeditions had been stopped by
312 ice, the existence of an ice free inner part of the Arctic Ocean was seriously discussed. Robert
313 Thorne, an English merchant, had already 1527 suggested that the continuous daylight during
314 summer should store enough heat in the water column to prevent ice formation in winter. Another
315 idea, favored by the Dutch mapmaker Peter Plancius, was that an ocean in perpetual motion would
316 not freeze. The Russian scientist Michail Lomonosov suggested that ice can only form in connection
317 with land and river runoff and the interior of the Arctic Ocean might be free of ice. In 1772 the Swiss
318 geographer and librarian Samuel Engel noticed that sea ice contains little salt and proposed that sea
319 water could not freeze. These ideas led to a few failed attempts to sail to the Pacific via the North
320 Pole.

321



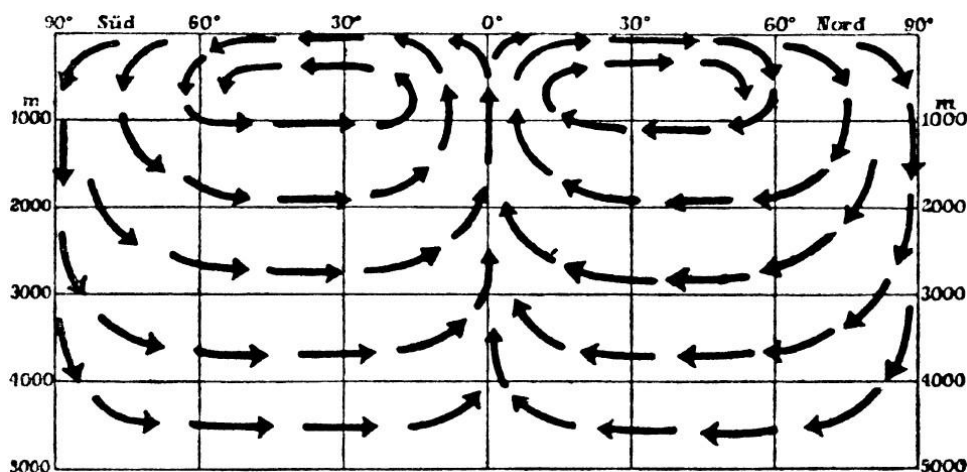
322 3.2 The deep circulation

323 In the age of sail the separation of the direct driving by the wind from the effects of the ocean
324 currents was not easy to make, and James Rennel studied the ship logbooks to determine the drift
325 caused only by the ocean currents. The results of his analyses were published in 1832, two years
326 after his death as *Investigations of the currents of the Atlantic Ocean and of those which prevail*
327 *between the Indian Ocean and the Atlantic* and supported the view that ocean currents are mainly
328 wind driven. However, Mathew Maury made a similar compilation of ocean current from logbooks,
329 which was published in 1855 as *“Geography of the Sea”*. Maury, by contrast, argued that differences
330 in density between water masses, due to temperature and salinity variations, might generate
331 stronger currents than the wind.

332 In 1751 captain Henry Ellis on the vessel *Earl of Halifax* made temperature
333 measurements in the deep tropical Atlantic by collecting water from different depths in a bucket
334 equipped with a thermometer. He found that the temperature decreased to about 9°C at 1200 m but
335 then stayed constant, as the measurements continued down to 1600 m. These observations,
336 although reported in the Philosophical Transaction of the Royal Society, did not receive much
337 attention until Benjamin Thompson (Count Rumford) almost 50 years later proposed that the cold
338 deep water was advected from higher latitudes, where the winters were cold enough to create water
339 of the observed temperature. Thompson (1797) also pointed out that ocean water does not attain its
340 maximum density at 4°C, but instead its density increases with decreasing temperature until freezing.

341 This was demonstrated by Emil von Lenz, who made deep temperature measurements
342 using thermometers protected in self-closing buckets on Otto von Kotzebue’s second
343 circumnavigation in 1823-1826, observing temperatures well below 4°C. Von Lenz returned to the
344 study of the ocean deep circulation later in his life and proposed a thermally driven deep circulation
345 symmetric about the equator, the water sinking at high latitudes and rising towards the surface at
346 the equator (von Lenz 1845) (Figure 3).

347



348

349

350 Figure 3: The symmetrical thermally driven meridional overturning circulation suggested by Emil von
351 Lenz 1845 (from Merz and Wüst, 1922).

352

353 In 1868 and 1869 William B. Carpenter and Charles Wyville Thomson sailed to the area
354 between Scotland and the Faroe Islands to prove, or disprove, Edvard Forbes' theory of an ocean
355 devoid of life below 800 m depth. They did prove that living creatures exist at the ocean bottom
356 regardless how deep they sampled. However, they also found deep water with temperatures
357 between 0°C and 0.5°C northeast of a line between the Shetland and the Faroe Islands, while the
358 deep temperatures west of the line were between 4.5°C and 8.5°C. These observations suggested
359 that waters cooled at higher latitudes were moving south along the bottom into the North Atlantic,
360 and Carpenter (1871) proposed an extensive meridional overturning circulation, where cooling at the
361 surface forces the surface water to sink at high latitudes to be replaced by warmer, lighter water
362 advected in the upper layer from the equatorial region, while the dense deep water moves towards
363 the equator, much like the circulation proposed by von Lenz (1845) and in agreement with the ideas
364 of Benjamin Thompson.

365 Carpenter was aware of warm and strong surface currents such as the Gulf Stream but
366 he considered these to be of minor importance and assumed that the effects of the Gulf Stream



367 ended in mid-Atlantic and did not influence the climate in Europe. The overwhelming part of the heat
368 carried northward by the ocean was instead due to the proposed massive, thermally driven
369 overturning circulation. Carpenter's grand generalization of the meridional ocean circulation was
370 initially not generally accepted and the main opposition came from James Croll.

371 Croll did not believe that heating of the surface water in the equatorial areas and
372 cooling at high latitudes could create a sea level slope steep enough to drive the water to higher
373 latitudes. He argued that the ocean currents carrying heat to the high northern and southern
374 latitudes were wind driven, and in the North Atlantic this circulation was dominated by the Gulf
375 Stream (see e.g., Croll, 1875). This debate lasted over five years but eventually abated. Croll returned
376 to his theory of the ice ages (Croll, 1875) and Carpenter became involved in the *Challenger*
377 expedition 1872-1876. Carpenter's thermally driven overturning circulation appeared in the end to
378 have gained the strongest support. However, the question of how ocean currents, at the surface and
379 in the deep, are driven was far from solved, and its complexity hardly appreciated by either
380 Carpenter or Croll (Mills, 2009).

381

382 3.3 The Nordic Seas

383 At the time of the *Challenger* expedition the Norwegian biologist G.O. Sars and meteorologist Henrik
384 Mohn proposed to the Norwegian government to send an expedition, akin to the Challenger
385 expedition, to the waters west of Norway, extending to Iceland and Greenland and northward to
386 Svalbard and northeastward into the Barents Sea. The proposal was accepted and resulted in the
387 Norwegian North Atlantic expedition 1876-1878 with *S/S Vøringen* to the "North Ocean", as Mohn
388 would call it in his comprehensive final report on the cruises (Mohn, 1887). The expedition thus
389 studied the area, where the formation of the cold deep water observed by Carpenter and Wyville
390 Thomson was expected to take place.

391 Mohn had worked with the mathematician Cato Guldberg on the thermal theory of
392 cyclones and had formulated the equations for the baric wind, where the pressure gradient is



393 balanced by the Coriolis force and the wind blows parallel to the isobars. Mohn noticed that the
394 circulation in the Nordic Seas resembled that of a cyclone and he tried to determine the density
395 distribution in depth from the temperature and salinity measurements made on the expeditions.
396 Assuming a level of no motion around 300 fathoms (1 fathom = 1.85 m) he found that the sea surface
397 was concave, being lowest at the center and standing higher along the Norwegian coast, where the
398 warm Atlantic water moved north, and along the Greenland coast where cold but less saline water
399 flowed south. This corresponds to a cyclonic circulation around the Nordic Seas where pressure is
400 balanced by the Coriolis force. Mohn also included the effects of the mean winds. Using air pressure
401 observations from existing meteorological stations, he computed the geostrophic wind and then
402 related the current speed empirically to the wind.

403 Mohn assumed that wind drives the surface water in the same direction, but as the
404 water is moving on a rotating earth the current becomes deflected to the right (northern
405 hemisphere), leading to a change in sea level slope that eventually balances the Coriolis force and
406 again makes the current parallel to the wind. The wind effect was added to the computed sea level
407 distribution and found to be larger than and reinforcing the sea level slope due to the density
408 distribution (Mohn, 1887).

409 The salinity observations made on the expeditions were, however, not of the standard
410 required for the computations Mohn attempted, but the cyclonic circulation present in the Nordic
411 Seas was reproduced. Furthermore, temperature observations indicated that below 700 m the
412 Nordic Seas were filled with water with temperatures below zero, and in Norwegian Sea southeast of
413 Jan Mayen an almost isothermal water column with temperature of -1.2C° was observed. The salinity
414 was comparatively high, and Mohn suggested that here a cooling and sinking of Atlantic water down
415 to the bottom took place (Mohn, 1880). The Norwegian Sea would then be one area, where the
416 water that filled the deeper layers of the oceans was produced.

417 Mohn's theoretical study was a first attempt to mathematically describe the oceanic
418 circulation but it was not immediately followed up. When it was reexamined twenty years later, it



419 was mainly its weaknesses that were noticed and its merits were not fully appreciated (Werenskiold,
420 1937). The inaccurate salinity determinations led to instabilities and to unrealistic circulation
421 patterns and Mohn's description of the wind driven currents was criticized. His suggestion of
422 convection and ventilation of the deeper layers by cooling of the Atlantic water were also almost
423 forgotten, when Fridtjof Nansen (1906) described the same phenomenon.

424

425 3.4 Warm Currents and ice cover

426 Croll had emphasized the importance of the heat carried by the Gulf Stream for the European
427 climate, but warm currents that enter the Arctic Ocean might also melt ice and lead to an open Arctic
428 Ocean beyond the region influenced by continental runoff. One strong advocate for an ice-free inner
429 Arctic Ocean was the geographer August Petermann, who examined the path of and the heat carried
430 by the Gulf Stream and traced Gulf Stream water along the Siberian shelf as far as Bering Strait
431 (Petermann, 1865). He also suggested that the best route to enter the inner part of the Arctic Ocean
432 would be over the Barents Sea east of Svalbard.

433 Petermann was perhaps the most ardent believer in an open Arctic Ocean and of the
434 importance of warm ocean currents, but he was not the only one. Captain Silas Bent (1872) argued
435 that the pathways into the Arctic Ocean were in the wake of the warm currents, and Van Campen
436 (1877) tried to convince the Dutch authorities to revive the Dutch Arctic explorations, which had
437 been so intense during the 17th century, by sending expeditions following different warm currents
438 into the Arctic Ocean.

439 However, there were also contrary views. Maury (1855) argued that since the
440 southward flowing cold water was found at the surface and had low salinity, it was instead warm and
441 saline water from the south that rose from the deep and brought heat to the surface, which melted
442 the ice and kept the inner parts of the Arctic Ocean open. The low salinity mixture of sea ice and cold
443 water then flowed south in the East Greenland Current and the Labrador Current. This would then be
444 a circulation akin to that suggested by von Weitz (1755) (see below).



445 Efforts to reach the open Arctic Ocean were made at all passages where warm surface
446 water was observed to flow north. Elisha Kane (1853-1855), Charles Hall (1866-1871) and George
447 Nares (1874-1875) tried to enter the Arctic Ocean west of Greenland, Julius Payer and Karl
448 Weyprecht sailed 1972 with the ship *Admiral Tegetthoff* towards the Arctic Ocean east of Svalbard,
449 and Charles de Long (1879-1881) entered through Bering Strait with *Jeanette* in 1879. All these
450 efforts failed and on several expeditions the ships were trapped in and eventually crushed by the ice
451 and the expedition members had to man the life boats. Some made it back, some perished. The
452 *Tegetthoff* expedition discovered Frans Josef Land but then the ship was caught in the ice and
453 crushed. The expedition members made it back in the life boats.

454 The *Jeanette* was trapped by the ice north of Bering Strait and drifted with the ice for
455 21 months in no obvious direction. After almost two years *Jeanette* broke up and vanished beneath
456 the ice. The expedition members were prepared and had put provisions, sledges and boats on the
457 ice, and they started the journey south towards Siberia. They reached open water in early August and
458 took to the boats, but a storm separated the three boats. One boat disappeared, one boat reached
459 the Lena river and the men were saved. De Long's boat made it to the Siberian coast, but they did
460 not meet anyone to help them finding food and all died by starvation. Three years later, in 1884,
461 objects from the *Jeanette* expedition were found by inuits on an ice floe close to Julianehåb on the
462 southwestern coast of Greenland, indicating that they had been carried by the ice from the wreckage
463 across the Arctic Ocean to the Nordic Seas and along the east coast of Greenland down to and
464 around Cape Farewell.

465

466 3.5 The drift of *Fram*

467 Henrik Mohn examined the drift of the *Jeanette* objects and proposed that there was a continuous
468 stream from the coastal region of eastern Siberia across the Arctic Ocean. This idea was taken up by
469 Fridtjof Nansen, who suggested that one possible way to enter the interior of Arctic Ocean would be
470 to work with the ice and the currents by letting a ship be carried by the ice drift over the Arctic



471 Ocean. The discovery of objects from *Jeanette* put a time scale on the ice movements across the
472 Arctic Ocean and on the duration of such a drift.

473 Nansen's plan split the scientific community. Some scientists were in favor but many
474 against, claiming it to be impossible. However, Nansen had the support of the Norwegian
475 government and eventually the idea gained the acceptance of a large fraction of the scientists. The
476 crucial part was the ship, *Fram*, which was built by the Norwegian master shipwright Colin Archer
477 specifically designed to withstand the ice pressure. *Fram* was rigged as a three masted schooner with
478 a support steam engine. The shape of the hull was smooth to avoid the ship being caught by the ice.
479 Instead, it would be forced upward as a cork onto the ice. The rudder could be drawn up into the hull
480 and the propeller was protected. The heating and ventilation were designed to avoid that moisture
481 collected on the inner walls of the ship and then froze to ice in the cold winters. *Fram* was also a
482 research vessel with laboratories to work with the observations and the samples collected during the
483 drift. *Fram* was in fact the first drifting scientific ice station.

484 *Fram* sailed from Oslo in June 1893 and in September she had reached the New
485 Siberian Islands, where she turned northward into the ice and was tied to an ice floe. The drift,
486 lasting until summer 1896, had begun. The first winter showed that *Fram* could withstand the ice
487 pressure. Meteorological and hydrographic observations were made regularly and depth
488 measurements indicated water depths close to 4000 m. The tacit assumption that the Arctic Ocean
489 was shallow was wrong and the possibility of finding large land masses in the Arctic Ocean was ruled
490 out.

491 The *Fram* expedition proved that the Arctic Ocean is an ice covered ocean, but also
492 that it was possible to enter the ice cover by moving with the ice, if the vessel was sturdy and well
493 enough designed. The existence of an ice drift, and possibly also a current, directed from Siberia
494 towards Greenland and Svalbard was demonstrated. The expedition also showed that the Arctic
495 Ocean in its central part is a deep ocean. The warm Atlantic water, by many assumed to enter the
496 Arctic Ocean and with its heat keep the Arctic Ocean open, was also observed, but at 150 m to 200 m



497 depth and separated from the ice cover by a cold, low salinity upper layer. What had not been
498 considered before was the magnitude of the freshwater input to the Arctic Ocean, and the fact that
499 sea ice melting on warm water creates a protective cold and low salinity melt water layer at the
500 surface that inhibits further melting (Nansen, 1912, see also below).

501 The drift of *Fram* did not, however, remove the ice and the obstacle it was for further
502 studies of the Arctic Ocean, and in the following forty years oceanographic studies were mainly
503 confined to the open areas and the marginal ice zone during the summer season. Planning for a
504 submarine expedition to the North Pole with a discarded submarine *Nautilus* was made in 1931 but
505 the expedition had to be abandoned just as it had started because failures with the diving rudders,
506 preventing the submarine to dive (Sverdrup and Soule, 1933). The Soviet ice breaker *G. Sedov* was
507 trapped in the ice in the late 1930s and involuntarily repeated the drift of *Fram*.

508 A major step forward in the research of the interior of the Arctic Ocean occurred in
509 1937, when the Soviet Union established the first drifting ice station, NP-1, at the North pole. The
510 station drifted rapidly south and the team was picked up by Soviet ice breakers in February 1938 in
511 the Greenland Sea. After the Second World War new ice stations were launched, mainly by the Soviet
512 Union, but also by the United States and Canada. The Soviet Union also organized airborne
513 expeditions each spring covering the entire Arctic Ocean, where water sampling, ice thickness
514 measurements and meteorological observations were made. The observations from the ice stations
515 and from the airborne expeditions provided the knowledge of the ice drift, the ocean circulation and
516 the water mass distribution in the Arctic Ocean as it existed around 1980, before the beginning of the
517 ice breaker and the submarine expeditions and the revolution in remote sensing and in mooring
518 techniques that have taken place the last 40 years (see e.g., Rudels, 2015, 2021).

519 The presence of an atmospheric high pressure cell over the Beaufort Sea that
520 generates an anticyclonic circulation of the ice, and the existence of the Transpolar Drift that
521 transports ice from Siberia towards Greenland became known. Observations of the density
522 distribution in the water column also showed that the wind field creates an anticyclonic geostrophic



523 circulation in the upper layers centered at the Beaufort Sea. The movements of the deeper Atlantic
524 layer were determined from the observed changes in TS properties of the Atlantic core, which
525 showed that the core temperature decreased around the Arctic basin, being highest north of
526 Svalbard and lowest north of Greenland, implying a cyclonic circulation of the Atlantic water around
527 the Arctic Ocean (Coachman and Aagaard, 1974).

528

529 3.6 ICES and technical and theoretical advances.

530 The drift of *Fram* was part of the tremendously active period in oceanography starting with the
531 *Challenger* expedition. Between 1899 and 1902 the International Committee for the Exploration of
532 the Sea (ICES) was established with its secretariat in Copenhagen and the ICES laboratory in Kristiania
533 (Oslo) with Nansen as director. One of the first task of ICES, really the reason for its founding, was to
534 coordinate a five years observation program, where the different member states should arrange
535 oceanographic expeditions in all seasons in their adjacent waters, thus covering much of the
536 northern North Atlantic, the Norwegian Sea, the Barents Sea, the North Sea and the Baltic.

537 As a response the Norwegian Fishery Board launched an extensive research program
538 in the Norwegian Sea between 1900 and 1904 with the research vessel *Michael Sars*. However, the
539 report on these expeditions, *The Norwegian Sea*, published by Bjørn Helland-Hansen and Nansen in
540 1909, described not only observations made within the program, but almost all available
541 observations and measurements were included in the report. *The Norwegian Sea* discussed all the
542 major water masses and currents and most of the major circulation features; the Atlantic water
543 entering from the south and flowing northward in the Norwegian Atlantic Current, the Norwegian
544 Coastal Current ultimately from the Baltic Sea and moving along the Norwegian Coast, the southward
545 flowing East Greenland Current and its branches the Jan Mayen Current and the East Iceland Current,
546 and the major cyclonic gyres in the different basins were all identified. Not only surface currents but
547 also the distribution and motions of the waters in the deeper layers were deduced and described.



548 Observations made in the North Atlantic from *RV Michael Sars* in 1910 (Helland-
549 Hansen, 1912) and from *Frithjof* 1910 (Nansen, 1913) showed that the North Atlantic drift brings
550 three branches of warm water towards the eastern part of the Greenland-Scotland Ridge. Two
551 branches cross the ridge. One branch joins the slope current west of Scotland and enters the Arctic
552 Mediterranean through the Faroe-Shetland Channel, where the most persistent, warmest and most
553 saline inflow takes place at the continental slope west of Shetland. This inflow then partly becomes a
554 continuation of the European Slope Current, which is observed at the continental slope west of Spain
555 and may be present also farther south (Nansen, 1913). The other branch crosses the ridge west of
556 the Faroes and flows first east and then moves south into the Faroe-Shetland Channel, where it
557 splits, one part turning northward into the Arctic Mediterranean and the other circulating around the
558 Faroe Islands. The third branch turns west along the ridge and flows south of Iceland into the
559 Irminger Sea, where the main part continues south along the Greenland slope as the Irminger
560 Current and finally enters the Labrador Sea. A small fraction separates from the stream and flows
561 northward into the Iceland Sea west of Iceland as the North Icelandic Irminger Current, described by
562 Martin Knudsen (1899) based on observations from the Danish *Ingolf* expeditions 1895 and 1896.

563 The main function of the ICES laboratory in Kristiania was to develop, test and
564 evaluate instruments and methods, formulas and tables to assure that reliable and repeatable
565 measurements could be made. A task that actually was achieved in the first decade of the 20th
566 century. The use of water bottles equipped with protected and unprotected reversing thermometers,
567 and the determination of chlorinity by Mohr-Knudsen titration and calibrated with standard sea
568 water provided by ICES became routine, and the salinity and density were calculated from the
569 Knudsen Hydrographic tables (1901). This routine lasted for more than fifty years.

570 At the turn of the century Vilhelm Bjerknes formulated the circulation theorem for a
571 stratified fluid on a rotating earth, which became the basis for the dynamic method by which the
572 geostrophic velocities, arising from the balance between the Coriolis force and the pressure gradient
573 can be determined (Bjerknes, 1898a, 1898b, 1901). How to use the circulation theorem to compute



574 ocean currents was described by Sandström and Helland-Hansen (1903) and Helland Hansen (1905).
575 Another advance, based on Nansen's observations on *Fram* that the ice drifted to the right
576 of the wind, was the formulation of the theory of wind driven ocean currents by Vagn
577 Walfrid Ekman (1905).

578

579 3.7 Deep water formation and the overturning circulation

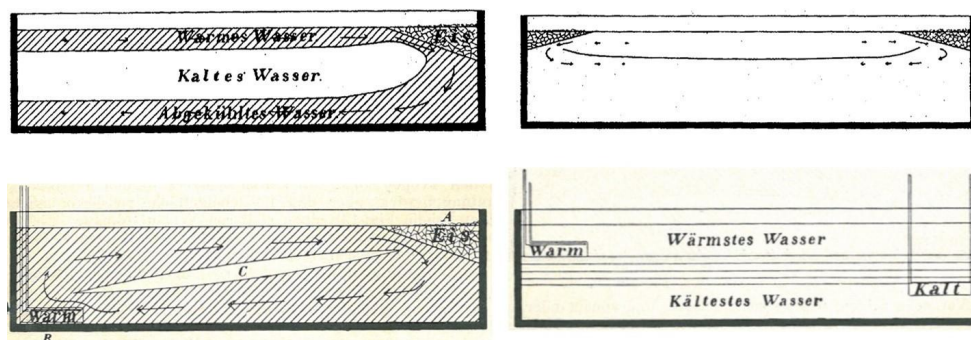
580 In 1901 Roald Amundsen made an extensive survey of the waters in the Greenland Sea, northern
581 Norwegian Sea and the Barents Sea onboard *Gjøa*, later famed as the first vessel sailing the
582 Northwest Passage. These measurements together with other available observations, especially from
583 Russian cruises in the Barents Sea (Knipovich, 1905), were compiled and interpreted by Nansen in his
584 monograph *Northern Waters* (Nansen, 1906). The observations in the central Greenland Sea showed
585 that the stability of the water column was weak and an almost homogenous dome of cold, -1.2°C ,
586 and saline, 34.92, water with only a thin layer of warmer and less saline water separating it from the
587 atmosphere. In winter seasonal cooling might increase the density of the surface water sufficiently
588 for it to sink and renew the water of the deep water dome.

589 The observations in the Barents Sea close to Novaya Zemlya, by contrast, showed
590 saline and cold bottom water, which Nansen interpreted as a result of brine rejection during ice
591 formation. Nansen thus identified two modes of convection; homogenization of the water column by
592 cooling in the open ocean, and the creation of dense saline water by brine rejection on the shelves.
593 Nansen (1912) examined the possible sources of the cold deep water in the North Atlantic and
594 concluded that dense water formed in the Nordic Seas might contribute to the North Atlantic deep
595 water but he expected the main source to be located south of Greenland in the Irminger Sea.

596 Sandström (1908) made laboratory experiment with saline water in a narrow tank to
597 describe the thermally driven circulation in the North Atlantic (Figure 4). He found that the
598 circulation, if only driven by cooling at the surface, was sluggish, and when cooling was applied at
599 both ends of the tank cold water filled the main depth of the tank and the circulation was confined to



600 a thin upper layer. However, if a heat source was applied at one end and a cold source at the other
601 end of the tank a strong overturning circulation was generated, when the warm source was placed
602 deeper than the cold source. By contrast, if the heat source was above the cold source the water
603 column became stagnant. Since in the ocean the heat and cold sources are both located at the
604 surface, this suggests that a thermally driven circulation is likely to be weak.
605



606
607

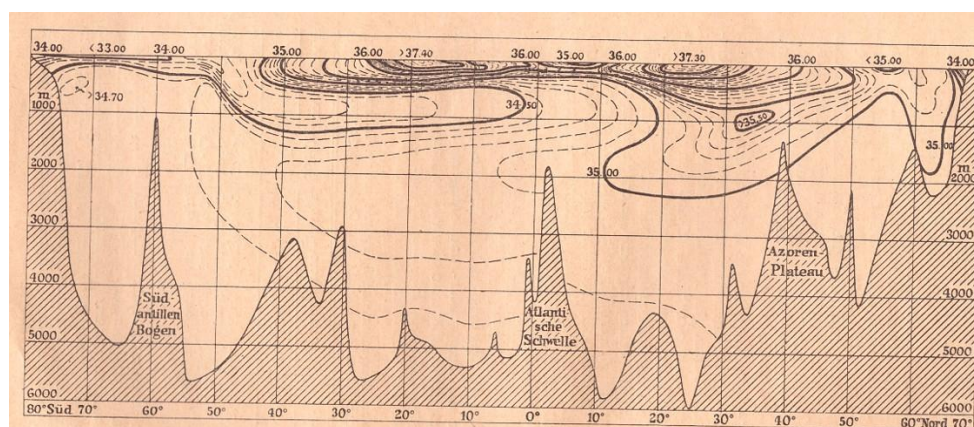
608 Figure 4 The Sandström experiment to simulate the circulation between lower and higher latitudes
609 driven by cooling at high latitudes. The upper panel shows the effect by just cooling, at the northern
610 hemisphere (left) and at both hemispheres (right). The circulation is sluggish. The lower panel shows
611 the circulation with the cold source located above the heat source (left), leading to a vigorous
612 circulation and the situation when the cold source is located below the heat source resulting in
613 stagnant conditions (from Sandström, 1908).

614

615 The density of sea water is determined not only by temperature but also by salinity
616 (and by pressure). This allows for a different circulation mode. In 1755 J.S. von Waitz, a German
617 mining engineer, estimated that evaporation in the Mediterranean Sea leads to a lower sea level,
618 which forces a surface inflow of Atlantic water through Gibraltar Strait. He noted that evaporation
619 removes freshwater but leaves the salt in the water column, which creates a more saline and denser
620 water column in the Mediterranean Sea. This reverses the pressure gradient in depth and gives rise
621 to a dense deep outflow to the Atlantic. Von Waitz was aware of the two-layer exchange through the
622 Bosphorus studied by Luigi Marsigli (1681), which showed less saline water from the Black Sea flowing



623 over a denser deep inflow from the Mediterranean Sea. Von Waitz extrapolated this and his own
624 findings to the world ocean. Heating and evaporation at lower latitudes would increase the salinity
625 and density of the surface water and force it to sink and be replaced at the surface of a flow of
626 colder, less saline and less dense water from higher latitudes. This would create an overturning
627 circulation in the opposite sense to that proposed by von Lenz and Carpenter.
628



629

630

631 Figure 5. A longitudinal salinity section in the Atlantic showing the present of the upper low salinity
632 input from the Southern Ocean, the saline North Atlantic deep water and the slightly less saline
633 bottom water from the Antarctic (from Merz and Wüst, 1922).

634

635 Merz (1922) and Merz and Wüst (1922) reexamined temperature and salinity

636 observations made in the South Atlantic on the *Challenger* expedition 1872-1876 and found that they

637 did not agree with the symmetric circulation scheme proposed by von Lenz and that both

638 temperature and salinity influenced the circulation. Merz and Wüst emphasized that theirs were no

639 new findings but had been noticed already in the original *Challenger* reports. The observed deep

640 circulation does not consist of two loops symmetric about the equator but of several layers of sinking

641 and advected water masses that extend from high latitudes across the equator into the other

642 hemisphere. Cold, low salinity water around 1000 m depth moves from the South Atlantic towards

643 the equator, while at 3000 m to 4000 m depth a more saline and colder layer flows south from the



644 North Atlantic, crossing the equator. The colder, slightly less saline bottom water originates in the
645 south, in the Antarctica, and moves northward crossing the equator (Figure 5). The deep circulation
646 in the Atlantic thus forms a large meridional overturning circulation comprising several different
647 layers that extend over the entire Atlantic connecting north and south and ultimately the North
648 Atlantic to the rest of the world ocean.
649



650 Section 4 The inflows and their forcing

651 The Arctic Mediterranean Sea is dominated by the interplay between the advection of heat, mass
652 and freshwater from lower latitudes and the local, strongly seasonal, forcing. Most heat is carried by
653 the atmosphere, which also provides the largest freshwater input to primarily the Arctic Ocean,
654 mainly as strongly seasonal runoff from the large catchment areas but also as direct local
655 precipitation.

656 The Pacific water that enters the Arctic Ocean through Bering Strait is driven by the
657 higher sea level in the North Pacific than in the Arctic Ocean (Stigebrandt, 1984). The sea level
658 difference is caused by the less dense water column in the North Pacific compared to that in the
659 North Atlantic. A difference that ultimately arises from the atmospheric flux of water vapor from the
660 Atlantic to the Pacific Ocean across the Isthmus of Panama (Weyl, 1968). However, also more local
661 processes play a role. The weaker transports in winter have been explained by the presence of
662 stronger, more northerly winds (Coachman et al., 1975). The inflow in summer is warm, creating the
663 Bering Strait summer water, while the inflow in winter is at the freezing temperature forming the
664 Bering Sea winter water, showing up as a temperature maximum and a deeper temperature
665 minimum respectively in the Canada Basin water column. The Pacific inflow is limited by the shallow
666 depth (85m) of the strait, and it does not carry any oceanic heat from lower latitudes. The warmer
667 water transported in summer is formed by local seasonal heating and is rather a part of the radiation
668 balance of the Arctic Mediterranean. Because of its low salinity the Pacific inflow also transports a
669 substantial amount of freshwater to the Arctic Ocean, adding to its stability.

670 By contrast the connection between the Arctic Mediterranean and the North Atlantic
671 over the Greenland-Scotland Ridge is deep and wide with mean sill depth of about 500m. The
672 thickness of the Atlantic water layer entering the Norwegian Sea is 300-400m and it transports
673 oceanic heat from lower latitudes to the Arctic Mediterranean. The Atlantic water flows north as the
674 Norwegian Atlantic Current in two branches. One follows the continental slope, while the second



675 branch separates from the slope at the Vøring Plateau and continues as a baroclinic current above
676 the Mohn-Knipovich Ridge towards Fram Strait.

677 As the Atlantic water at the slope reaches the Barents Sea opening it splits. One
678 branch enters the Barents Sea but then again splits. The major part continues eastward toward
679 Novaya Zemlya, while a smaller stream turns north in the Hopen Deep, where it again splits with one
680 part flowing eastward north the Central Bank and the other returning as cold bottom water to the
681 Norwegian Sea south of Bear Island. The Norwegian Coastal Current that flows between the Atlantic
682 water and the coast, carrying low salinity water from the Baltic Sea and runoff from the Norwegian
683 coast, also enters the Barents Sea and continues eastward close to the coast as the Murman Current.

684 The branch of Norwegian Atlantic Current that remains at the slope continues
685 northward to Fram Strait, where it partly merges with the outer Mohn-Knipovich branch. Both
686 branches then split. One stream enters the Arctic Ocean along the continental slope close to
687 Svalbard, and a second stream flows around the Yermak Plateau to rejoin the inner branch farther
688 east. A smaller eastward flow crosses the Nansen Ridge that connecting the Yermak Plateau to the
689 Svalbard slope into the Sofia Deep (Gascard et al., 1995). A substantial fraction of the Atlantic water,
690 however, recirculates westward and does not enter the Arctic Ocean. Instead, it flows south along
691 the East Greenland shelf and slope. This recirculation of Atlantic water was noticed early by Carl
692 Ryder (Ryder 1892). The cooling of the Atlantic water in the Norwegian Sea increases its density
693 sufficiently for it to become overflow water that could contribute to the deep return flow of the
694 North Atlantic overturning circulation.

695 In contrast to Bering Strait the mechanisms driving the Atlantic water into the Nordic
696 Seas are not well known. The warm Atlantic water derives from the Gulf Stream and from the
697 Subtropical gyre. As the warm water in the North Atlantic Drift approaches Scotland it splits. The
698 upper layer moves mainly south and remains in the subtropical gyre, while the deeper layers, below
699 300m, raise to the surface and flow north into the Subpolar gyre (Brambilla and Talley, 2006;
700 Burkholder and Lozier, 2011). The functioning of this valve and how it might affect the properties of



701 the northward flowing Atlantic water is not adequately known but likely depends on the
702 characteristics of the North Atlantic Drift, the circulation in the Subpolar gyre and on the properties
703 of the waters exiting the Arctic Mediterranean.

704 The more fundamental question is if the inflow across the Greenland-Scotland Ridge is
705 driven by winds and large weather systems like the North Atlantic oscillation, or if the cooling of the
706 Atlantic water and the convection taking place in the Nordic Seas draw the warm Atlantic water
707 across the ridge in the manner envisaged by Carpenter? This would have a large impact on how the
708 Arctic Mediterranean responds to changes in climate and we return to this question later.

709



710 Section 5 The ice cover and ocean ice atmosphere interactions

711 The most outstanding feature of sea ice is that it floats. It is not unique but rare that a substance,
712 when solidified by cooling, becomes less dense than its liquid phase. In freshwater this is preceded by
713 a density maximum at 4°C, above the freezing point, which means that further cooling creates its
714 own upper stable stratification, limiting the amount of water that must reach freezing temperature
715 before ice is formed. Sea water with salinity $S > 24.7$, by contrast, is densest at its freezing point and
716 the entire water column has to be cooled to freezing temperature or down to a density gradient
717 caused by an advective input of a denser water mass. As ice starts to form above a water column at
718 the freezing point no heat is supplied by the underlying water and the only heat source for the
719 atmosphere is the release of latent heat of freezing, and a balance between the heat lost at the ice
720 surface and the heat conducted through the ice is created. A balance that gradually shifts as the
721 thickness of the ice cover increases and the ice surface temperature decreases, which reduces the ice
722 growth at the ice-sea interface.

723 The solid ice cover allows snow to accumulate during winter, which isolates and
724 further reduces the heat loss to the atmosphere and to space. A white snow cover implies a high
725 albedo and when the sun rises in spring most of the shortwave radiation is reflected back to space.
726 This is the perhaps most often mentioned Arctic feedback mechanism. Warmer air, less snow, more
727 absorbed shortwave radiation, warmer air, less snow, etc. However, another mechanism that may be
728 even more important is increased advection of moist air from lower latitudes, which increases the
729 downward longwave radiation and may start melting snow and ice before sunrise (Mortin et al.,
730 2018).

731 During summer the incoming solar radiation increases the air and water temperatures
732 and snow and sea ice start to melt, creating an upper melt water layer that, however, remains close
733 to melting temperature as long as ice is present. If the ice cover is not compact, shortwave radiation
734 penetrates into and through the melt water layer and creates a warmer layer below. This heat is
735 isolated from the ice until autumn, when ice again starts to form and the salinity of the melt water



736 layer increases. These two layers might then merge, which would temporarily slow down the
737 seasonal ice formation. If not, the warmer layer becomes a permanent temperature maximum in the
738 water column, the Near Surface Temperature Maximum (Jackson et al., 2010).

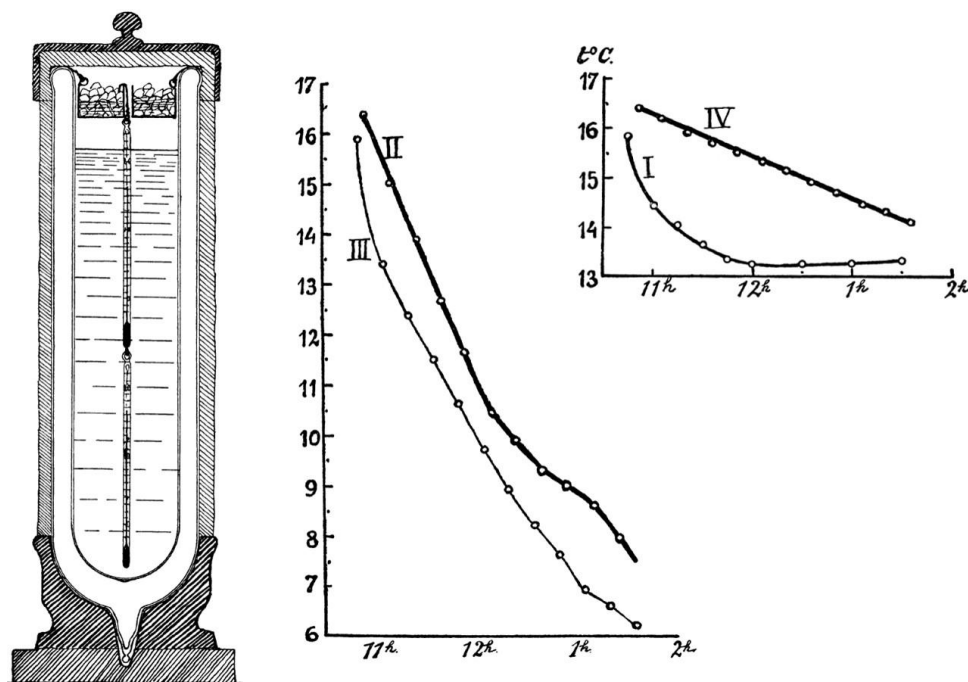
739 A stable seasonal cycle of ice formation and ice melt would eventually lead to an
740 equilibrium thickness of the ice cover. The equilibrium is reached because the ice formation in winter
741 depends more upon the ice thickness than the ice melt in summer. Thinner ice leads to rapid growth
742 in winter and the ice cover becomes thicker. If the ice is initially thick, little ice growth takes place in
743 winter, while a larger amount melts in summer and the ice thickness decreases (Maykut, 1986).

744 As sea ice forms, either by growing directly from the underside of the ice cover or
745 created as frazil ice in the water column, salt and freshwater become separated into ice and brine.
746 The sea ice becomes thicker and the water below saltier, and in the case of frazil ice formation the
747 ice crystals rise to the surface and “droplets” of brine sink. The smaller brine droplets soon lose their
748 identity as they sink and the salt diffuses into the surrounding water. This creates a thicker, slightly
749 unstable layer that eventually must convect into the underlying ocean (Rudels, 1986a). However, the
750 frazil ice that is collected as a “mushy” layer (Wettlaufer et al., 1997) at the surface traps a large
751 fraction of the brine, and as the mushy layer solidifies the brine is eventually squeezed out of the ice
752 and sinks. The brine parcels rejected out of the mushy layer are likely to be larger than the droplets
753 formed together with the frazil ice and might sink as individual parcels to greater depth before the
754 salt anomaly is diffused away.

755 Until now we have only looked at the case when the upper layer temperature is close
756 to the freezing/melting temperature and not considered what happens, when sea ice encounters and
757 melts on warmer water. Nansen (1912) studied this situation by laboratory experiments. A vessel
758 with warm, saline water was cooled from above in three different manners. First a jar with sea ice
759 was held above the water surface and the water was cooled by radiation. Then the jar was allowed to
760 float on the water, cooling the water by conduction. Finally, the ice was added at the surface and
761 coming in direct contact with the ice (Fig. 6). The temperature evolution at the bottom and at the



762 center of the vessel was measured in all experiments. The difference between the three experiments
763 is striking. In the case of just radiative cooling the temperature decrease of the water is small and
764 slow, while the conductive cooling of the water leads to a rapid and large temperature change in the
765 vessel, indicating that thermal convection is established. The experiment where the ice is melting
766 directly at the sea surface is the most revealing. A short rapid cooling takes place but after that the
767 temperature remains essentially constant. The warm water melts the ice, which leads to the
768 formation of a cold, less saline and less dense surface layer that isolates the ice from the warm water
769 below. Sea ice evidently protects itself from heat input from below by creating a stratification that
770 limits the heat transfer.
771



772

773

774 Figure 6. Nansen's experiments with cooling of sea water. Experiment I is when the ice is placed
775 directly on the water, which leads to the formation of a low salinity melt water layer and no or little
776 convection in and cooling of the water column. Experiments II and III show the results when the ice is
777 put in a jar, which is floating at the water surface. The cooling at the surface leads to convection and
778 cooling of the water column. In experiment IV the jar with ice is held above the water surface. The
779 water is cooled slowly by radiation and the convection is weak (from Nansen, 1912).



780

781 Nansen's experiments were idealized. No turbulence was present in the vessel and the
782 experiments were performed at room temperature. In the ocean wind will generate turbulence,
783 either directly or by driving the ice, which entrains water across the interface into the upper layer.
784 Furthermore, in summer the main sea ice melting occurs at the surface and the melt water prevents
785 heat from below to reach the ice. In winter, however, the air temperature is low and the summer
786 melt water layer is gone. As the warm water gets in contact with and melts the ice, an upper, cooler
787 and less saline and less dense layer develops and deepens as warm water is entrained from below.

788 Assuming that the deepening of the upper layer can be described by a Kraus-Turner
789 energy balance model (Kraus and Turner, 1967; Niiler and Kraus, 1977), where the turbulent energy
790 added at the surface is used not only to entrain denser water from below but also to mix melt water
791 from above into the mixed layer. The entrainment velocity w_e then becomes:

792

$$793 \quad w_e = \frac{2n_o u_*^3}{g[\beta(S_A - S_1) - \alpha(T_A - T_1)]} - \frac{\varepsilon B}{g[\beta(S_A - S_1) - \alpha(T_A - T_1)]} \quad (1)$$

794

795 Here n_o is a constant usually put to 1.25, u_* is the friction velocity, T_A , T_1 , S_A and S_1 are the
796 temperatures and salinities of the upper and lower layer respectively, α , the coefficient of heat
797 expansion and β the coefficient of salt contraction. The sign of α is explicit in the expression. g is the
798 acceleration of gravity, B is the buoyancy input and ε is a parameter put to 1 if the buoyancy input is
799 positive and 0.05 if the buoyancy is negative to take the weak mixing rate of convection into account
800 (Stigebrandt, 1981). If the density is taken only to depend upon salinity, the second term becomes
801 equal to w_e and the input of fresh (melt) water at the surface thus reduces the entrainment by a
802 factor of 2 (Rudels, 1989).

803 The entrained heat not only melts ice, in winter the heat loss to the atmosphere also
804 has to be supplied by the entrained water. The distribution of the entrained heat to sea ice melting
805 and to the atmosphere is crucial for the evolution of the upper layer, and one suggestion is that the



806 fraction of heat going to ice melt is the one that leads to minimum ice melt (Rudels et al., 1999a) This

807 fraction ϕ_o is found to be:

808

$$809 \quad e\phi_o = \frac{2\alpha L}{c(\beta S_A - \alpha \Delta T)} \approx \frac{2\alpha L}{c\beta S_A} \quad (2)$$

810

811 L is the latent heat of melting and c the heat capacity of sea water and ΔT the temperature

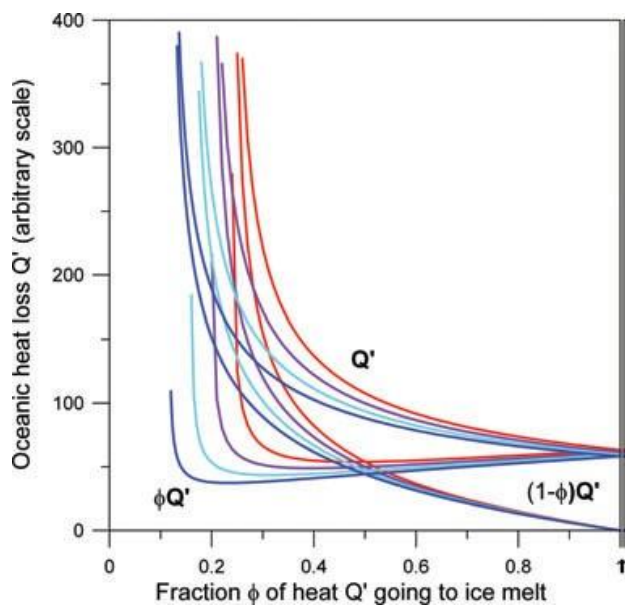
812 difference between the Atlantic and the melt water layer. (Rudels et al., 1999a). α decreases with

813 decreasing temperature and Figure 7 shows the total heat loss Q' , the heat loss to ice melt $\phi_o Q'$, the

814 heat loss to the atmosphere $(1-\phi_o)Q'$ as functions of ϕ for different ΔT and the corresponding values

815 of α .

816



817

818

819 Figure 7. Curves showing the total heat loss Q' , the heat going to ice melt $\phi Q'$ and the heat going to

820 the atmosphere $(1-\phi)Q'$ as function of ϕ , the fraction going to ice melt. Red curves have $\Delta\alpha T = 8^\circ\text{C}$

821 and $\alpha = 0.781 \times 10^{-4}$, purple curves $\Delta\alpha T = 6^\circ\text{C}$ and $\alpha = 0.654 \times 10^{-4}$, cyan curves $\Delta\alpha T = 4^\circ\text{C}$ and $\alpha =$

822 0.526×10^{-4} , blue curves $\Delta\alpha T = 2^\circ\text{C}$ and $\alpha = 0.390 \times 10^{-4}$. $\beta = 8 \times 10^{-4}$, $c = 4000 \text{ J kg}^{-1} \text{ K}^{-1}$, $L = 0.335 \times$

823 10^6 J kg^{-1} . The fraction ϕ_o giving minimum ice melt decreases with decreasing temperature and

824 decreasing α .



825

826 As the created upper layer deepens its salinity and temperature decrease, while the
827 stability increases with time until the freezing temperature is reached. The salinity S_1 in the upper
828 layer is then given by:

829

$$830 \quad S_1 \approx \frac{S_A}{\left(1 + \frac{2\alpha}{\beta S_A}(T_A - T_f)\right)} \quad (3)$$

831

832 T_A is the temperature of the lower layer and T_f the freezing temperature of the upper layer. The
833 stable salinity step $\beta(S_A - S_1)$ is about twice the unstable temperature step $\alpha(T_A - T_1)$ giving a stability
834 ratio of 2 at the interface. The problem is the choice of α , which depends strongly on temperature
835 and as the upper layer deepens and cools α decreases to a minimum at the freezing point. A smaller
836 α leads to a deeper upper layer with higher salinity.

837 When the freezing temperature is reached, the upper layer has become so deep that
838 the amount of entrained warm water is not enough to supply heat both to ice melting and to the
839 atmosphere and ice again starts to form. The stability at the interface then decreases and
840 entrainment starts to increase. Whether this leads to a stable situation with a deepening of the
841 upper layer, more melting and a thinning of the ice cover, or to an increase in salinity and density of
842 the upper layer eventually leading to deep convection will be discussed in section (10) below. Here
843 we might just add that the fraction ϕ_o of minimum heat going to ice melt is twice the fraction leading
844 to marginal stability. A fraction smaller than $\phi_o/2$ will not stabilize the water column and it overturns.
845 This is also evident from the stability ratio $R_p = \beta\Delta S/\alpha\Delta T = 2$ reached when the upper layer has
846 attained freezing temperature.

847



848 Section 6 The Atlantic inflows to the Arctic Ocean

849 The Atlantic water that enters the Arctic Ocean through Fram Strait soon encounters and starts to
850 interact with sea ice. In winter the melting sea ice and entrained Atlantic water create a less saline
851 melt water layer that is eventually cooled to freezing temperature. An area of open water often
852 forms north of Svalbard, the “Whalers’ Bay”. Whether heat entrained by mechanical mixing from the
853 Atlantic layer below is sufficient to melt the ice and create a polynya, or if convection of the entire
854 upper layer, driven by ice formation and brine rejection after it has reached freezing temperature, is
855 also required, remains an open question. The Whalers’ Bay normally becomes ice covered later in
856 winter, either by locally formed ice or by ice advected from the interior of the Nansen Basin.

857 The formation of the less saline upper layer implies that part of the Atlantic water that
858 was cooled in the Norwegian Sea and transformed into high density water, potentially contributing
859 to the overturning circulation, instead will leave the Arctic Mediterranean as less dense upper water.
860 The now stratified Atlantic water column continues as a boundary current eastward along the
861 Eurasian continental slope and in the following summer sea ice melting by shortwave radiation
862 creates a seasonal surface melt water layer.

863 The fate of the water that enters the Barents Sea is more varied and more difficult to
864 follow. The Norwegian Coastal Current and the main Atlantic inflow branch flow eastward towards
865 Novaya Zemlya and the heat advected by the Atlantic water is sufficient to keep the southern half of
866 the Barents Sea free of ice the year around. The heat loss is large and the Atlantic water becomes
867 considerably colder than the Atlantic water entering the Arctic Ocean through Fram Strait. In the
868 southern Barents Sea ice is only formed close to the coast and over the shallow areas west of Novaya
869 Zemlya, which are mainly covered by water from the less saline coastal current and where the entire
870 water column is cooled to freezing in winter.

871 The northern Barents Sea is different. It is shallow, mainly comprising the about 120 m
872 deep Grand Bank. It connects to the Arctic Ocean between Svalbard and Franz Josef Land with the
873 deepest trough being the 500m deep Victoria Channel west of Franz Josef Land. The northern



874 Barents Sea is strongly stratified and seasonally ice covered. The source(s) of the low salinity upper
875 layer is(are) not obvious. Its characteristics suggest that it is not directly supplied from the Arctic
876 Ocean, but it might enter from the Kara Sea in the Persey Current, which flows westward south of
877 Franz Josef Land. Another possibility is that the upper layer is formed in the Barents Sea by sea ice
878 melting on the warmer Atlantic and coastal waters that move north towards the passage to the Kara
879 Sea between Franz Josef Land and Novaya Zemlya. The low salinity, cold upper water is eventually
880 exported from the northern Barents Sea to the Norwegian Sea in the Bear Island Current. The more
881 saline and denser deep and bottom waters in the northern Barents Sea are supplied by the branch of
882 Atlantic water that mainly recirculates in the Hopen Deep, but also penetrates northward onto the
883 Grand Bank.

884 In the 2010s the ice cover in the northern Barents Sea became significantly reduced
885 and the stability between the upper layer and the Atlantic water below weakened. This was
886 suggested due to an increased inflow of warmer Atlantic water that reduced the stability and melted
887 the sea ice from below (Lind et al., 2012; Lind et al., 2018). The change would be part of a larger shift
888 that is presently occurring in the Arctic Ocean, the “Atlantification” of the Arctic Ocean, which
889 implies a reduction of the upper layer thickness and stability and a stronger upward transport of heat
890 from the Atlantic layer to the ice (Polyakov et al., 2017). This phenomenon was first reported from
891 the eastern Nansen Basin north of the Laptev Sea, and the changes observed in the Barents Sea were
892 taken as signs that the same pattern was expanding. The heat advected from the North Atlantic
893 would in the near future dominate not only the Norwegian Sea but also the Nansen Basin and the
894 Barents Sea and reduce the extension of the ice cover (Lind et al., 2018). In the later part of the
895 2010s the reduction of the ice cover in the northern Barents Sea stopped and it started to recover,
896 but it is still far from its extent in the 1980s.

897 Not only the ice cover but also the water mass characteristics in the Barents Sea have
898 changed considerably during the last decades. In the 1980s the ice cover and the low salinity upper
899 layer extended farther south and occasionally covered the Central Bank. In some years ice formation



900 and brine rejection over the bank led to haline convection to the bottom and the formation of a cold,
901 dense water column over the bank that eventually contributed to dense water formation in and
902 dense water export from the Barents Sea (Quadfasel et al., 1992; Schauer et al., 2002). In years with
903 strong inflow of warm Atlantic water the Central Bank, by contrast, became covered by Atlantic
904 water and no ice and no dense water was formed over the bank. In the 2000s and 2010s the Atlantic
905 water has been warmer, more saline and denser than in the 1980s. The convection over the Central
906 bank has been thermal and the created waters have been denser than those formed by brine
907 rejection in the 1980s.

908 The dense water formation in the Barents Sea has altered not only over the Central
909 Bank but also farther east, above the Central Depression and over the shallow areas west of Novaya
910 Zemlya. The Atlantic water cooled in winter is presently denser than in the 1980 and shows up as
911 warmer bottom water below a less saline water mass with temperature close to freezing (Lien and
912 Trofimov, 2013; Dmitrenko et al., 2015). The salinity indicates that the upper layer could be created
913 by sea ice melting on top of the denser Atlantic water. This is in contrast to observations made in the
914 early 1900s, when the water created by ice formation and brine rejection west of Novaya Zemlya was
915 the densest water formed on the Barents Sea (Knipovich, 1905; Nansen, 1906). Dense water
916 formation by brine rejection still occurs but now it appears to mainly take place north rather than
917 west of Novaya Zemlya (Lien and Trofimov, 2013).

918



919

920 Section 7 The circulation in the Arctic Mediterranean Sea

921 Section 7.1 Atlantic water in the Eurasian Basin

922 The two Atlantic inflow branches meet again in the St. Anna Trough in the western Kara Sea. The

923 Fram Strait branch, flowing as a boundary current along the Eurasian continental slope, follows the

924 bathymetry southward on the western side of the trough, while the Barents Sea branch enters the

925 trough from southwest through the passage between Novaya Zemlya and Franz Josef Land. The

926 properties of the branches are now different. The Atlantic core of the Fram Strait branch has been

927 shielded from the surface processes by the less saline upper layer created by ice melting north of

928 Svalbard and has retained its warm and saline characteristics. The main part of the Barents Sea

929 inflow branch, by contrast, has been strongly cooled by the atmosphere in the southern Barents Sea

930 and when it encounters and melts sea ice in the northeastern Barents Sea the salinity and density of

931 the melt water layer become higher than that covering the Fram Strait branch.

932 The part of the Fram Strait branch that flows close to Franz Josef Land enters the

933 Barents Sea and circulates around Franz Josef Land to return to the Arctic Ocean, rejoining the

934 boundary current upstream. Most of the Fram Strait branch, however, interacts in the St. Anna

935 Trough with water of similar density from the Barents Sea, forming a colder and less saline Atlantic

936 core that remains on the slope and moves eastward between the Kara Sea shelf and the warmer

937 Fram Strait branch at the slope. The denser waters formed in the Barents Sea sink down the eastern

938 flank and along the deepest part of the St. Anna Trough and enter the boundary current as cold, less

939 saline intrusions beneath the warm core of the Fram Strait branch.

940 Two of the largest Siberian rivers, Ob and Yenisey, discharge into the Kara Sea, but

941 most of their runoff does not appear to cross the Kara Sea shelf break. The major part of the river

942 input instead flows through the Vilkitsky Strait to the Laptev Sea before it, together with runoff from

943 the Lena, crosses the shelf break and enters the deep Eurasian Basin. This shelf outflow is less saline

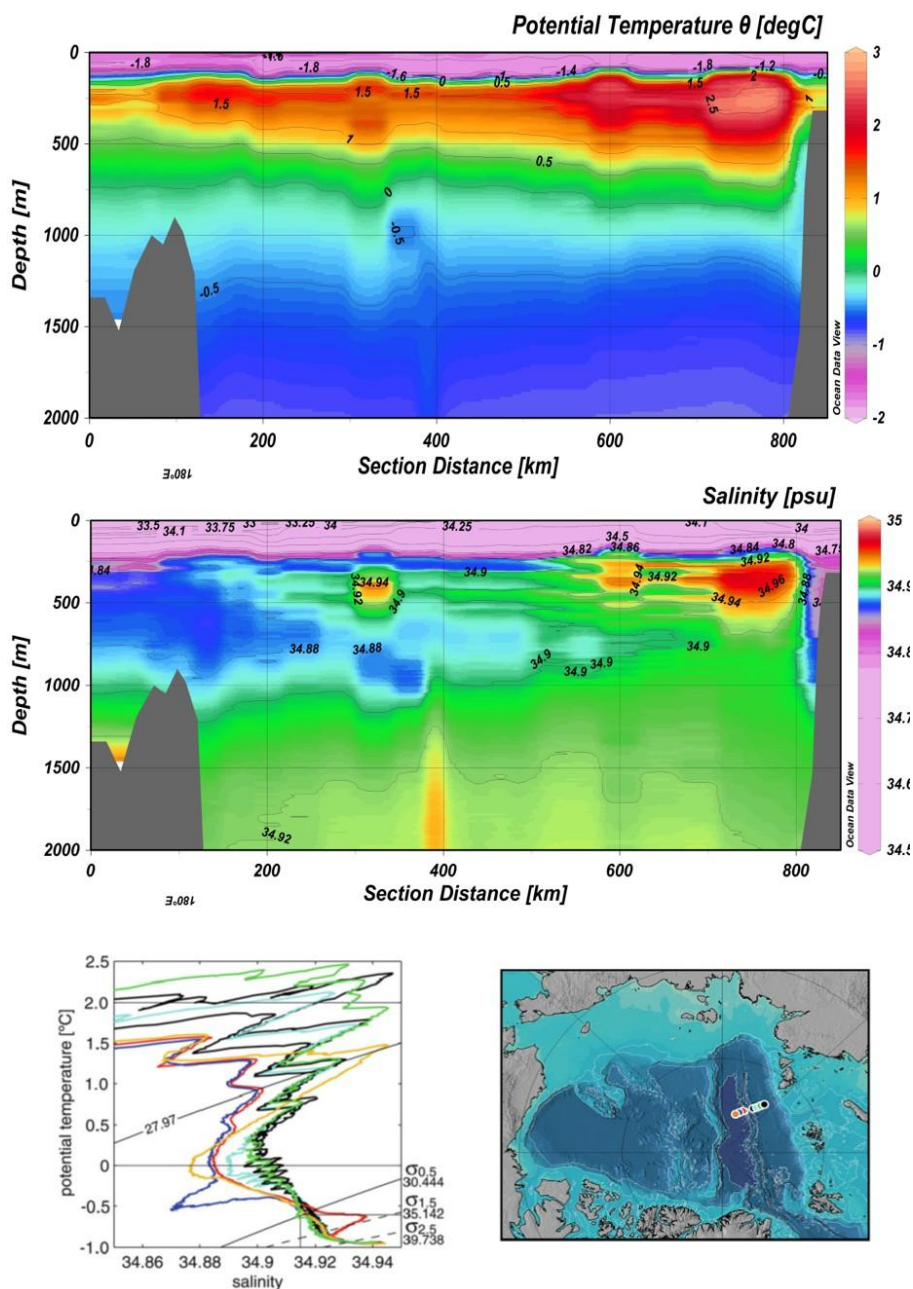
944 and less dense than the surface layer created north of Svalbard and increases the stability of the



945 upper part of the water column. The Atlantic water becomes more isolated from the ice cover, the
946 sea surface, and the atmosphere and most of the observed property changes are due to interactions
947 in the deep between the two inflow branches.

948 The upper, colder stream follows the shelf break until it reaches Severnaya Zemlya.
949 Here the slope and shelf narrow and the stream is forced into the basin and starts to interact
950 isopycnally with the warm core of the boundary current (Rudels et al., 1994; Schauer et al., 1997).
951 Inversions and thermohaline intrusions are created between the colder, less saline shelf stream and
952 the warmer, more saline slope current (Fig. 8). Intrusions are observed in all possible background
953 stratifications; above the temperature maximum where the water column is unstable in
954 temperature, between the temperature and the salinity maxima where the water column is stable in
955 both properties, and below the salinity maximum where the water column is unstably stratified in
956 salinity.

957



958

959 Figure 8. Potential temperature and salinity sections taken 1996 by *FS Polarstern* from the eastern
960 Kara Sea shelf across the Nansen and Amundsen basins and the Lomonosov Ridge into the Makarov
961 Basin. The θ S curves are from the same section, showing interleaving as well as eddies in the
962 different waters. The station positions are shown on the map (The lower panel is from Rudels et al.,
963 2012).

964



965 Theoretically, instabilities and interleaving may form spontaneously, if one component
966 is unstably stratified (Stern 1967; Turner, 1973), but if the background stratification of both
967 components are stable, finite external disturbances are needed to bring the waters across the front
968 to generate the property inversions that drive the intrusions. At the slope such disturbances could be
969 generated by trapped tidal or inertial waves (Toole and Giorgi, 1981). However, the intrusions
970 penetrate into the opposite water mass only as long as an unstable distribution of the driving
971 component remains. Once it is removed, the interleaving stops. One question is then: How far from
972 the slope into the basin do the intrusions influence the lateral mixing between the two streams?

973 Interleaving structures are observed at the Kara Sea slope but also in the interior of
974 the Eurasian Basin at least as far as the Gakkel Ridge. However, a core of warm, saline Fram Strait
975 branch water showing no or weak intrusions is located between these interleaving structures (Fig. 8).
976 It thus appears that the intrusions formed at the slope do not reach to the center of the warm core.
977 On the basin side of the warm core there is no obvious front that can generate intrusions.
978 Furthermore, the only source of colder, less saline water in this density interval is the Barents Sea
979 inflow branch.

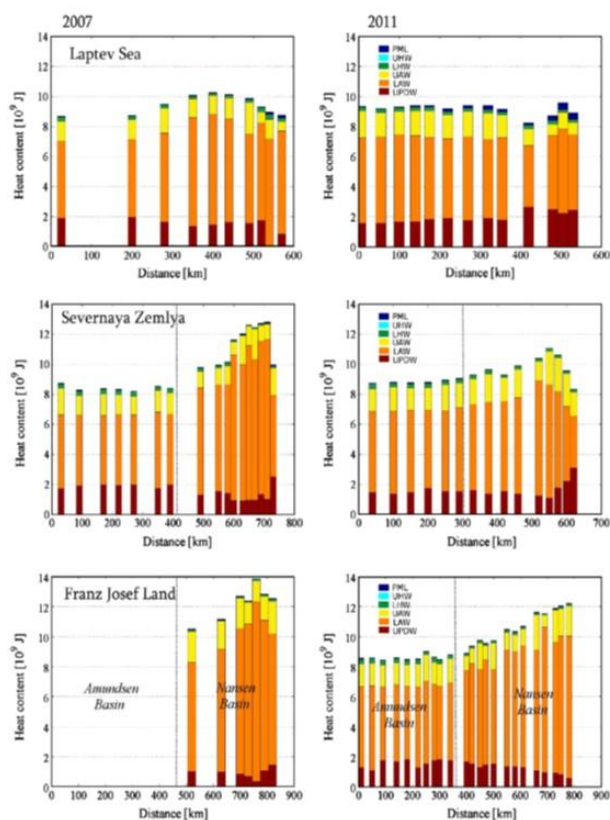
980 One explanation for the presence of thermohaline intrusions in the central Nansen
981 Basin is that the two branches, as they reach the Laptev Sea slope, turn and flow back towards Fram
982 Strait in the Nansen Basin and over the Gakkel Ridge (Rudels et al., 1994). This implies that the
983 intrusions do not spread as far as their presence suggests. Instead, the observed interleaving
984 structures in the interior of the basin are rundown and fossil and are passively advected with the
985 main circulation. In fact, they could be used as tracers for the circulation (Rudels et al., 1994).

986 The water column is not only characterized by interleaving and gyre circulation. There
987 are also several eddies present, which appear to move independently of the gyres, carrying their
988 original properties into different surroundings (Fig. 8, lower panel).

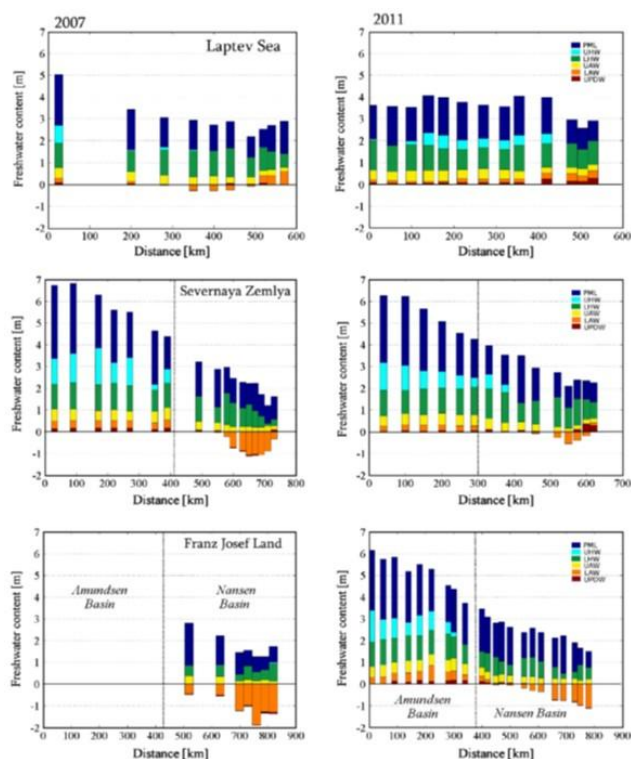
989 The interleaving between the two branches leads to cooling of the Fram Strait branch,
990 but because mass is added the cooling does not necessarily imply a heat loss to the overlying water



991 and to the ice and atmosphere. The heat has already been lost elsewhere, mainly in the Barents Sea.
992 Not only is the Atlantic core cooled, the salinity also decreases significantly (Figure 10). To mix
993 freshwater or low salinity water mechanically and vertically into the deep is energy consuming and
994 the more obvious process is isopycnal mixing between the two branches. The low salinity water
995 added from the Kara Sea west of Severnaya Zemlya enters, freshens and cools the Atlantic core in
996 contrast to the low salinity water from the Laptev Sea, which enters in the surface layer (Fig. 9). To
997 understand how present, and especially how possible future changes in inflow strength and
998 characteristics of the Atlantic water might influence the future condition in the eastern Nansen
999 Basin, it is necessary to consider both inflow branches, how they are transformed individually and
1000 how they interact.
1001



1002



1003

1004

1005 Figure 9. Heat (upper panels) and freshwater (lower panel) content in the upper 1000 m of the water
1006 column (the height of the columns, except where the freshwater content is negative in the Atlantic
1007 water) and the different water masses observed on sections taken in the Eurasian Basin in 2007 and
1008 2011. The different waters are; the Polar Mixed Layer (PML), located above the upper temperature
1009 minimum indicating winter convection, upper halocline water (UHW), found below the upper
1010 temperature minimum and with $S < 34$, lower halocline water (LHW) defined by $\theta < 0^\circ\text{C}$ and $34 < S$,
1011 Atlantic water I (AWI) $0^\circ\text{C} < \theta$, and above the temperature maximum. Atlantic water II (AWII) $0^\circ\text{C} < \theta$,
1012 but below the temperature maximum, upper Polar Deep Water $\theta < 0^\circ\text{C}$, below AWII and above 1000
1013 db. Especially the increase in freshwater content (reference salinity 34.9) in the Atlantic layer on the
1014 eastern sections and the input of freshwater to the upper layer across the Laptev Sea shelf break are
1015 clearly seen (figure from Rudels et al., 2015).

1016

1017 Interleaving has vertically alternating salt finger and diffusive interfaces and between
1018 the background temperature and salinity maxima the buoyancy transports through the salt finger
1019 and diffusive interfaces are roughly equal and the property steps diminishes with time but are not
1020 removed. However, if intrusions are created in the upper part of the water column, above the
1021 temperature maximum, the diffusion of buoyancy through the diffusive interfaces is larger than that



1022 through the salt finger interfaces due to the larger property steps created at the diffusive interfaces.
1023 This may lead to overturning of the salt finger interfaces, which transforms the interleaving into a
1024 thermohaline step structure with thick homogenous layers separated by thin diffusive interfaces with
1025 large temperature steps and small stability ratios (Rudels, 2021). Such thick diffusive layers have
1026 been observed in the eastern Nansen Basin above the temperature maximum and they would
1027 contribute to a vertical rather than a lateral heat transport (Polyakov et al., 2012).

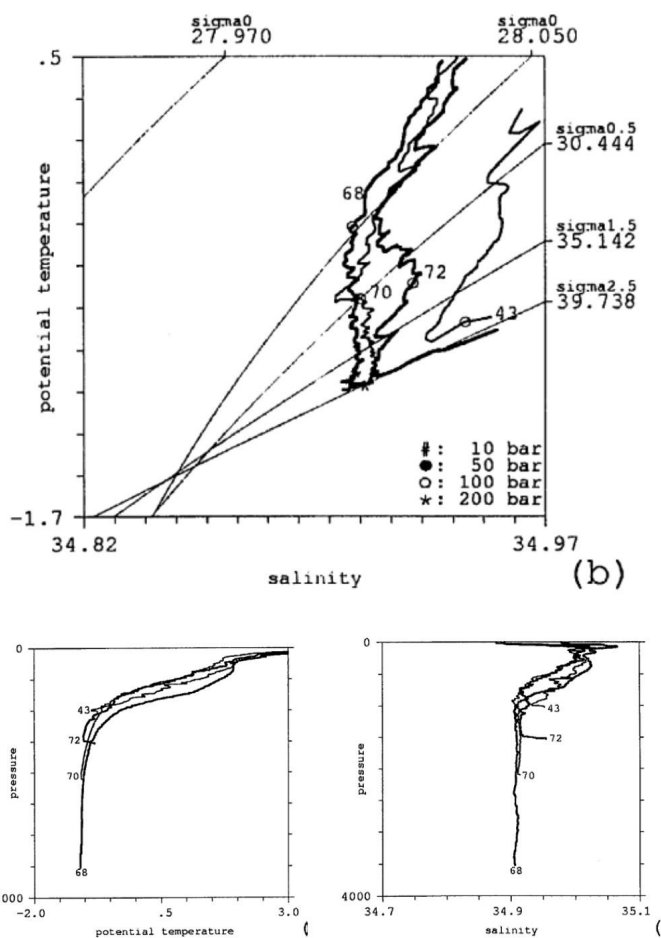
1028 The temperature of the Atlantic water in the Nansen Basin was in 1990 observed to
1029 have increased by about 1°C compared to the climatology (Quadfasel et al., 1991). During the 1990s
1030 more changes in the Arctic Ocean water masses were observed. Higher Atlantic water temperatures
1031 were also seen in the Makarov Basin and the Pacific water that previously supplied the upper layer in
1032 the Makarov Basin had retreated from the Lomonosov Ridge to the Mendeleev Ridge (Carmack et
1033 al., 1993). Also, the runoff normally advected from the Laptev Sea to the Eurasian Basin was absent,
1034 and the more saline melt water layer extended to the sea surface also in the Amundsen Basin,
1035 bringing the Atlantic water closer to the sea surface and the ice cover. By contrast, in the Canada
1036 Basin the upper layer had become thicker and less saline, while the Atlantic water was pressed down
1037 and located at deeper levels (Morison et al., 1998).

1038 These changes in the Arctic Ocean water column were likely due to changes in the
1039 atmospheric circulation. During the 1990s the North Atlantic Oscillation Index was positive and high,
1040 showing that the Icelandic low pressure system was strong and extended north into the Barents Sea,
1041 perhaps farther. This not only brought more Atlantic water into the Arctic Mediterranean, it also
1042 forced the runoff from the large Siberian rivers to leave the shelves farther to the east, into the
1043 Makarov and Canada basins (Maslowski et al., 2000).

1044 Several later pulses of warm Atlantic water have entered through Fram Strait and
1045 been followed as they moved around in the different gyres in the Arctic Ocean (Polyakov et al., 2005,
1046 2011.). Changes have, however, also occurred in the Barents Sea branch. In the 1980s the Barents
1047 Sea branch water that entered the Arctic Ocean was colder, less saline and denser and showed up as



1048 a salinity minimum between 800m and 1200m in the Eurasian Basin (Rudels et al., 2013, see also
1049 figure 8). In the 2000s, by contrast, the water that enters and passes over the Barents Sea to the
1050 Arctic Ocean has been warmer, more saline and denser and has instead been identified as a salinity
1051 maximum around 2000 m (Rudels, 2021).
1052



1053

1054

1055 Figure 10. Potential temperature and salinity profiles and θ -S curves observed from FS Valdivia west
1056 of Svalbard in 1986. The increase in salinity and temperature in the deepest layer indicates brine
1057 enriched water from Storfjorden that has entrained intermediate warm Atlantic water during its
1058 descent (adapted from Rudels et al., 1999b).

1059



1060 The densest water created by ice formation and brine rejection on the shallow areas
1061 west and north of Novaya Zemlya, however, does not show up clearly in the Arctic Ocean water
1062 column. Its presence has been deduced from an increase in temperature in thin saline bottom layers
1063 at the slope (Rudels et al., 2001). The high salinity is due to brine rejection and accumulation of saline
1064 water at the shelves, and the temperature increase is caused by entrainment of intermediate warm
1065 Atlantic water as the plumes sink into the deep. This process has, however, been followed in more
1066 detail in the western Barents Sea (Fig. 10), where brine enriched dense outflows from Storfjorden in
1067 southern Svalbard sink into the deep Fram Strait, entraining warm Atlantic water (Quadfasel et al.,
1068 1988).

1069 There are two different conceptual models for the descending plumes. The shaving
1070 plumes (Aagaard et al., 1985), where the interfacial stress on the upper part of the plume causes the
1071 plume to gradually lose mass to the surrounding water as it sinks into the deep. The second model
1072 pictures thin plumes passing through and entraining the intermediate layers (Rudels, 1986a). The
1073 turbulence is generated by bottom stress and to accommodate the increased mass transport the
1074 plumes do not grow vertically but laterally and their thickness is retained.

1075 Shaving plumes are initially fairly thick and carry a substantial amount of dense water
1076 from the shelf into the deep and redistribute it to the ambient water column as they sink. This is a
1077 picture that would fit the denser water descending down the t. Anna Trough, and perhaps also the
1078 dense overflow plumes crossing the Greenland-Scotland Ridge. The entraining plumes, by contrast,
1079 would be thin and carry but little water from the shelf but instead incorporate intermediate water
1080 from bypassed layers and bring it into the deep. The Atlantic water flowing along the slope thus
1081 becomes transported downwards and transformed into deeper and denser water masses. The
1082 observations shown in Fig. 10 suggest entraining plumes.

1083

1084 Section 7.2 A possible wind driven circulation

1085 The two Atlantic inflows partly cross the Lomonosov Ridge and enter the Amerasian Basin, partly



1086 remain in the Eurasian Basin and return directly to Fram Strait, mostly along prominent bathymetric
1087 features such as the Lomonosov Ridge and the Gakkel Ridge. The forcing of the Atlantic water
1088 circulation in the Arctic Mediterranean deep basins is not well established and several conceptual
1089 models have been proposed and here the approach taken by Nøst and Isachsen (2003) will be
1090 examined.

1091 Nøst and Isachsen (2003) assumed that the circulation is wind driven and computed
1092 the vorticity input at the surface from the NCEP/NCAR reanalysis data (Kalnay et al., 1996, 1997) and
1093 the thermal wind transports from the observed seasonally averaged hydrographic fields. They found
1094 that these did not balance and a Sverdrup circulation, where the added wind torque drives a
1095 meridional transport, is not present in the Arctic Mediterranean Sea. The vorticity added at the sea
1096 surface must then be removed by nonzero bottom velocities and bottom friction.

1097 Nøst and Isachsen suggested either quadratic or linear bottom friction laws to
1098 represent the bottom torque. The applied meteorological forcing corresponds to a vertical velocity of
1099 about 10^{-6}ms^{-1} , and the vertical velocity generated by the bottom torque must be of the same order.
1100 The bathymetry of the Arctic Mediterranean consists of several basins that display closed
1101 topographic contours H and also closed geostrophic contours f/H , H being the depth and f the
1102 Coriolis parameter. Assuming that the bottom circulation follows the geostrophic contours and that
1103 the width of the bottom streams is equal to the width of the continental slopes, the bottom
1104 velocities can be estimated to 10^{-1}ms^{-1} , which is close to the observed bottom velocities (Newton and
1105 Sotirin, 1997; Nøst and Isachsen, 2003). The picture is then an almost barotropic deep circulation in
1106 the Arctic Mediterranean that largely follows the f/H contours and that the wind forcing is balanced
1107 by the bottom torque.

1108 The neglect of thermodynamics, except that present in the observed and used density
1109 field, prevents the model from addressing the changes in the stratification that take place in the
1110 Arctic Mediterranean. Aaboe and Nost (2008) tried to remedy this limitation by introducing a
1111 variation in bottom density along the f/H contours. The bottom density is highest in the Nordic Seas



1112 and lower in the Arctic Ocean and especially in the Canada Basin. This generates a cyclonic flow in
1113 the Nordic Seas, which weakens and eventually changes to anticyclonic in the Arctic Ocean. This
1114 change can be explained by a shift from a strong barotropic circulation in the Nordic Sea to a larger
1115 contribution of the baroclinic part of the circulation (Aaboe and Nøst, 2008). No thermodynamics is
1116 included in the model that can explain the bottom density changes, but one possibility could be that
1117 the input of shelf water and the Pacific inflow at the surface push the boundary current to deeper
1118 levels and replace the water column at the chosen f/H contour with a less dense one from higher up
1119 on the slope.

1120 Nøst et al. (2008) made a theoretical and experimental study of two connected basins
1121 with sloping bottom and with one basin driven by either cyclonic or anticyclonic forcing. They found
1122 that cyclonic forcing at one basin also made the second basin exhibit a cyclonic circulation. By
1123 contrast, a weak anticyclonic forcing in one basin creates an anticyclonic circulation in the second
1124 basin. However, when the anticyclonic forcing increases the circulation in the second basin shifts to
1125 cyclonic. It thus appears that a cyclonic circulation is more stable than an anticyclonic one. Another
1126 interesting detail is that cyclonic forcing in one basin can also drive a cyclonic circulation in an
1127 adjacent basin. This implies that an atmospheric forcing in the Nordic Seas could drive the circulation
1128 along the geostrophic contours also in the Arctic Ocean. If the cyclonic wind forcing in the Subpolar
1129 gyre can drive the Atlantic inflow to the Arctic Mediterranean is an interesting possibility.

1130



1131 Section 8 The circulation in the Amerasian Basin
1132 East of the Laptev Sea and the New Siberian Islands the nature of the circulation changes. It is no
1133 longer characterized by the two Atlantic inflows but by freshwater input from rivers and from the low
1134 salinity Pacific inflow. The resulting freshwater storage confines the atmospheric forcing and the
1135 oceanic response to the upper part of the water column. The mainly wind driven circulation is
1136 centered below the atmospheric high pressure cell above the Beaufort Sea in the Canada Basin. The
1137 anticyclonic wind field forces the less dense surface waters towards the center of the Beaufort Sea,
1138 leading to a higher sea level and to an anticyclonic geostrophic circulation, the Beaufort Gyre, in the
1139 upper few hundred meters. In the Eurasian Basin, by contrast, the low pressure cell extending from
1140 Iceland into the Barents Sea creates a cyclonic circulation that drives Atlantic water from the
1141 Norwegian Sea into the Arctic Ocean and forces much of the continental runoff from Eurasia into the
1142 Amerasian Basin.

1143 The two gyre systems are brought together and interact in the Transpolar Drift, where
1144 the Siberian branch originating in the Laptev Sea flows towards Greenland and Fram Strait in the
1145 Amundsen Basin parallel to the rim of the Beaufort Gyre. Waters are exchanged between the two
1146 gyres and the denser Siberian branch intrudes into and supplies water to the deeper levels of the
1147 Beaufort Gyre (Morison et al., 2012). Both streams transport sea ice and especially the Laptev Sea
1148 has been considered an important formation site for the sea ice exported from the Arctic Ocean.

1149 The existence of the Transpolar drift was demonstrated by the drift of *Fram* 1893-
1150 1896. Roald Amundsen tried to repeat the drift with *Maud*, 1918-1925, but by starting from the East
1151 Siberian Sea farther to the east, he hoped to have a greater possibility to drift over the North Pole.
1152 This plan did not work. *Maud* remained in the East Siberian Sea trapped by the ice and did not pass
1153 beyond the shelf break. The main source of the Transpolar drift thus appears located west of the
1154 New Siberian Islands. while the East Siberian Sea, in contrast to the Laptev Sea, more acts as an ice
1155 sink for the inner Arctic Ocean. This is partly confirmed by Zacharov (1976), who estimated the ice



1156 export from Siberian shelves and concluded that the Laptev Sea ice export was about ten times as
1157 large as that from the East Siberian Sea.

1158 The ice cover in the East Siberian Sea has diminished drastically in recent years and has
1159 now changed to seasonal from being present almost the year around. This is but one indication of
1160 the changes taking place in the Arctic Ocean ice cover. The decline in ice cover extent has since the
1161 beginning of the satellite observations in the 1970s been followed almost in real time, but
1162 information about sea ice thickness is more difficult to obtain. Not until upward-looking sonar
1163 observations were made from the submarine USS Pargo in 1993 could sea ice thickness
1164 measurements be compared with those made about 30 years earlier. The thickness of the Arctic
1165 Ocean ice cover had decreased by 40%, from an average thickness of about 3 m to 1.8 m (Rothrock et
1166 al., 1999).

1167 The effects of these changes were clearly demonstrated by the ship *Tara*, which in
1168 2008 within the EU-DAMOCLES (Developing Arctic Modeling and Observing Capabilities for Long-
1169 term Environmental Studies) program repeated the drifts of *Fram* and *G.Sedov* in only 18 months
1170 compared to 3 years for the earlier drifts, showing that thinner ice moves more quickly than the thick
1171 ice cover in the past. The reduction in ice cover thickness and extent does not appear to have
1172 significantly changed the sea ice export to the Nordic Seas through Fram Strait (Spren et al., 2009).
1173 The ice grows as it drifts and thinner ice grows more quickly, and the reduced ice thickness is also
1174 compensated by the more rapid flow. However, the storage of freshwater as ice in the Arctic Ocean
1175 has declined significantly, and the seasonal ice formation manages to supply the ice export but
1176 cannot rebuild any large reservoir of older, thicker ice within the Arctic Ocean. Some of the more
1177 dramatic reductions in the ice cover have been connected with atmospheric circulations and winds
1178 favoring a large ice export through Fram Strait as in 2007, the year of the second lowest summer ice
1179 extent on record.

1180 The loss of sea ice has not resulted in a reduction of the total freshwater storage in the
1181 Arctic Ocean. The total freshwater volume has increased by 4500km³ and the liquid freshwater that



1182 has accumulated in the Beaufort Gyre has increased the freshwater storage there by 5000km³,
1183 between 2000s and the 1980s and 1990s. This more than compensate for the about 3500km³ loss of
1184 sea ice (Haine et al., 2015).

1185 The circulation in the Beaufort Gyre is complex. The anticyclonic winds collect the low
1186 salinity upper water in the center of the gyre and this accumulation is balanced by instabilities in the
1187 deeper layers that shed eddies into the surroundings (Manucharyan and Spall, 2016). However, the
1188 balance between these two processes is yet not reached, and the present storage of about 20 m of
1189 freshwater relative to a salinity of 34.8 could increase to more than 30 m (Manucharyan and Spall,
1190 2016; Manucharyan et al., 2016). Another, additional, process has therefore been suggested, the ice-
1191 stress governor, resembling the valve that in the 19th century prevented steam engines from running
1192 amok (Meneghello et al., 2018).

1193 The accumulation of low salinity water by the wind in the center of the gyre creates a
1194 baroclinic density field that drives an anticyclonic geostrophic circulation around the gyre. If the wind
1195 stress on the ice surface is taken up by the internal stresses in the ice cover, the ice cover is no longer
1196 forced by the wind. Instead, its motion ceases and it begins to retard the geostrophic circulation of
1197 the water below, which in turn reduces the slope of the isopycnals and the accumulation of
1198 freshwater. This process should then act together with the instability mechanism to reduce the
1199 freshwater storage in the Beaufort Gyre (Meneghello et al., 2018). However, if the ice cover becomes
1200 less compact, or perhaps disappear, the ice-stress governor ceases to function and more freshwater
1201 would again be collected in the Beaufort Gyre (Doddridge et al., 2019).

1202 With more freshwater accumulated in the Beaufort Gyre the stability increases and
1203 the upper layer becomes isolated from the bathymetry. The balance between the input of vorticity at
1204 the surface and its removal by bottom stress, as proposed by Nøst and Isachsen (2003), might then
1205 disappear and another balance is needed. One, albeit speculative, possibility could be a Sverdrup
1206 balance. The anticyclonic wind field generates a southward transport, which is balanced by an inertial
1207 return flow on the western side of the gyre, like the Transpolar drift. The flow would intensify as long



1208 as f increases, but when the highest latitudes is passed f starts to decrease and the boundary current
1209 begins to diverge. This is but speculation.

1210 In the Amerasian Basin the input of low salinity water from the shelves, and the Pacific
1211 inflows that create a temperature maximum around 75m in summer and form a temperature
1212 minimum between 200m and 300m in winter, further isolate the Atlantic water from the energy
1213 input at the sea surface. The temperature minimum also involves an increase of salinity, suggesting
1214 that in winter ice has formed in the Bering and Chukchi seas, and the bottom water salinity has
1215 increased by brine rejection. This is in agreement with the mechanism for creating the cold Arctic
1216 Ocean halocline proposed by Aagaard et al. (1981), which isolates the deeper layers from the surface
1217 processes. The cold, saline water also has high nutrient content, indicating regeneration of nutrients
1218 from the bottom sediments (Jones and Anderson, 1986).

1219 The thermocline between the Pacific winter water and the temperature maximum of
1220 the Atlantic layer displays step structures and homogenous layers, suggesting that heat is
1221 transported upwards by double diffusion. The individual diffusive layers and steps appear to be
1222 coherent over several kilometers, giving a horizontal to vertical ratio of about 10000 to 1
1223 (Timmermans et al., 2008). However, over the same distance large temperature differences are
1224 present in both the upper and the lower part of the thermocline. The vertical diffusive heat flux
1225 reduces the temperature of the Atlantic core, but the lost heat becomes trapped in and warms the
1226 temperature minimum of the Pacific winter water. The temperature in the central part of the
1227 thermocline, however, remains more or less constant, suggesting that here the heat fluxes through
1228 the lower and upper diffusive interfaces are balanced. This implies that the thermocline and the
1229 diffusive layers are advected over the basin on time scales of several years. The layers are coherent
1230 in time rather than in space.

1231 The stability ratios $\beta S/\alpha T$ at the interfaces are large, 3-4. This implies that parcels
1232 convecting from the interfaces can homogenize the existing layers but could not have created the
1233 initial layers. The layers, or embryos of the steps and layers might then be present already as the



1234 Atlantic water enters the Amerasian Basin and the larger number of layers and interfaces compared
1235 to the Eurasian Basin would be due to a decreased buoyancy of the rising and sinking plumes. They
1236 are then no longer able to stir and homogenize the entire layer but only the part close to the
1237 interfaces, and new interfaces are created at mid-depth.

1238 The Atlantic water that returns from the Amerasian Basin lies too deep to exit through
1239 the Canadian Arctic Archipelago. Instead, it appears, at least partly, to leave the North American
1240 continental shelf and slope and move northward as a boundary current along the Lomonosov Ridge.
1241 There it passes through gaps in the ridge from the Makarov to the Amundsen Basin and then returns
1242 south towards Greenland (Björk et al., 2010). Some Atlantic water may also cross the Lomonosov
1243 Ridge at the continental slope directly to the Amundsen Basin.

1244 In the mid-20th Century the commonly accepted view was that the deep and bottom
1245 water source in the Arctic Mediterranean was located in the Greenland Sea and that cold, dense
1246 deep water penetrated into the Arctic Ocean through Fram Strait and its temperature increased with
1247 the distance from the source (Wüst, 1941). However, on the US expedition Ski-jump 1951 and 1952
1248 L.V. Worthington noticed that the deep water temperatures below about 1600 m in western Arctic
1249 Ocean, away from Fram Strait, remained almost constant around -0.5°C , significantly higher than in
1250 the Greenland Sea. Worthington suggested that the higher temperature was caused by a submarine
1251 ridge that prevented the deepest and coldest water from spreading to the entire Arctic Ocean
1252 (Worthington, 1953). Unknown to Worthington this ridge, the Lomonosov Ridge, had been
1253 discovered by the Soviet airborne high-latitude expeditions in 1948.

1254 It was later noticed that not only the deep temperatures but also the deep salinities
1255 were higher in the Amerasian Basin beyond the Lomonosov Ridge than in the Eurasian Basin
1256 (Aagaard, 1980). This implied that the deep Arctic Ocean was not stagnate and that water mass
1257 renewals must take place. The situation was akin to the one Nansen had encountered with the
1258 erroneous, too high, salinity measurements from *Fram*. Nansen had initially suggested that these
1259 salinities could be due to brine enrichment of the bottom waters on the shallow shelves and a



1260 subsequent sinking of the dense shelf water down the continental slope (Nansen, 1906). An idea that
1261 he later abandoned, when he found that the deep salinities measured north of Svalbard agreed with
1262 those observed in the Greenland Sea (Nansen, 1915). Now the Arctic Ocean was suddenly recognized
1263 as an additional active source for the deep water in the Arctic Mediterranean and Aagaard et al.
1264 (1985) and Rudels (1986a) proposed a connected system, where the Greenland Sea supplies the
1265 colder, less saline end member and the Arctic Ocean the saline, warmer end member and the two
1266 sources communicate through Fram Strait.

1267 The water columns in the Eurasian Basin and in the Amerasian Basin differ. The
1268 Eurasian Basin is warmer and more saline in its upper part while the Amerasian Basin is warmer and
1269 more saline in the deep. The changeover occurs at different depth levels for temperature and
1270 salinity. The Amerasian Basin becomes warmer than the Eurasian Basin below 900 m, well above the
1271 sill depth of the Lomonosov Ridge, but it becomes more saline first at 1400 m, closer to the sill depth,
1272 but still in a depth range, where the different basins communicate with each other.

1273 These differences must be due to slope convection and the entrainment into the
1274 sinking boundary plumes. The colder deep water in the Eurasian Basin could be explained by the
1275 entrainment of much colder ambient water as the plumes sink through the deeper part, while the
1276 more saline characteristics of the Amerasian Basin may be caused by the less dense upper part of the
1277 water column, which requires the initial shelf contributions to be much more saline to reach the
1278 deepest layers than those descending from the Eurasian shelves.

1279 Below about 1500 m to 2000 m the deep waters in the different basins communicate
1280 less freely and they have acquired their different characteristics. The deep water columns in the
1281 Nansen, Amundsen and Canada basins are similar. The temperature decreases and the salinity
1282 increases until about 1000 m from the bottom, where a temperature minimum is encountered.
1283 Below this level the temperature increases slightly and the salinity continues to rise until a
1284 homogenous, 600 m to 800m thick bottom layer is encountered. The temperature increase and the
1285 homogenous bottom water have been explained by geothermal heating, which could homogenize



1286 the bottom layer by convection from below and perhaps eventually remove the temperature
1287 minimum (Timmermans et al., 2003; Björk and Winsor, 2006; Carmack et al., 2012). The presence of
1288 a temperature minimum in the three basins is not obvious. In the Canada Basin it can be explained by
1289 advection of deep water from the Makarov Basin across the Alpha and Mendeleev ridges, but no
1290 such source can be identified in the Nansen and Amundsen basins.

1291 The Makarov Basin is different. No deep temperature minimum is present and the
1292 salinity increase with depth stops about 1000 m from the bottom, while the temperature continues
1293 to decrease until 500 m from the bottom. Below this level a homogenous bottom layer is found. This
1294 feature was explained by Jones et al. (1995) by a spillover across the Lomonosov Ridge of colder, less
1295 saline deep water from Amundsen Basin, which could then sink to the bottom, aided by the higher
1296 compressibility of colder water. However, when the deepest sill at the Lomonosov Ridge was reached
1297 and studied by *IB Oden* in 2005, no such overflow was found. Instead, warm and saline deep water
1298 from the Makarov Basin was observed entering the Amundsen Basin (Björk et al., 2007). If there is a
1299 spillover from Amundsen Basin to the Makarov Basin, it must be intermittent.

1300

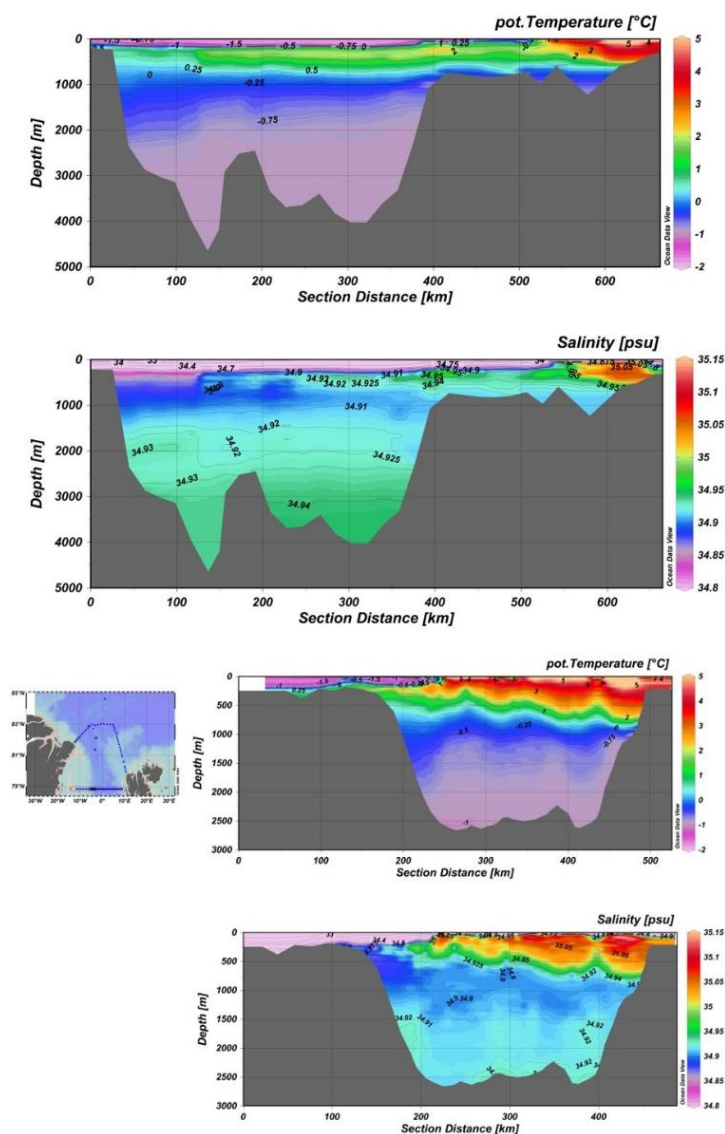


1301 Section 9 Fram Strait.

1302 The downstream conditions of the inflow to the Arctic Ocean through Fram Strait and the upstream
1303 conditions for the return flows to the strait are shown in Fig. 11. The inflow involves not only Atlantic
1304 water, which mainly enters over the shelf north of Svalbard, but also denser, deeper lying waters,
1305 which cannot pass directly eastward and have to circulate along the Nansen Ridge and the northern
1306 slope of the Yermak Plateau before they can join the shelf inflow at the continental slope east of
1307 Svalbard. Farther north the water returning to Fram Strait in the northern Nansen Basin, over the
1308 Gakkel Ridge and in the Amundsen Basin dominate.

1309 The Arctic Atlantic water returning in the Eurasian Basin is warmer and more saline
1310 than the Arctic Atlantic water that has passed through the Amerasian Basin and approaches Fram
1311 Strait along the Greenland slope. The water that has entered the Arctic Ocean over the Barents Sea is
1312 identified as a less saline layer at 1000 m depth, but it is difficult to separate intermediate waters
1313 returning directly from the Eurasian Basin and those that have passed through the Amerasian Basin,
1314 except by location. The deep water from the Amerasian Basin shows up as a salinity maximum
1315 around 2000m at the Greenland slope, and the colder and denser Eurasian Basin deep water fills the
1316 deeper layers on the northern section (Fig. 11).

1317



1318

1319

1320 Figure 11. Two potential temperature and salinity sections, one taken from Svalbard along the
1321 Nansen Ridge and over the Yermak plateau into the Nansen Basin and the westward to Greenland
1322 and the second along the sill in Fram Strait showing the exchanges between the Arctic Ocean and
1323 the Nordic Seas (sections taken by *FS Polarstern* 2004).

1324

1325 On the southern section, taken along 78°50'N in Fram Strait (Figure 11), there is an

1326 inflow of mainly Atlantic water in the West Spitsbergen Current but also of intermediate and deep



1327 waters from the Nordic Seas. The deep waters in general are slightly less saline in Fram Strait than
1328 farther north in the Nansen Basin. The central part of the strait exhibits a strong recirculation of
1329 Atlantic water towards the west. The recirculation is largely carried by barotropic and baroclinic
1330 eddies that appear to move westward towards Greenland. The main southward flow from the Arctic
1331 Ocean takes place to the west in the East Greenland Current. The recirculation in Fram Strait is strong
1332 and only a narrow space is available for the outflowing water between the recirculating Atlantic
1333 water and the Greenland continental slope.

1334 The East Greenland Current is more baroclinic than the West Spitsbergen Current and
1335 carries several different water masses. The upper layer is dominated by low salinity waters
1336 comprising river runoff, occasionally contributions from the Pacific inflows, and halocline water
1337 created from ice melted on the warm Atlantic water entering north of Svalbard. The cold, low salinity
1338 water flows above warm recirculating Atlantic water that penetrates into the East Greenland Current
1339 above the transformed Arctic Atlantic water that is returning along the Greenland continental slope.
1340 The warmest Arctic Atlantic water derives from the Fram Strait branch that mainly remains in the
1341 Eurasian Basin while the colder contributions are supplied by the Barents Sea inflow branch that
1342 circulates around the Makarov and Canada basins. The Barents Sea inflow also forms an intermediate
1343 water mass with distinct doubly stable θ_S characteristics, salinity increasing and temperature
1344 decreasing with depth.

1345 At the western slope two outflows of the Arctic Ocean deep waters can be identified.
1346 A warm saline core centered around 1800m depth, which ultimately derives from the Amerasian
1347 Basin, and a colder core with similar salinity located at sill depth, indicating an outflow of Eurasian
1348 Basin deep water. The comparatively warm and saline characteristics of the Arctic Ocean deep
1349 waters indicate that they are created by slope convection as shelf water made dense by ice
1350 formation sinks down the slope entraining ambient warmer water. The salinity then decreases and
1351 the temperature increases and the plumes continue to sink until their density matches that of the
1352 surrounding water column. The deep and bottom water of the Arctic Ocean thus become warmer



1353 and more saline than deep water created by open ocean convection. The entrainment into the
1354 boundary plumes transports Atlantic water downward in the water column and its density increases
1355 as it mixes with the cold, saline shelf outflow. The interaction with sea ice formation and sea ice
1356 melting thus separates the inflowing Atlantic water into both less dense and denser waters.

1357 Fram Strait is the only deep passage to the Arctic Ocean and most of the entering
1358 Atlantic water must exit through Fram Strait. The low salinity waters can, however, leave the Arctic
1359 Ocean either through Fram Strait or through the narrow and shallow passages of the Canadian Arctic
1360 Archipelago. The largest runoff enters the Kara and Laptev shelves and since the shelf outflow from
1361 the Laptev Sea to the Amundsen Basin has salinity between 32 and 33 the runoff must mix with an
1362 advective saline water mass, and the only one available on these shelves is the water of the
1363 Norwegian Coastal current that enters the Barents Sea and continues eastward to the Kara Sea and
1364 Laptev Sea shelves.

1365 The Chukchi shelf is flooded from behind by the Pacific inflow, which also supplies
1366 saline water to the East Siberian Sea, where, in addition, upwelling of saline water from the Makarov
1367 Basin takes place. The melting of sea ice on the entering Atlantic water, either north of Svalbard or in
1368 the Barents Sea, creates the densest upper layer water and the densest water that can pass through
1369 Nares Strait, the deepest passage in the Canadian Arctic Archipelago (Rudels et al., 2004; Díckson et
1370 al., 2007).

1371 The major driving forces behind the exchanges through Fram Strait are not identified
1372 with certainty, but the largest transports take place at the slopes, which could indicate either a
1373 barotropic wind driven flow along geostrophic contours as that suggested by Nøst and Isachsen
1374 (2003), but also baroclinic transports of mainly less dense upper layer waters along the coastal
1375 boundaries (Werenskiold, 1935), or a combination of both. The sea level in the Arctic Ocean is higher
1376 than in the Nordic Seas, which favors a southward flow in the East Greenland Current. It could also
1377 obstruct the northward flow in the West Spitsbergen Current and force a westward recirculation in
1378 the strait.



1379 The presence of eddies leads to weak horizontal coherence of the velocities and
1380 makes it difficult to determine the transports by direct current measurements. Existing hydrographic
1381 sections, by contrast, have a much higher horizontal and vertical resolution which allows for better
1382 identification of the transports of different waters. The temporal resolution is of course much less,
1383 one section per year compared to one record per hour. Several attempts to compute the geostrophic
1384 volume transports through the strait and to estimate the heat and freshwater fluxes have been
1385 made. One weakness always present is the choice of the unknown barotropic reference velocities,
1386 which to some extent must be subjective. However, this and other difficulties may also offer an
1387 opportunity to reflect upon what the obtained results really imply and we will discuss in some detail
1388 the exercise made by Rudels et al. (2008).

1389 Rudels et al. (2008) noticed that the deep water from the Arctic Ocean is more saline
1390 than the deep inflow from the Nordic seas, and that the deep inflow also has to leave the Arctic
1391 Ocean as deep water ($28.06 \leq \rho_\theta$). They postulated that 0.4 Sv of deep water ($S = 34.935$) is produced
1392 in the Arctic Ocean and that 0.2 Sv of deep water ($S = 34.910$) enter from the Nordic Seas. This
1393 implies a net deep outflow M , of $0.4 \cdot 10^6 \text{ m}^3\text{s}^{-1}$, carrying a net salt export S of $13.973 \text{ kg}^6\text{s}^{-1}$. They
1394 applied these constraints on the deep part of the strait and required that the kinetic energy of the
1395 added barotropic reference velocities should be a minimum. The barotropic reference velocities
1396 extend to the sea surface, but no corrections are applied on the shallow parts of the strait, where no
1397 deep water is present. The applied constraints promote a saline deep outflow on the western and
1398 the less saline inflow on the eastern side of the strait, in accordance with observations.

1399 The northward and southward volume transports in Fram Strait are not balanced. This
1400 implies that computed heat and freshwater transports depend upon the choice of reference
1401 temperature and reference salinity. Rudels et al. (2008) put the reference salinity equal to the mean
1402 inflow salinity and the reference temperature equal to the mean outflow temperature. This implies
1403 that the inflow carries no freshwater and the outflow no heat.



1404 Computing the geostrophic transport through 16 hydrographic section obtained
1405 between 1980 and 2005 along the sill in Fram Strait the total in and outflows ranged from 5 Sv to
1406 almost 15 Sv with an averaged inflow of 6 Sv and an average outflow close to 9 Sv. This is, as
1407 expected, less than the transports obtained by direct current measurements, but not alarmingly so.
1408 The mean net outflow, 2.5 Sv, 2.8 Sv if the southward flow on the Greenland shelf is included, is
1409 larger than that found from the current meter array.

1410 The transports through the other passages of the Arctic ocean are only in one
1411 direction. Inflows take place over the Barents Sea and through Bering Strait and runoff and net
1412 precipitation add freshwater. The only other outflows occur through the Canadian Arctic
1413 Archipelago. The shelf outflows and the Pacific inflow are cooled to freezing temperature but the
1414 part of the Barents Sea inflow that enters the deeper layers of the basins has a mean temperature
1415 around -0.5°C . We assume that the transports through the other passages are known, and use the
1416 estimates provided by Dickson et al. (2007). It is then possible to determine the amount of heat
1417 entering and the amount of freshwater leaving the Arctic Ocean through Fram Strait and also how
1418 the advective heat is lost in the Arctic Ocean.

1419 The net volume transport, the mean outflow temperature and the northward heat
1420 transport referenced to the outflow temperature were computed for each section. The average
1421 values 2.8 Sv, $T_{\text{ref}} = 0.7^{\circ}\text{C}$ and 25 TW obtained from the sections were taken to represent the
1422 transports and used to determined how the inflowing heat might be distributed in the Arctic Ocean.

1423 Assuming that 1.2 Sv of the Barents Sea inflow with temperature -0.5°C enter the
1424 deeper layers and leave the Arctic Ocean through Fram Strait, this cold water transports $c \times (T_{\text{ref}} -$
1425 $(-0.5)) \times 1.2 \times 10^9 = 5.8 \text{ TW}$ into the Arctic Ocean. $c = 4000 \text{ Jkg}^{-1}\text{K}^{-1}$ is the heat capacity of sea water.
1426 The remaining part of the net outflow of 1.6 Sv is less saline and at the freezing point and exits as
1427 upper layer water transporting $c \times (T_{\text{ref}} - (-1.8)) \times 1.6 \times 10^9 = 16 \text{ TW}$ heat northward. The northward
1428 heat transport in the East Greenland Current of 22 TW then has to be balanced by outflowing
1429 warmer returning and recirculating Atlantic water. This implies that almost all 25 TW of the



1430 northward heat transport through the strait return south as warmer water in the East Greenland

1431 Current.

1432 The remaining 3 TW could melt sea ice north of Svalbard and with an Atlantic inflow
1433 temperature of 3.1°C this implies that 0.15 Sv is cooled to freezing temperature and that the fraction
1434 $\phi = 2\alpha L(c\beta S_A)^{-1}$ (see section 5) or about one third of this heat loss, is used to melt ice and the rest
1435 goes to the atmosphere. The amount of melted ice added to the created upper layer is then 0.003 Sv.

1436 Introducing the obtained freshwater and volume transports through Fram Strait in the
1437 volume and freshwater balances for the Arctic Ocean made by Dickson et al. (2007) Rudels et al.
1438 (2008) found that the freshwater fluxes into and out of the Arctic Ocean were almost in balance but
1439 the volume transports were unbalanced by 1.17 Sv. This indicates that the barotropic velocities
1440 added in Fram Strait are too small. However, since the chosen reference salinity is the mean salinity
1441 of the inflowing water, we can add a barotropic correction to the northward transports without
1442 affecting the freshwater balance. If a barotropic northward transport of 1.1 Sv is added also the
1443 volume fluxes become almost balanced. The northward heat transport, however, then increases.

1444 The difference between the mean inflow temperature, 1.6 °C, and the mean outflow
1445 temperature 0.7 °C is 0.9 °C, which increases the heat transport by 4 TW. The net outflow that has to
1446 be heated to 0.7 °C decreases from 2.8 Sv to 1.7 Sv, implying that only 0.5 Sv of the cold surface
1447 water must be warmed to 0.7 °C, which requires 5 TW. The heat transport through Fram Strait that
1448 enters the Arctic Ocean then becomes 19 TW. If all this heat goes to ice melt by cooling the Atlantic
1449 water to the freezing point about 1 Sv of Atlantic water is converted to low salinity upper water. 7 Tw
1450 go to melting sea ice and 12 TW are lost to the atmosphere. This mean that 0.021 Sv of ice is melted
1451 and the salinity of the upper layer becomes 34.3.

1452 These values are realistic and agree with other estimates of the Arctic Ocean heat and
1453 freshwater balances (e.g., Rudels et al., 2015). It appears that the heat and the effects of the heat
1454 carried by the Atlantic water into and around the Arctic Ocean are less than commonly expected. The
1455 existence of strong warm inflow pulses of Atlantic water could perhaps alter this situation and



1456 increase the effects of the Atlantic inflow. However, the persistence of the high temperatures in the
1457 Atlantic inflow pulses as they circulate around the Arctic Ocean basins (Polyakov et al, 2005, 2011)
1458 rather indicates that the heat remains in the Atlantic layer and the heat is eventually returned to the
1459 North Atlantic through Fram Strait.
1460



1461

1462 Section 10 The Greenland Sea

1463 The Nordic Seas were early identified as a possible source area for the cold, dense deep waters of the
1464 oceans. Wyville-Thomson and Carpenter found cold, dense bottom water south of the Faroes, Mohn
1465 identified a cold, almost homogenous water column southeast of Jan Mayen, and Amundsen's
1466 observations from *Gjøa* in the Greenland Sea in 1901 showed a cold homogenous dome of water
1467 extending from the bottom almost reaching the surface (Nansen, 1906). However, Nansen (1912)
1468 judged that the deep convection observed in the Greenland Sea had little global impact and instead
1469 postulated that the bulk of the ocean deep water is formed farther south, in the Irminger Sea
1470 southeast of Greenland, or in the Labrador Sea.

1471 In the 1970s this view began to change. Satellite observations showed a polynya in the
1472 Weddell Sea ice cover 1977 to 1979 and hydrographic observations confirmed that the polynya was
1473 related to a cold, less saline water column indicating recent convection (Gordon, 1978). This
1474 stimulated a search for and studies of convection, or chimneys (Killworth, 1979), and in the
1475 Greenland Sea satellite observations showed several rapid events of ice formation and subsequent
1476 disappearance of sea ice, suggesting sinking of cold brine enriched surface water, which was replaced
1477 by upwelled warmer water, melting the ice.

1478 Convection occurs as small-scale short events in winter, usually during bad weather
1479 conditions making it difficult to observe and study. In the 1970s field experiments dedicated to
1480 convection studies were initiated in known convection sites, in the Mediterranean Sea and in the
1481 Labrador Sea, and in the 1980s and 1990s most observational and theoretical work in the Greenland
1482 Sea was concentrated to convection studies and many new techniques were introduced. At the same
1483 time the importance of the Greenland Sea convection for the formation of dense deep water that
1484 could drive the Atlantic meridional overturning circulation, or the global thermohaline circulation as
1485 it was then commonly called, was realized, and perhaps more urgent, what were the consequences,
1486 if the convection and deep water formation should weaken. In retrospect, in 2026, the three decades



1487 between 1980 and 2010 were decades when the largest known changes in the Greenland Sea
1488 convection occurred, and when our understanding of the deep water formation in the Arctic
1489 Mediterranean deepened.

1490 In the mid-20th century the principal sign of deep convection, a homogenous water
1491 column extending from the surface to the bottom, had not been observed in the Greenland Sea and
1492 the early observations by Mohn and Amundsen were not fully trusted because the instruments used
1493 then were not of the same quality as those deployed during the 1950s. Metcalf (1955) suggested a
1494 sloping descent of the dense water that would not be captured by vertical hydrographic casts but this
1495 idea was never really accepted. The water column in the central Greenland Sea had structure that
1496 appeared to be conserved, even if its deep and bottom waters were renewed. Generally, it consisted
1497 of a low salinity upper layer above a deep temperature maximum and further down a salinity
1498 maximum below which the temperature and salinity decreased with depth until the homogenous
1499 Greenland Sea bottom water was encountered. How could this structure be explained?

1500 Carmack and Aagaard (1973) suggested that the deep and bottom water formation
1501 was driven by double-diffusive transports through diffusive interfaces, Atlantic water circulating
1502 around the Greenland Sea gyre penetrates towards the center while losing heat upward to the colder
1503 surface water but retaining its high salinity. When it finally reaches the center of the gyre, its density
1504 has become high enough to renew the deep water and perhaps sink to the bottom. The fact that the
1505 convecting water is not in direct contact with the atmosphere could also explain the low oxygen
1506 content observed in the Greenland Sea deep water (Carmack and Aagaard, 1973). This idea was
1507 further developed by McDougall (1983), who found that the amount of dense water that could be
1508 created by this process corresponded well with existing estimates of deep water formation in the
1509 Greenland Sea.

1510 Deep convection areas are usually related to cyclonic circulation that forces the
1511 surface water towards the rim and allows the deeper layers at the center to rise as a dome towards
1512 the surface. A smaller volume of upper layer water must then be cooled before convection starts and



1513 the water column overturns more readily (Killworth, 1979, 1983). The smaller volume also allows for
1514 the possibility that the convection occurs in a filling box mode, where the upper layer density
1515 increases in winter, becomes unstable and convects to the bottom, bypassing the intermediate layers
1516 (Baines and Turner, 1969). The difficulty with this explanation, in contrast to e. g. brine rejection over
1517 the shelves, is that it is not possible to accumulate dense water at the surface. A Rayleigh number
1518 based on the ocean depth would directly make the water column unstable, and even with a Rayleigh
1519 number based on the penetration depth of the heat anomaly from the surface (Howard, 1967) no
1520 large positive anomaly could accumulate before convection starts.

1521 This fact and satellite observations showing an interplay between the ice tongue
1522 Odden and the ice free Nordbukta, suggesting rapid formation and melting of the ice cover in the
1523 central Greenland Sea, opened for the possibility that open ocean deep convection could be driven
1524 by ice formation (Rudels, 1986a). As the water is cooled to freezing temperature, ice will form and
1525 rise to the surface, leaving more saline water droplets behind. These droplets sink through and their
1526 excess salinity diffuses into the ambient upper layer. As the droplets eventually lose their salinity it is
1527 instead the ambient upper layer that has become saline and dense with respect to the underlying
1528 water and starts to convect. The density and thickness of the unstable layer can be estimated from
1529 how long it takes for the salinity anomaly to diffuse, using molecular diffusion coefficients, into the
1530 ambient water, and how fast the parcels sink, computed from Stokes' resistance law.

1531 The unstable upper layer then sinks as entraining plumes or thermals into the deep
1532 until the plumes reach their neutral density level, where they spread out. Convection, however,
1533 continues and the upper part of the water column becomes gradually denser until its density is high
1534 enough for the convection to penetrate still deeper. The transformed upper layer then convects into
1535 the deep and becomes replaced by warmer water from below that starts to melt the ice and the
1536 convection stops. If the cooling persists, the upper layer is again cooled to freezing temperature and
1537 ice starts to form, brine is rejected, and another convection cycle startsZX (Rudels. 1986a). Since it is
1538 cold water that convects, it is possible that the thermobaric effect, arising because cold water is

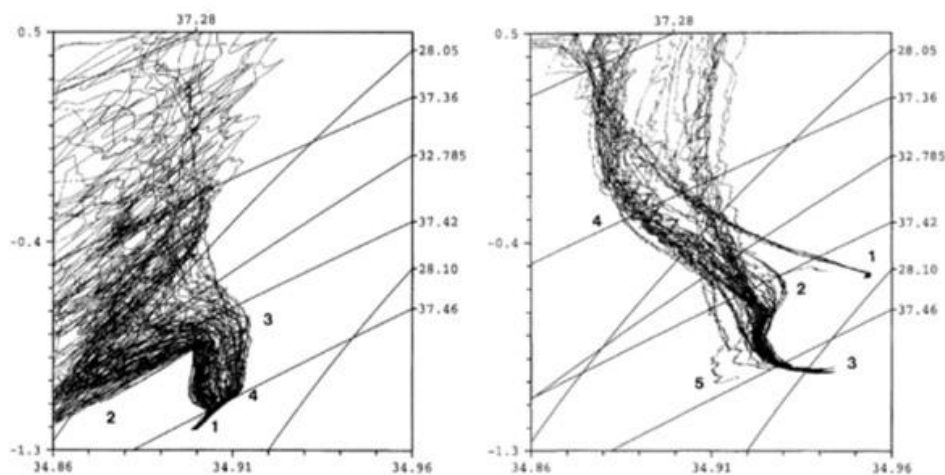


1539 more compressible than warm water, further increases the density of the plumes if the convection
1540 reaches sufficiently deep.

1541 This scenario is highly speculative, perhaps even controversial, and field studies were
1542 initiated in the Greenland Sea to capture at least some of the involved processes (Quadfasel and
1543 Rudels, 1990). During strong cooling and ice formation a sediment trap was deployed 0.5 m below
1544 the sea surface to capture the released brine droplets. The brine was collected in sample bottles in
1545 initially deflated plastic bags. The sampling interval was 40 minutes and seven samples were
1546 collected. To observe the buildup and ejection of the saline top layer a 25m long drifting tube with
1547 temperature and conductivity sensors at 2.5m and 22.5m was deployed. The experiment only lasted
1548 about six hours, but a gradual increase and a sudden lowering of the salinity was observed at the
1549 upper instrument but not seen at 22.5m. This perhaps could indicate a buildup and release of a
1550 salinity anomaly (Quadfasel and Rudels, 1990; Rudels and Quadfasel, 1991.).

1551 With the advent of the CTD the resolution and accuracy of the salinity and
1552 temperature measurements increased tremendously and unexpected details were observed in the
1553 Greenland Sea water column. θ_S structures on stations taken in the Greenland Sea in 1993 by *FS*
1554 *Valdivia* are shown in figure 12. The densest water is the Greenland Sea bottom water concentrated
1555 in a narrow θ_S range with temperature and salinity decreasing towards the bottom. Above the
1556 bottom water the salinity range increases with increasing temperature and two salinity maxima can
1557 be identified. The highest salinities are found over the Greenland continental slope, along the Jan
1558 Mayen Ridge and at the Mohn-Knipovich Ridge and the lowest at the center of the Greenland Sea
1559 gyre. This implies that saline deep waters are advected from north along the Greenland slope and
1560 become deflected eastward to circulate around the rim of the Greenland Sea.

1561



1562

1563 Figure 12. Left panel blow-up of θS curves from stations taken by *FS Valdivia* in 1993 in the
1564 Greenland Sea. The numbers indicate (1) Greenland Sea bottom water, (2) locally formed Arctic
1565 intermediate water, (3) intermediate temperature and salinity maxima, (4) deep salinity maximum.
1566 Right panel blow-up of θS curves from stations taken by *IB Oden* in the Arctic Ocean 1991. The
1567 numbers indicate (1) the deep and bottom water in the Makarov Basin, (2) the salinity maximum in
1568 the Eurasian Basin derived from the Amerasian Basin, (3) the salinity maximum of the Eurasian Basin
1569 deep water, (4) stations from the Amundsen Basin showing interleaving, (5) traces of Norwegian Sea
1570 deep water north of the Yermak Plateau (from Rudels, 1995).

1571

1572 The saline deep waters must ultimately arrive from the Arctic Ocean and Fig. 12 also

1573 shows θS curves from stations in the Arctic Ocean obtained by the icebreaker *Oden* in 1991. Two

1574 saline deep water modes are clearly seen. Warmer and saline deep and bottom water are observed

1575 in the Makarov Basin close to the Lomonosov Ridge. Some of this deep water crosses the sill (1800

1576 m) of the Lomonosov Ridge and enters the Amundsen Basin, where it can be identified as a salinity

1577 maximum around 1700m (Anderson et al., 1994; Björk et al., 2007). The deep and bottom waters

1578 formed in the Eurasian Basin are colder and denser but slightly less saline. The density of the

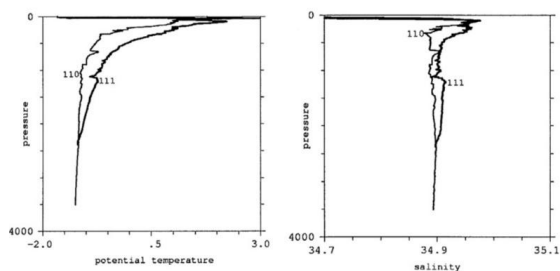
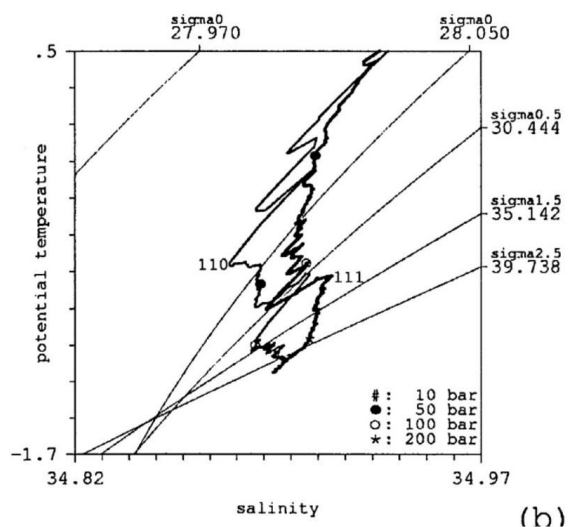
1579 Eurasian Basin Deep water corresponds well with the deeper salinity maximum observed in the

1580 Greenland Sea, while the density of the upper salinity maximum, also forming a deep temperature

1581 maximum in the central Greenland Sea, indicates the presence of the Amerasian Basin deep water.



1582 These observations show that the deep waters in the Arctic Mediterranean Sea are
1583 supplied by two sources. The open ocean convection area in the Greenland Sea supplying the colder,
1584 less saline endmember and the Arctic Ocean the saline, warmer endmember. The deep waters
1585 communicate through Fram Strait and depending on the regional climate, one or the other source
1586 will dominate (Aagaard et al., 1985; Rudels, 1986a).
1587



1588

1589 Figure 13. Potential temperature and salinity profiles and θS curves obtained in 1988 from *RV Lance*
1590 from stations over the Greenland continental slope. The stations show an isopycnal exchange of
1591 eddies between the slope and the central Greenland Sea (adapted from Rudels et al., 1999b).

1592

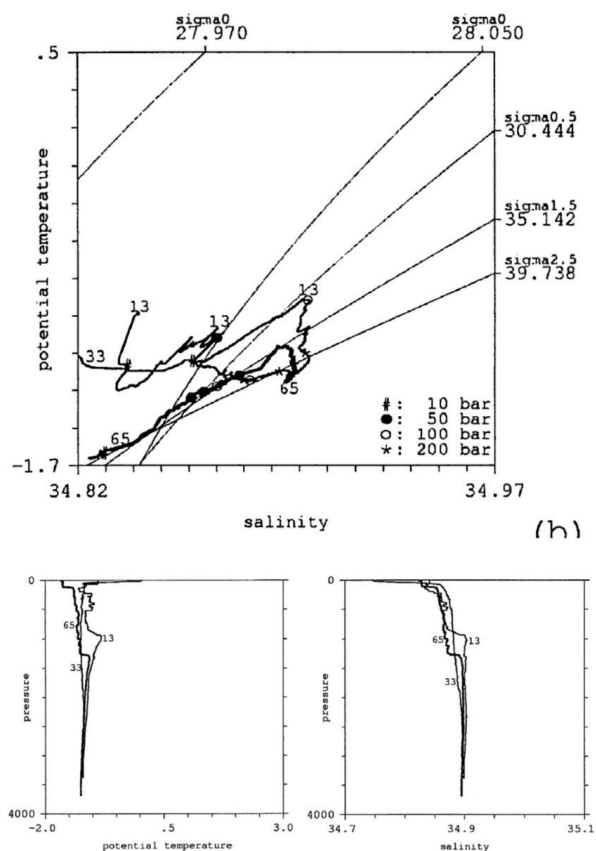
1593 The salinity maxima are weakest in the central part of the Greenland Sea as is seen in

1594 Fig. 13 taken by *RV Lance* 1988, where an eddy exchange between the center and the rim of the

1595 Greenland Sea is captured. The exchange is isopycnal and the profiles show the doming of the



1596 density field in the central Greenland Sea, shifting the water from the rim upwards and that from the
1597 center to deeper levels at the rim. It is thus likely that the saline Arctic Ocean deep waters that
1598 penetrate to the inner part of the Greenland Sea become diluted by the convection taking place
1599 there largely removing their temperature and salinity anomalies.
1600



1601

1602 Figure 14. Potential temperature and salinity profiles and $\theta\sigma$ curves obtained by *FS Valdivia* in 1988
1603 (65 and 33) and 1993 (13) in the central Greenland Sea, showing the evolution of the convection in
1604 during 1988 and the shallower convection observed in 1993 (adapted from Rudels et al., 1999b).

1605

1606 Figure 14 displays the potential temperature and salinity profiles and the $\theta\sigma$ curves of
1607 two stations taken in the center of the Greenland Sea in 1988, station 65 in February and station 33
1608 in June and a third station, 13, taken in 1993, all from *FS Valdivia*. The February station shows



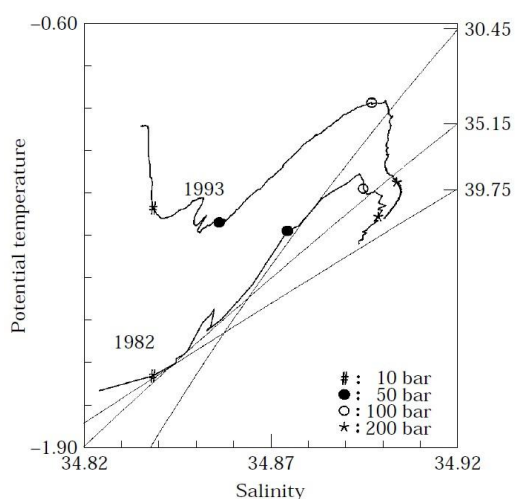
1609 convection deeper than 1000m and the formation of a homogenous, less saline layer covered by
1610 cold, low salinity surface water and located above a more saline deep layer. In June the profiles
1611 indicate that convection has continued and reached deeper than 2000m. The salinity in the upper
1612 1000m has increased and the salinity in the deeper part has decreased, implying that during late
1613 winter the upper layer density has increased and the two layers have been homogenized. The density
1614 of the low salinity surface layer has to increase, first by cooling to freezing temperature and if this
1615 not sufficient for convection, ice formation and brine rejection continue to increase the density to
1616 above that of the layer below, and the surface layer then convects. The density of the first layer
1617 below is then increased sufficiently for it to convect into the second deep layer below. The two layers
1618 then merge, forming a more than 2000 m deep, homogenous water column.

1619 Station 13 in Fig. 14 shows a warmer, more saline water column and deep coinciding
1620 temperature and salinity maxima. The convection here extends to the temperature maximum and
1621 the convected water forms a temperature minimum above the temperature maximum. The deeper
1622 salinity maximum has become more saline and the Greenland Sea bottom water salinity has
1623 increased. That the convection is shallower implies that the Arctic Ocean deep water will not be
1624 transformed in the central Greenland Sea and the deep salinity maxima become more prominent.
1625 This especially applies to the deeper maximum from the Eurasian Basin.

1626 Figure 15 shows two stations, one from 1982 taken by *RV Hudson* and one *Valdivia*
1627 station from 1993. The temperature and salinity of the deep salinity maximum have increased and
1628 also the Greenland Sea bottom water has become warmer and more saline. The salinity increase in
1629 the bottom water can only be caused by turbulent mixing from above and Meincke et al. (1997)
1630 estimated the vertical diffusion coefficient for the deep mixing in the Greenland Sea by assuming a
1631 balance by the lateral advection of Eurasian Basin deep water to the center of the gyre and the
1632 vertical mixing into the bottom water. The obtained mixing coefficient was surprisingly high, $\kappa_v \approx 3.7$
1633 $10^{-3} \text{ m}^2 \text{ s}^{-1}$. The renewal time for the deep salinity maximum was estimated to 6 years, corresponding
1634 to a through flow of 0.3 Sv. If the removal of the Greenland Sea bottom water, 0.2 Sv, is included 0.5



1635 Sv of deep water is exported from the Greenland Sea (Meincke et al., 1997). Later studies made by
1636 Somavilla et al. (2013) and Marnela et al. (2016) have indicated similar high vertical mixing
1637 coefficients.
1638



1639
1640 Figure 15. θ S curves from two stations taken 11 years apart from *RV Hudson*, 1982 and *FS Valdivia*
1641 1993.

1642 The changes in the Greenland Sea water column continued during the 1990s and a
1643 temperature maximum started to develop at mid depth (Budéus et al., 1998), indicating that the
1644 Amerasian Basin deep water penetrating towards the center of the Greenland Sea no longer was
1645 removed or weakened by mixing with convecting cold, less saline Arctic intermediate water. The
1646 water locally formed in winter has become less dense and only the water column above the
1647 temperature maximum is ventilated by convection. The temperature maximum, by contrast, is
1648 renewed by advection, locally from the Greenland slope but ultimately from the Arctic Ocean, which
1649 gradually increases its temperature. The temperature maximum also moved downwards in the water
1650 column (Budéus and Ronski, 2009), implying that the local convection, although less dense than the
1651 water of the temperature maximum, did not stop sinking when it reached its neutral density level.
1652 Instead, its layer thickness increased, indicating that it was pressing the underlying water column



1653 downwards, by continuity forcing the bottom water towards the rim and eventually to leave the
1654 Greenland Sea.

1655 This radically changed the density structure of the central Greenland Sea. Instead of
1656 displaying a dome of dense water reaching towards the surface the density surfaces formed a bowl
1657 depressed in the center and rising towards the rim. This change implies that the doming, which was
1658 earlier considered generated by wind forcing and a necessary preconditioning for convection
1659 (Killworth, 1983; Marshall and Schott, 1999) instead is a consequence of open ocean convection.
1660 When deep convection ceases, the doming cannot be maintained and the density surfaces relax.

1661 During this phase deep reaching cold, vertically almost homogenous anticyclonic
1662 vortices were observed in the Greenland Sea (Gascard et al., 2002; Wadhams et al., 2002). Their
1663 lateral extent was 10 to 15 km, close to the local Rossby radius, which prevented them from breaking
1664 up. The vortices reached deep (>2000 m) and penetrated into the temperature maximum. The upper
1665 part of the vortices was denser but their lower part less dense than the ambient water column. The
1666 vortices were, as the rest of the Greenland Sea, capped by a low salinity layer in summer. However,
1667 the large vertical extent of the vortices made this upper layer less thick and it would more rapidly
1668 become dense in winter and convect into the vortices, recharging them with dense water. This early
1669 started and confined convection could also be a cause for the deep vertical penetration of the
1670 vortices. The fact that the vortices were less dense than the ambient water between 1500 m and
1671 2000 m made them, however, unlikely candidates for a renewal of the Greenland Sea deep and
1672 bottom water, but they stand out as intriguing features in the water column. Vortices were observed
1673 during a 10 years period but then disappeared.

1674 In 1996 a tracer release experiment to study the convection was conducted in the
1675 central Greenland Sea. A cloud of Sulphur Hexachlorid was injected in the central gyre at the density
1676 surface $\sigma_{0.5} = 30.4268$ and its spreading and mixing were monitored during the following years
1677 (Watson et al., 1999). The first winter was one with comparably strong ice formation, which likely
1678 influenced the mixing of the tracer. Outside the gyre the tracer cloud only spread little vertically but



1679 in the gyre the tracer was redistributed vertically from the surface down to 1300 m. The highest
1680 tracer concentration was reduced and the maximum was shifted slightly upward.

1681 One interpretation of these changes is that cooling or ice formation and brine
1682 rejection created denser water at the surface that convected into the deep as entraining plumes that
1683 passed through the tracer cloud and redistributed the tracer to deeper levels. By mass continuity a
1684 compensating upward flow through the tracer cloud then brought tracer also to shallower levels. The
1685 one-dimensional convection model applied by Watson et al. (1999) agrees with this picture.

1686 With time the temperature of the cold Arctic intermediate water above the
1687 temperature maximum gradually increased and eventually it became higher than the temperature of
1688 Amerasian Basin water, which instead only was identified as a sharp salinity increase below the
1689 ventilated intermediate water. By mid 2010s the ventilated intermediate water had also become
1690 more saline than the Amerasian Basin water and its salinity maximum disappeared.

1691 This is a likely consequence of the increase in salinity and temperature of the upper
1692 layer in the Greenland Sea due to interaction with recirculating Atlantic water in the East Greenland
1693 Current, which counteracts the atmospheric cooling taking place in the central gyre (Latarius and
1694 Quadfasel, 2016). The salinity and temperature of the upper layer in the Greenland Sea are now the
1695 highest observed in the Greenland Sea water column. This has made the Greenland Sea similar to the
1696 Labrador Sea and the convection now resembles that of a gradual cooling and deepening of the
1697 upper layer in winter.

1698 The cold, less saline Greenland Sea bottom water has also disappeared and the θ_S
1699 characteristics of the bottom water are now those of the Eurasian Basin deep water (Marnela et al.,
1700 2016). The features of the water column that identified two competing sources of the deep water in
1701 the Arctic Mediterranean (Aagaard et al., 1985; Rudels, 1986a) have disappeared, and presently the
1702 Arctic Ocean source dominates and the Greenland Sea deep water is renewed by advection. If the
1703 Arctic Ocean source also have weakened, it has not yet been detected in the Greenland Sea because
1704 its larger reservoir in the Arctic Ocean. The cause behind these changes is likely the warming climate



1705 that no longer creates water dense enough to ventilate the deep Greenland Sea by open ocean

1706 convection.

1707



1708

1709 Section 11 Overflows.

1710 The Arctic Ocean and Greenland Sea deep waters are mostly confined to the Greenland Sea by the

1711 Jan Mayen fracture zone and the Mohn-Knipovich Ridge and contribute but little to the overflows.

1712 When the intensive studies of the Nordic Seas started in the 1970s and 1980s an outflow of

1713 Greenland Sea deep water to the Norwegian Sea was observed in the about 2200m deep channel in

1714 the Mohn Ridge just north of Jan Mayen. In the late 1990s this flow had changed direction and

1715 instead deep water from the Norwegian Sea entered the Greenland Sea, implying that the Greenland

1716 Sea deep water density had been reduced and that the deep pressure gradient had reversed

1717 (Østerhus and Gammelsrød, 1999). Since no deep water is formed in the Norwegian Sea, this

1718 indicated that water, earlier exported from the Greenland Sea, was returning. This situation probably

1719 persisted only a short period since, due to continuity, the deep water from the Arctic Ocean entering

1720 the Greenland Sea has to leave, either through gaps in the Mohn-Knipovich Ridge to the Norwegian

1721 Sea or return to the Arctic Ocean through Fram Strait.

1722 The deepest passage across the Greenland-Scotland Ridge to the North Atlantic is the

1723 Faroe Bank Channel (>840 m) and the densest deep water that enters the Norwegian Sea from the

1724 Greenland Sea must eventually exit the Arctic Mediterranean through this passage. For less dense

1725 water there is also the possibility of spillover across the 500 m deep ridge segment between Iceland

1726 and the Faroes. The Faroe Bank Channel is a continuation of the Faroe Shetland Channel and Fig. 16,

1727 showing bottom temperature and bottom salinities in the northeastern North Atlantic, reveals the

1728 narrowness of the channel and also the spillover of cold, less saline water across the Iceland-Scotland

1729 Ridge. Not all dense water that passes through the Faroe-Shetland Channel reaches the Faroe Bank

1730 Channel. Some less dense water continues south and crosses the Wyville Thomson Ridge and enters

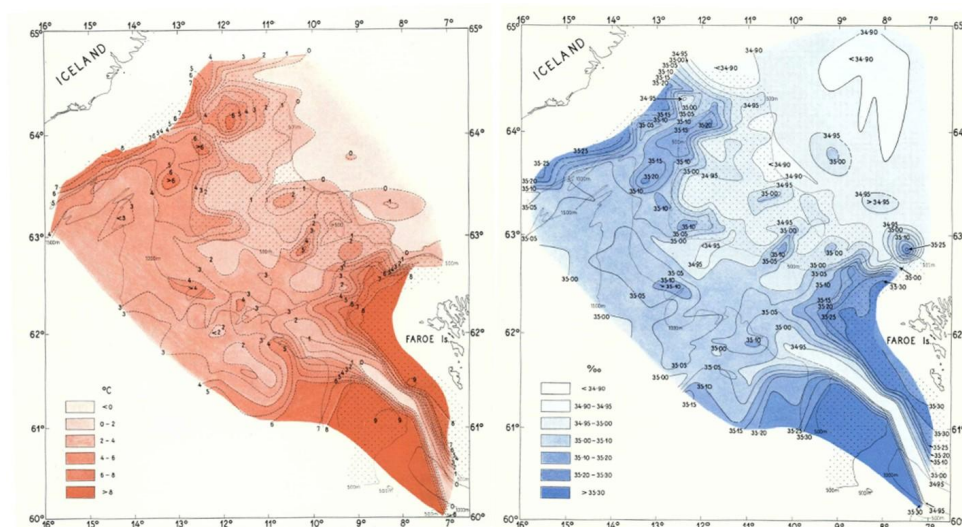
1731 the Rockall Basin. As the name of the ridge suggests, this is where Carpenter and Wyville Thomson

1732 first observed the cold water entering the Northeast Atlantic from the north.

1733



1734



1735

1736

1737 Figure 16. The bottom temperature (left) and salinity (right) distributions observed between Iceland
1738 and the Faroes during ICES's Overflow-60 experiment. Especially the cold and less saline water
1739 flowing through the Faroe Bank Channel is conspicuous compared to the cold water spilling over the
1740 Iceland Faroe Ridge and clearly reveal the narrowness of the channel (from Tait et al., 1967).

1741

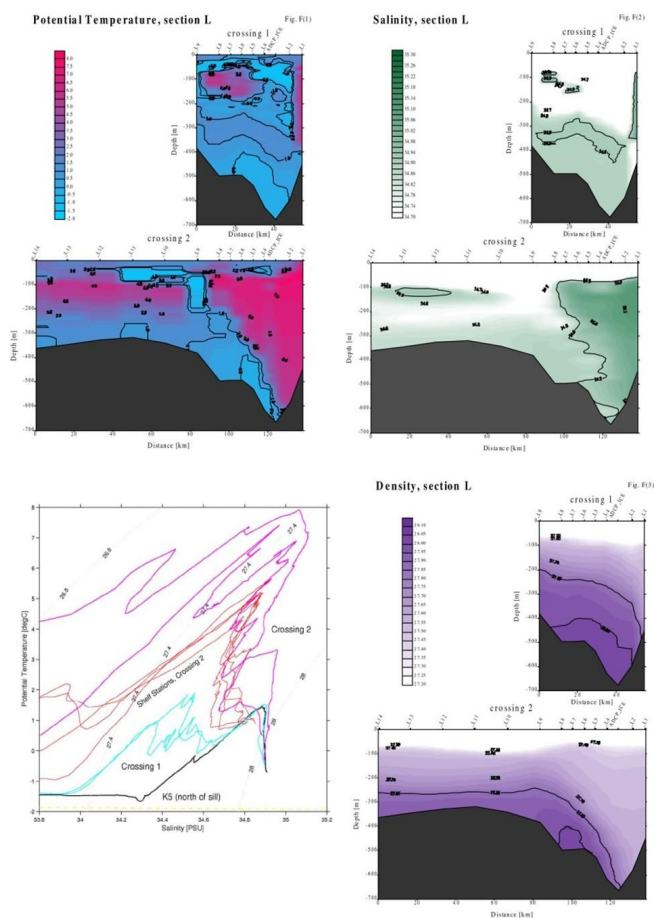
1742 Not all the overflow water from the Norwegian Sea derives from the Greenland Sea. A
1743 substantial fraction of the East Greenland Current that crosses the Jan Mayen Fracture Zone and
1744 enters the Iceland Sea continues eastward in the East Icelandic Current into the Norwegian Sea. The
1745 East Icelandic Current is deep, about 600 m, and carries not only low salinity surface water but also
1746 denser waters that especially contribute to the spillover across the Iceland-Faroe Ridge. In a drifter
1747 experiment with RAFOS floats with a drifting depth of 600m in the Iceland Sea all of the floats
1748 deployed east of the Kolbeinsey Ridge moved southeastward into the Norwegian Sea, and also some
1749 deployed west of Kolbeinsey Ridge entered the Norwegian Sea. However, most of the floats
1750 deployed west of the ridge either exited through Denmark Strait or grounded on the northwestern
1751 Icelandic shelf (De Jong et al., 2017).



1752 The eastern overflow entrains strongly the ambient waters and as the overflow
1753 reaches its neutral density level the overflow volume has more than doubled. The overflow water
1754 moves toward the equator but when it reaches the Gibbs Fracture Zone in the Mid-Atlantic Ridge it
1755 splits and some, maybe the major part, leaves the Iceland Basin and enters the Irminger Basin and
1756 then moves north towards Iceland. The initial low temperature and salinity characteristics of the
1757 eastern overflow has rapidly been removed and it has attained a potential temperature between 2°C
1758 and 3°C and a salinity around 34.925.

1759 The western overflow in Denmark Strait is more complicated. It is not a deep, almost
1760 stagnate reservoir that gradually drains south over a sill, but instead a region where several current
1761 branches and water masses converge. The upper part of the East Greenland Current that passes over
1762 the sill depth of the Jan Mayen Fracture Zone (1700m) comprises not only low salinity Polar water,
1763 but also Arctic Atlantic and denser intermediate waters from the Arctic Ocean, as well as warm and
1764 saline Atlantic water recirculating in Fram Strait and Arctic Intermediate waters created in and
1765 exported from the Greenland Sea. There is also the recently discovered North Icelandic Jet roughly
1766 following the 600m isobath on the northern Iceland shelf westward to Denmark Strait (Jónson and
1767 Waldimaron, 2004). In addition, the warm and saline North Icelandic Irminger Current enters the
1768 Denmark Strait from the south. The sill depth in Denmark Strait is 640m, but the deep channel is
1769 narrow and waters from north and south contend for space and passage. Changes take place from
1770 one week to the next and Fig. 17 shows two sections along the sill taken by *RV Aranda* one week
1771 apart. On the first section waters from the north dominates, on the second water from the south.
1772 The second section extended farther towards Greenland because of favorable ice conditions (Rudels
1773 et al., 1999).

1774



1775

1776 Figure 17. Potential temperature, salinity and potential density sections from two crossings between
1777 Greenland and Iceland along the sill in Denmark Strait taken one week apart. The θS diagram shows
1778 the θS curves from the two crossings, the first crossing in cyan and the second crossing in red and
1779 magenta. (The figure is adapted from Rudels et al., 1999c).

1780

1781 Overflow water is commonly defined as water with potential density above 27.8 and
1782 the second section shows that waters with density above 27.8 are present on the shelf, which implies
1783 that even when the North Iceland Irminger Current dominates in the deep channel the overflow, or
1784 at least part of it, could instead take place over the shelf and then sink down the continental slope
1785 into the Irminger Basin. However, the East Greenland Current is not the only source of overflow
1786 water. In fact, the densest water crossing the sill is supplied by the North Icelandic Jet. The jet has
1787 been traced eastward towards its unknown source area and it is observed along the entire northern

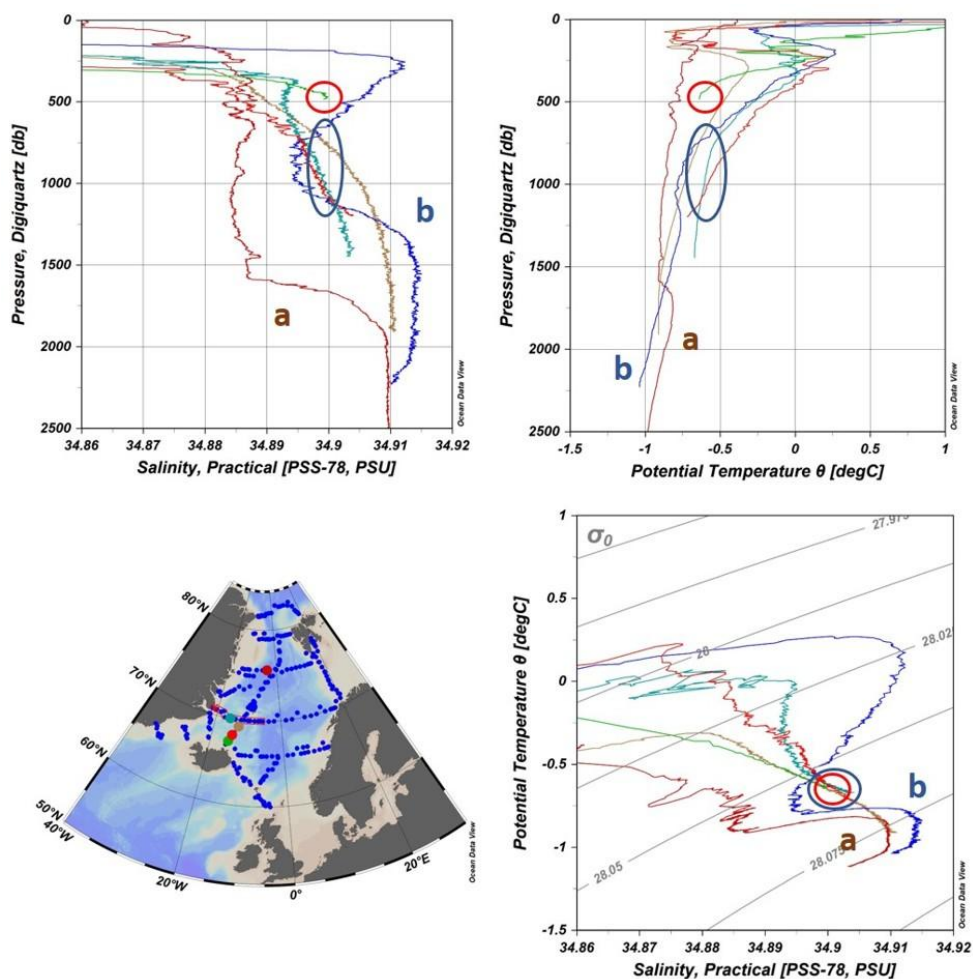


1788 shelf break (Våge et al., 2011). Våge et al. (2011) suggested that the water of the North Icelandic Jet
1789 is supplied by two sources, the first would be the cooling of the North Icelandic Irminger Current as it
1790 flows eastward on the shelf. The second contribution would come from mixing with the denser water
1791 in the interior of the Iceland Basin as the cooled water returns towards Denmark Strait, further
1792 increasing its density. The problem with this explanation is that the atmospheric cooling observed in
1793 the area is not strong enough to create the observed θ_S properties of the jet (Segtman et al., 2011;
1794 Latarius and Quadfasel, 2016). Furthermore, the seasonal convection in the Iceland Sea is usually
1795 limited to the upper 200 m and only in the northern part of the Iceland Sea does the winter mixed
1796 layer occasionally attain the θ_S observed in the North Icelandic Jet (Våge et al., 2015).

1797 That the formation of dense water in the Iceland Sea in winter and its subsequent
1798 export in summer and fall was the main process supplying the Denmark Strait overflow was proposed
1799 by Swift et al. (1980) and Swift and Aagaard (1981) as an alternative to the cooling of the Atlantic
1800 water in the Norwegian Sea and its recirculation in Fram Strait and export in the East Greenland
1801 Current suggested by Worthington (1970). However, Mauritzen (1996a, 1996b) did not find any
1802 strong seasonality of the overflow, which speaks against seasonal sources in the central basins of the
1803 Nordic Seas and rather indicates a steady flow, which could be supplied by the gradually cooled
1804 Atlantic water returning to the North Atlantic through Denmark Strait.

1805 Waters with the θ_S characteristics of the deepest overflow are present in the northern
1806 Iceland Sea and in the East Greenland Current. These θ_S properties are, however, observed at much
1807 deeper levels, 750m to 1500m, than the about 500m depth, where the core of the North Icelandic Jet
1808 is found. Moreover, it is likely that these waters are formed farther north and have been advected
1809 across the Jan Mayen Fracture Zone to the Iceland Sea. If the East Iceland Current transports a major
1810 part of the upper 600m of the water column to the Norwegian Sea, the deeper levels might, if they
1811 are advected southward, ascend to shallower depth as they approach the Iceland Continental slope
1812 and then feed the North Icelandic Jet (Fig. 18; Rudels, 2021).

1813



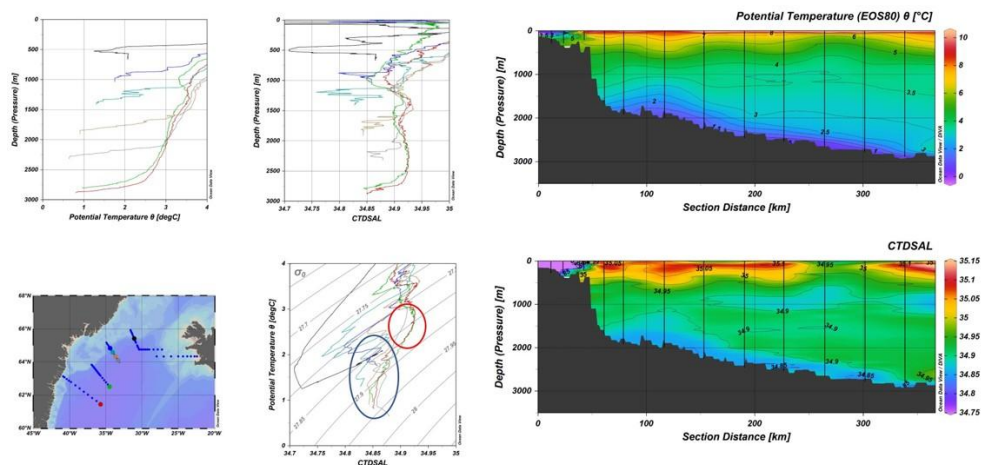
1814

1815

1816 Figure 18. Profiles of potential temperature and salinity and θ S curves from stations in the Iceland
 1817 Sea and the Greenland Sea. The green station (red circles) found at 480 m depth at the Iceland slope
 1818 has similar θ S properties as the densest overflow and also properties akin to those observed below
 1819 750 m and still deeper on stations farther north in the Iceland Sea, indicated by blue ellipses. These
 1820 properties are located at deeper levels, if a warmer Atlantic layer also is present, suggesting that it is
 1821 pushed downward by the Atlantic water. The θ S curves from these stations have similar shape as the
 1822 upper Polar deep water (temperature decreasing and salinity increasing with depth), but are colder
 1823 and located lower in the θ S diagram. The θ S properties could be created by mixing between the
 1824 upper Polar deep water and the less saline and colder Arctic Intermediate water formed in the
 1825 Greenland Sea. However, the smooth θ S curves do not indicate recent interleaving and mixing but
 1826 rather suggest long residence time and slow renewal. Stations a and b shows the difference between
 1827 the central gyre and the southern rim of the Greenland Sea. The observations are from from RV
 1828 *Knorr* 2002 (Figure from Rudels, 2021).



1829 As a curiosity, the deep salinity maxima shown in Fig. 18 derive from the Jan Mayen
1830 Fracture Zone (blue station) and the central Greenland Sea (red station) and have about the same
1831 density, but the maximum at the station at the rim is located at shallower depth than the maximum
1832 at the station in the central Greenland Sea. This implies that the convection in the Greenland Sea has
1833 compressed the underlying water column, creating the deep part of a bowl, which then rises towards
1834 the rim. These stations were taken in 2002, when the Greenland Sea convection had become
1835 shallower, and it should be compared with the stations in Fig. 13 in section 10, taken in 1988, when
1836 the denser water is found at shallower levels in the center than at the rim.
1837



1838

1839

1840 Figure 19. Potential temperature and salinity profiles and ΘS curves from the Greenland slope south
1841 of Denmark Strait. The sections show the overflow as a cold, less saline bottom layer, the warm
1842 Irminger Current in the upper layer and the presence of the more saline and warmer Iceland-
1843 Scotland overflow water below 2000 m. The profiles and the ΘS curves reveal the downstream
1844 evolution of the overflow properties, especially the low salinity lid but also the difference between
1845 the two overflows, the Iceland-Scotland overflow indicated by red ellipse and the Denmark Strait
1846 overflow by blue ellipse in the ΘS diagram (data from *RV Alexander von Humboldt* 2004) (Figure from
1847 Rudels, 2021).

1848

1849

1850

The overflow plume in Denmark Strait is stratified. It comprises a cold, $< -0.5^{\circ}\text{C}$,
bottom layer with salinity ≈ 34.9 below a temperature and a salinity maximum of 2°C and 34.91



1851 respectively, and it is capped by a salinity minimum, a low salinity lid (Figure 19). As the plume leaves
1852 the sill its bottom temperature increases rapidly to above 0°C but remains below 1°C even when the
1853 plume has descended deeper than 3000m in the Irminger Sea, and the low salinity lid is present
1854 almost as deep. The initial rapid increase in bottom layer temperature suggests that a direct mixing
1855 between the overflow water and the northward flowing North Iceland Irminger Current takes place
1856 already at the sill in Denmark Strait. There the deepest and densest part of the overflow becomes in
1857 almost direct contact with the warm and saline Irminger Current water, and the observed increase in
1858 plume temperature could result from a mixing ratio of 1 to 4, significantly less than the estimated
1859 entrainment for the Faroe Bank overflow.

1860 The temperature minimum and the low salinity lid, by contrast, must derive from the
1861 Greenland shelf, where waters of the observed properties are found. The fact that especially the low
1862 salinity lid survives as the plume descends deeper than 2000m also indicates that the entrainment of
1863 ambient water through the upper boundary of the plume is weak. However, the low salinity lid
1864 suggests that if the less dense water can remain in contact with the densest part of the plume in the
1865 early stages, when it starts to descend the slope, it will remain attached to the plume and sink into
1866 the deep. One factor that can facilitate the descend of the cold low salinity upper part of the plume is
1867 the thermobaric effect, which increases the relative density of colder water as the pressure
1868 increases.

1869 If the dense water that flows southward on the Greenland shelf reaches the shelf
1870 break farther south, where the shelf narrows, the entrainment appears to be stronger and the
1871 plumes will remain on the upper part of the slope and not connect to the deeper overflow. This
1872 appears to be the case for the Greenland spill jet, identified by the density surfaces rising towards
1873 the shelf, which indicates velocities increasing with depth (Pickart et al., 2001). It flows as a separate
1874 core above the deep overflow plume towards Cape Farewell and eventually the density surfaces
1875 flatten and the spill jet disappear (Pickart et al., 2001). As the Denmark Strait plume descends it sinks



1876 through the overflow water from the Faroe Bank channel that shows up as a salinity maximum above
1877 the colder, less saline Denmark Strait overflow. Both overflows then continue to the Labrador Sea.

1878 The overflows contribute together with the dense water formed by open ocean
1879 convection in the Labrador Sea to the North Atlantic deep water and to the Atlantic Overturning
1880 Circulation. The overturning circulation has been monitored since 2004 by the RAPID-MOCHA
1881 (Meridional Overturning Circulation and Heat-flux Array) array deployed at 26°N. One of the
1882 drawbacks with this array is that it is located too far south to separate the overturning circulation,
1883 sinking into the deep, from the horizontal recirculation of cooled upper water in the subtropical gyre.
1884 An additional array, OSNAP (Overturning in the Subpolar North Atlantic Program), located north of
1885 the subtropical gyre has therefore been proposed and accepted, and the first deployment was in
1886 2014. The array extends from Scotland to Greenland (OSNAP east) and from Greenland to Labrador
1887 (OSNAP west). The first deployment ended in 2016 and when the results from the first 20 months
1888 were published (Lozier et al., 2019) the title “A sea change in our view of overturning in the subpolar
1889 North Atlantic” suggests that the results, at least for some of the researchers involved, have come as
1890 a surprise. The convection and dense water formation in the Labrador Sea contributes, as estimated
1891 by the OSNAP west array, but little, 2.1 ± 0.3 Sv, to the overturning circulation. By contrast the
1892 transformation to denser water measured by the OSNAP east array was 15.6 ± 0.8 Sv, almost an
1893 order of magnitude larger. Since some recirculation takes place, the measured total overturning is
1894 somewhat less, 14.9 ± 0.9 Sv.

1895 For those who have been working in the Arctic Mediterranean Sea and on the
1896 exchanges across the Greenland-Scotland Ridge these numbers are not surprising and should also be
1897 familiar to those remembering L.V. Worthington’s 1976 monograph on the North Atlantic circulation.
1898 The observations made during the NA CLIM project (North Atlantic CLIMate) indicated an overflow of
1899 5.8 Sv (Østerhus et al., 2019). Assuming a doubling of the volume due to entrainment into the
1900 plumes and some contribution from the spill jet the numbers almost match.



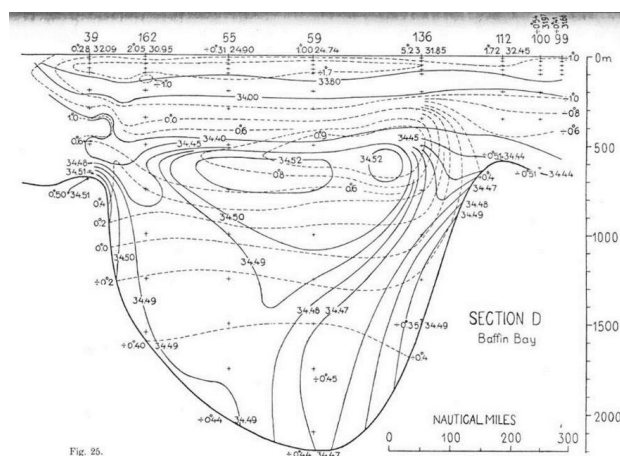
1901 The small volume of Atlantic deep water formed in the Labrador Sea comes as a
1902 surprise though. It suggests that seasonal deep convection is not a process that creates and drives an
1903 overturning circulation. It rather forms MODE waters than deep water (McCartney, 1977; McCartney
1904 and Talley, 1982). To create the dense water that supplies the overturning circulation, a sill and an
1905 isolated basin might be required. This would inject water with substantially higher density that can
1906 sink down and entrain ambient water, creating a significant volume of deep water with distinct
1907 properties. The fact that also the much weaker Mediterranean overflow shows up in and
1908 characterizes the Atlantic water column over a large region suggests that this could be the case.

1909 Observations from the RAPID array indicates a reduction of the overturning circulation
1910 by 2.5 Sv in 2009. The weaker overturning has persisted but no further reduction has been observed
1911 (Bryden et al., 2020). The reduction has, surprisingly, taken place in the denser part of the
1912 overturning circulation, which is supplied by the overflow from the Arctic Mediterranean. During the
1913 same time the EU projects THOR (ThermoHaline Overturning at Risk) and NACLIM were running and
1914 no reduction was observed, not in the overflows, nor in the northward inflows of Atlantic water to
1915 the Arctic Mediterranean.

1916 The RAPID array showed that reduction of the overturning circulation was
1917 compensated by an increase in the recirculation in the subtropical gyre by 2.5 Sv, about 15% of the
1918 overturning circulation. This implies that less warm Atlantic water is transported by the North
1919 Atlantic drift to the subpolar gyre, which leads to a cooling of the northeast Atlantic. This might break
1920 the warming trend in the Atlantic water that has prevailed almost two decades from the mid-1990s.
1921



1922 Section 12: Polar outflows and the Canadian Arctic Archipelago and Baffin Bay
1923 The water leaving the Arctic Mediterranean Sea consists not only of dense overflow water but also of
1924 cold, less saline and less dense polar water that interacts with the upper part of the subpolar North
1925 Atlantic. There are two main, but interacting, outflows, the outflow of Polar Water through Fram
1926 Strait in the East Greenland Current that follows the Greenland shelf and coast southward through
1927 Denmark Strait to Cape Farewell, and the polar water that flows through the narrow and shallow
1928 passages in the Canadian Arctic Archipelago to Baffin Bay and then continues through Davis Strait to
1929 the Labrador Sea. These two flows interact. A part of the East Greenland Current turns north after it
1930 has rounded Cape Farewell and forms the West Greenland Current, which enters Baffin Bay from the
1931 south. The upper, polar, part of West Greenland Current mixes with the outflows from Nares Strait,
1932 Jones Sound and Lancaster Sound and the mixing product is transformed by ice formation during
1933 winter into a distinct, about 200 m deep upper layer with temperature of -1.6°C and salinity of 33.7
1934 (Fig. 20).
1935



1936
1937
1938 Figure 20. Temperature (dotted lines) and salinity (full lines) sections taken by *Godthaap* 1928 in
1939 Baffin Bay from Davis Strait (left) to Smith Sound (right), showing the cold upper layer, the
1940 intermediate temperature and salinity maxima and the cold, slightly less saline bottom water (from
1941 Riis-Karstensen, 1936).

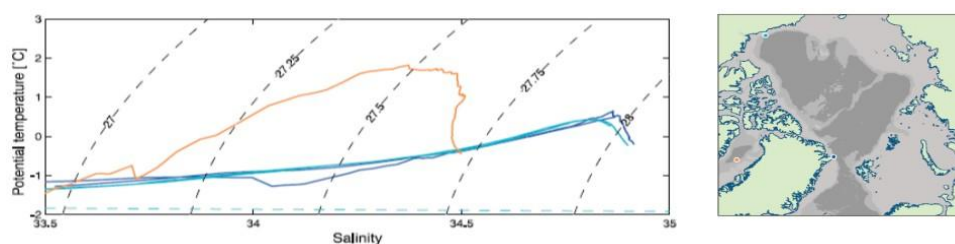


1942

1943 Below the low salinity upper water, a warm, 3-4°C, but rather fresh, 34.5-34.6, Atlantic
1944 layer is present. The Atlantic water enters Baffin Bay through Davis Strait in the West Greenland
1945 Current and the low salinity indicates that it was originally a part of the Irminger Current that has
1946 been diluted by cold, low salinity water from the East Greenland Current south of Denmark Strait.

1947 The bottom water in Baffin Bay is again colder, about -0.45°C with salinity 34.45. The
1948 origin of the Baffin Bay bottom water has been debated, Sverdrup et al. (1942) considered it to be a
1949 mixture between Labrador Sea water and Baffin Bay surface water, and local formation by
1950 convection was suggested by Bourke and Paquette (1991). Bailey (1956) found TS characteristics at
1951 sill depth north of Nares Strait similar to those of the Baffin Bay bottom water and proposed that
1952 bottom water entered from the Arctic Ocean. Figure 21 shows the TS curves from one station in
1953 Baffin Bay and two stations from the Arctic Ocean, one from the continental slope in the Canada
1954 Basin and the other from the slope northeast of Greenland, indicating that the Baffin Bay bottom
1955 water could derive from the Arctic Ocean.

1956



1957

1958

1959 Figure 21. TS curves from Baffin Bay (yellow) and from north of Canada (cyan) and north of
1960 Greenland (blue), showing that the Baffin Bay bottom water could derive from the Arctic Ocean
1961 (from Rudels et al., 2004).

1962

1963 The TS curves also show the warm but less saline characteristics of the Baffin Bay
1964 Atlantic water compared to the Arctic Atlantic water to the north. They also, interestingly, indicate
1965 that the entrainment of ambient water into the deep inflow must be small. If the inflow entrains



1966 much, it will become warmer, which reduces its density. This, in turn, requires a denser initial inflow.
1967 However, that would also mean a warmer inflow, which would lead to different TS characteristics in
1968 the Baffin Bay bottom water.

1969 To determine the export of low salinity polar water by direct current measurements is
1970 difficult. Drifting ice and bad weather conditions complicate not only the deployment and recovery
1971 but also the survival of the moorings. Since one primary object is to determine the freshwater fluxes,
1972 it is essential to obtain measurements close to the surface and the ice, where most of freshwater is
1973 located. In spite of these difficulties measurements of volume and freshwater fluxes have been
1974 made, at least for shorter periods, in all the major passages; Lancaster Sound (Peterson et al.,2012),
1975 Jones Sound (Cardigan Strait and Hells Gate) (Melling et al., 2008), and Nares Strait (Münchow et al.,
1976 2008) in the Canadian Arctic Archipelago, in Davis Strait (Curry et al., 2011, 2014), and on the shelf
1977 area east of Greenland (De Steur et al., 2009; De Steur et al., 2016). The techniques used in the
1978 different passages are distinct and adapted for the local challenges such as the presence of sea ice
1979 and the closeness to the magnetic North Pole that complicates the direction measurements. Details
1980 of these observations are given in Melling et al. (2008) and in Rudels (2021).

1981 The difficulty to perform field observation, especially for monitoring purpose, makes it
1982 tempting to use existing simple models to estimate the transports of Polar water through the
1983 different passages. One approach follows Werenskiold (1935), who derived an expression for the
1984 geostrophic transport M in a coastal current based only on the depth of the upper layer at the coast,
1985 H_1 , and the density difference $(\rho_2 - \rho_1)$ between the upper layer and the lower layer at rest, which
1986 extends to the surface one Rossby Radius away from the coast.

1987

1988
$$M = \frac{(\rho_2 - \rho_1)gH_1^2}{2f\rho_2} \quad (4)$$

1989



1990 The density in cold Arctic waters is mainly controlled by salinity and can be written as $\rho = \rho_r(1 + \beta S)$,
1991 where ρ_r is the reference density and β the coefficient of salt contraction. Taking the density of the
1992 lower layer as the reference density the reduced gravity ρ' becomes $g\beta(S_2 - S_1)$.

1993 There are three straits that are wider than the Rossby Radius and can transport at full
1994 capacity, Fram Strait, Lancaster Sound and Nares Strait. The total transport through these passages
1995 comprises the liquid freshwater added to the water column by rivers and by the low salinity Pacific
1996 inflow and the entrained lower layer water M_2 . The Pacific inflow is here separated into freshwater
1997 and lower layer water. This gives:

1998

$$1999 \quad M_2 + F = \frac{3g\beta(S_2 - S_1)}{2f} \quad (5)$$

2000

2001 The salinity of the upper layer becomes $S_1 = FH_1/(M_2 + F)$, where F is the freshwater input. The
2002 freshwater fraction in the upper layer, m , can then be written as:

2003

$$2004 \quad m = \frac{(S_2 - S_1)}{S_2} = \frac{FH_1}{(M_2 + F)} = \left(\frac{2fF}{3g\beta S_2}\right)^{\frac{1}{2}} \quad (6)$$

2005

2006 And the total outflow becomes:

2007

$$2008 \quad (M_2 + F) = \left(\frac{3g\beta F}{2f}\right)^{\frac{1}{2}} H_1 \quad (7)$$

2009

2010 The Rossby Radius Ro is independent of the entrainment and only depends on the freshwater input:

2011

$$2012 \quad Ro = \frac{[g\beta(S_2 - S_1)H_1]^{\frac{1}{2}}}{f} = \left(\frac{2g\beta S_2 F}{3f^3}\right)^{\frac{1}{4}} \quad (8)$$

2013



2014 The Rossby radius is about 10 km, which confirms that both Lancaster Sound and Nares Strait are
2015 wide enough to transport with full capacity.

2016 If we assume that the depth H_1 is the same in all channels and equal to the depth of
2017 the upper layer in the Arctic Ocean, the liquid freshwater storage in the Arctic Ocean can be
2018 estimated. Introducing $g = 9.83 \text{ ms}^{-2}$, $f = 1.4 \times 10^{-4} \text{ s}^{-1}$, $\beta = 8 \times 10^{-4}$, $F = 0.20 \times 10^6 \text{ m}^3 \text{ s}^{-1}$ and setting S_2 equal
2019 to 35 and the salinity of sea ice to zero the liquid freshwater storage becomes 8.24 m. The area of
2020 the Arctic Ocean is $10 \times 10^{12} \text{ m}^2$ and with a freshwater input of 0.2 Sv the residence time becomes 13
2021 years, or half of this if only the deep part of the Arctic Ocean is considered. The freshwater storage
2022 increases as $F^{1/2}$ but its residence time decreases as $F^{-1/2}$ (Rudels, 2010).

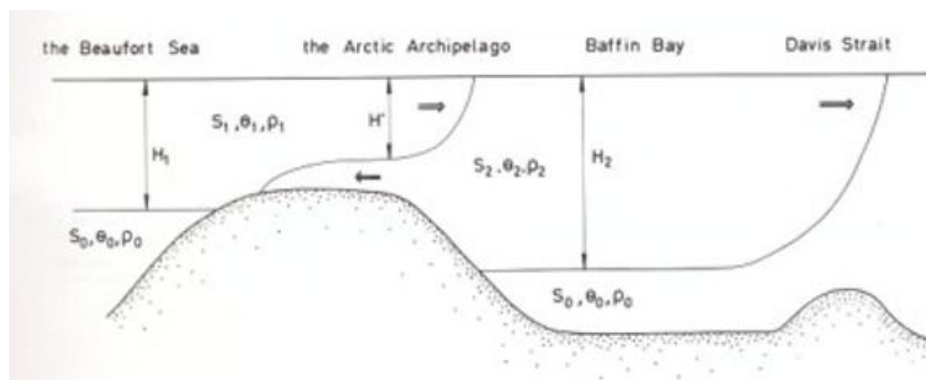
2023 The thickness of the ice cover was in the 1960s estimated to 3 m, about one third of
2024 the liquid freshwater storage, but had decreased by almost 50% by the 1990s (Rothrock et al., 1997),
2025 and if the ice export $F_i = 0.9 \text{ Sv}$, remains constant, its residence time is between 2.6 and 5.3 years
2026 depending upon the area considered. If only a seasonal ice cover were present and no sea ice were
2027 exported the liquid freshwater storage would increase to a little above 10 m (Rudels, 2010). The
2028 liquid freshwater in the Arctic Ocean is, however, not a lid lying on top of a deeper water mass but is
2029 distributed over a large, spatially varying, depth range in the Arctic Ocean water column. The
2030 conditions in the three passages are also not equal. Especially the characteristics of the second layer
2031 differ between the passages, which affects the transports of both volume and freshwater.

2032 The second passageway from the Arctic Ocean to the North Atlantic, the Canadian
2033 Arctic Archipelago and Baffin Bay, offers additional challenges but also other opportunities to
2034 theoretically estimate the transports. The geostrophic transports depend upon the number of
2035 openings (Stigebrandt, 1981) and two passages, Lancaster Sound and Nares Strait, transport Polar
2036 water from the Arctic Ocean to Baffin Bay. In addition, the West Greenland Current carries water,
2037 ultimately from Fram Strait and the Arctic Ocean, into Baffin Bay from the south. These inflows have
2038 to exit through one opening, Davis Strait, to the Labrador Sea.



2039 The outflow from the Arctic Ocean is ultimately due to the higher sea level in the
2040 Arctic Ocean, which implies that the upper layer in Baffin Bay must be denser than that in the Arctic
2041 Ocean and its depth should be greater than the depth of inflows to Baffin Bay. There will be a
2042 pressure reversal in depth in Baffin Bay, below which the pressure gradient forces the Baffin Bay
2043 water to enter the inflow channels. The water from Baffin Bay does not enter the Arctic Ocean but it
2044 forms a lower boundary below the inflows that is taken as the depth of the transports to Baffin Bay.
2045 The depth and density of the Baffin Bay upper layer determine the geostrophic transport out of
2046 Baffin Bay, which should balance the inflows. The Arctic Ocean is connected to the deeper layers in
2047 Baffin Bay through Fram Strait and across the sills of the Greenland-Scotland Ridge and Davis Strait,
2048 removing any deep pressure gradient (Figure 22).

2049



2050

2051

2052 Figure 22. Idealized three reservoir system representing the Beaufort Sea, the Canadian Arctic
2053 Archipelago, Baffin Bay, Davis Strait and Labrador Sea system (from Rudels, 1986b).

2054

2055 Assuming that the temperature and salinity of the Baffin Bay upper layer are -1.6°C
2056 and 33.7, the upper layer depth in Baffin Bay can be found, and the geostrophic transports through
2057 the system can be determined as functions of the Polar water salinity (Rudels, 1986b). The transports
2058 decrease with increasing salinity of the Polar water, since the density difference between the layers
2059 then is reduced.



2060 However, the characteristics of the Baffin Bay upper layer are not due only to the
2061 mixing between the entering waters but also influenced by the cooling and ice formation taking place
2062 in winter. The cooling and the ice formation only depend on the atmospheric forcing and are
2063 independent of the inflows, and a higher salinity of the entering Polar water would require an
2064 increased transport into Baffin Bay to reproduce the observed salinity of the Baffin Bay upper water.

2065 Since one estimate gives a transport decreasing with increasing salinity and the other
2066 an increasing transport with increasing salinity, a salinity must exist for which these transports are
2067 equal. This salinity is then set as the salinity of the Polar water leaving the Arctic Ocean. The Polar
2068 outflow, the freshwater export, and the ice export through the Canadian Arctic Archipelago-Baffin
2069 Bay system can then be determined (Rudels, 1986b). However, the outflow estimate obtained by this
2070 approach, 0.7 Sv, was lower than the 2 Sv then commonly cited. One serious weakness of this
2071 approach is that it requires a residence time for the Polar water in Baffin Bay of at least one year for
2072 the transformation into the Baffin Bay upper layer to take place. Especially the inflow through
2073 Lancaster Sound that enters close to Davis Strait may pass through Baffin Bay into the Labrador Sea
2074 in a time shorter than one year.

2075 The expected change into a warmer climate has brought melting of the Greenland ice
2076 cap into focus. Intensified melting has been observed in the Jacobhavn isbrae in Baffin Bay, but also
2077 the low salinity East Greenland Coastal Current (Sutherland and Pickart, 2007), flowing on the
2078 Greenland shelf inshore of the East Greenland Current, indicates that freshwater is supplied from
2079 Greenland as runoff and as ice melt. This freshwater input, either directly to Baffin Bay and/or
2080 advected through Davis Strait into Baffin Bay, will lower the salinity of the upper layer in Baffin Bay.

2081 The density contrast between the Polar water and the Baffin Bay upper layer then
2082 diminishes and the transport through the Archipelago becomes smaller. The expected increase in
2083 mass and freshwater fluxes from the Arctic Ocean to the North Atlantic in a warmer climate, might
2084 then not take place through the Canadian Arctic Archipelago. Instead, much of this increased outflow

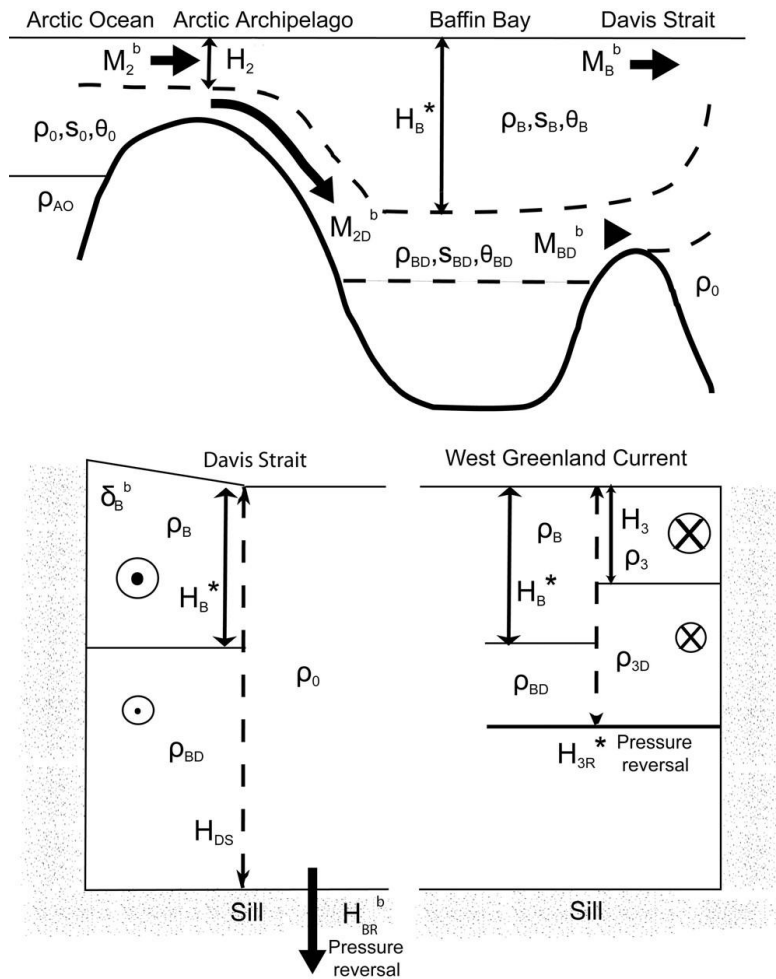


2085 could be channeled through Fram Strait, which might affect the dense water formation and
2086 convection both in the Greenland Sea and in the Irminger and Labrador seas (Rudels, 2011).

2087 It should be noted that in Rudels (2011) the ice formation and ice export are
2088 computed from the mass and salt balances in Baffin Bay using the postulated salinity of the Baffin
2089 Bay upper layer. It is then not independent of the inflow salinities. This in contrast to the approach in
2090 Rudels (1986b), where the ice formation was considered due to the atmospheric heat loss and
2091 unrelated to the salinities of the transports. It could then be used, together with the salinity of the
2092 upper layer, to determine the salinity of the Polar water entering Baffin Bay. The author appears, 25
2093 years later, to have forgotten this aspect.

2094 The Baffin Bay water column comprises not only transformed Polar water but also
2095 Atlantic water advected from the south and cold deep and bottom waters originating in the Arctic
2096 Ocean. These waters must eventually leave Baffin Bay, which requires a deep circulation in Baffin Bay
2097 that has not, so far, been considered. Rudels (2011) tried to theoretically estimate this deep
2098 circulation and how it relates to the upper layer exchanges by assuming that the inflows of upper
2099 water through the northern channels and in the West Greenland Current, now considered as part of
2100 the Polar inflow, are shallower than the depth of the pressure reversal. This allows for inflows from
2101 the deeper layers to Baffin Bay. Furthermore, the pressure reversal between the Arctic Ocean and
2102 Baffin Bay does not occur in Baffin Bay but in the Labrador Sea, below the sill depth in Davis Strait.
2103 The pressure head due to the higher sea level in the Arctic Ocean is thus not removed in Baffin Bay
2104 and it forces not only a deep inflow in the north but also a deep outflow to the Labrador Sea. The
2105 pressure reversal in the West Greenland Current, by contrast, occurs above the sill depth and the
2106 deep Atlantic inflow recirculates in Baffin Bay and then exits through Davis strait together with, but
2107 above, the outflow of the deep waters from the Arctic Ocean (Fig. 23).

2108



2109

2110

2111 Figure 23. Drawing showing the inflow of Polar surface water M_2^b and denser water M_{2D}^b through
 2112 Nares Strait and the outflow of upper layer water M_B^b and intermediate water M_{BD}^b through Davis
 2113 Strait for the barotropic case. The depth of the upper layer H_3 and the depth of the pressure reversal
 2114 H_{3R}^* in the West Greenland Current. The depth of the H_B^* and the sill depth H_{DS} in Davis Strait. The
 2115 depth of the pressure reversal in the Davis Strait outflow H_{BR}^b is located below the sill depth. δ_B^b
 2116 indicates the barotropic sea level difference between Baffin Bay and the Labrador Sea δ_3 is the
 2117 density of the upper layer and δ_{3D} is the density of the intermediate layer in the West Greenland
 2118 Current, δ_{BD} is the density of the intermediate layer in Baffin Bay and ρ_0 is the density of the Labrador
 2119 Sea water and of the deep inflow through Nares Strait. ρ_{AO} is the density of the deeper layer in the
 2120 Arctic Ocean.

2121



2122 The deep inflows decrease with increasing salinity of the Polar water, but the deep
2123 outflow through Davis Strait increases with the salinity of the Polar water. This implies that there is a
2124 salinity, 33.2 in this case, of the Polar water for which the deep exchanges in Baffin Bay are balanced.
2125 The deep outflow from the Arctic Ocean, taking place in the deepest channel, Nares Strait is 0.62 Sv,
2126 which is almost as large as the upper layer outflow of 0.77 Sv. The added barotropic pressure
2127 gradient also increases the outflow of Polar water from the Arctic Ocean to the North Atlantic and
2128 the total outflow through the Canadian Arctic Archipelago- Baffin Bay system becomes about 2.2 Sv,
2129 somewhat larger than the about 1.5 Sv presently determined from observations (e.g., Curry et al.,
2130 2014). For details of this theoretical approach the reader is referred to Rudels, (1986b, 2011).
2131

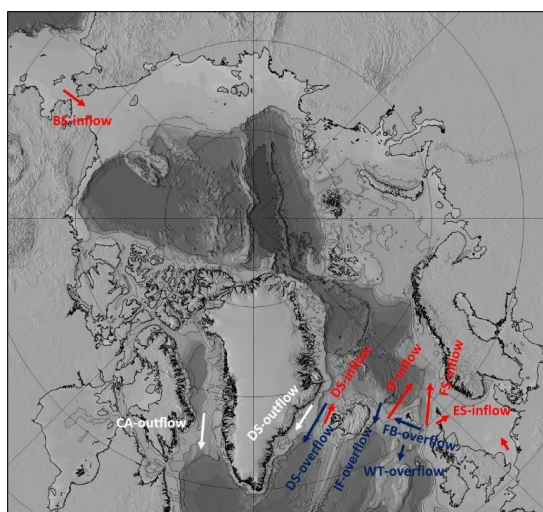


2132 Section 13. The Subpolar gyre

2133 All waters that circulate around the Arctic Mediterranean eventually flow south, entering the
2134 subpolar gyre in the North Atlantic. For most waters it is a return to where they started as warm,
2135 saline Atlantic inflows crossing the Greenland-Scotland Ridge. Only the Pacific inflow is added to the
2136 water entering the subpolar gyre from the north. We may remark here that in spite of the Pacific
2137 inflow bringing low salinity water to the Arctic Mediterranean, it supplies a net input of salt to the
2138 Atlantic Ocean that crosses the equator and is exported to Southern Ocean.

2139 The Atlantic water entering the Arctic Mediterranean becomes transformed in many
2140 ways by several different processes but, essentially, it is separated into denser and less dense waters
2141 by cooling and by receiving or rejecting freshwater, mainly through sea ice melting or sea ice
2142 formation. Waters that return to the North Atlantic either as dense overflows or buoyant outflows.

2143



2144

2145

2146 Figure 24: Map showing the volume balance of the Arctic Mediterranean Sea. BS: Bering Strait inflow,
2147 DS: Denmark Strait inflow, IF: Iceland-Faroe inflow, FS: Faroe-Shetland inflow, ES: European shelf
2148 inflow, CA: Canadian Arctic Archipelago outflow, DS: Denmark Strait outflow, DS: Denmark Strait
2149 overflow, IF: Iceland Faroe overflow, FB: Faroe Bank overflow, WT: Wyville Thomson overflow
2150 (adapted from Østerhus et al., 2019).

2151



2152 Østerhus et al. (2019) compiled the measured volume transports through all different
 2153 control sections to find if the volume fluxes balance (Figure 24 and Table 1). They found an inflow of
 2154 9.1 Sv and an outflow of 9.5 Sv, the exchange being almost in balance. However, an imbalance of 0.1
 2155 Sv would in one year lead to a sea level change in the Arctic Mediterranean of 0.2 m. This is more
 2156 than that observed and indicates that the direct current measurements may still be improved.
 2157

2158 Table 1: Inflows, outflows and overflows in the different passages of the Arctic Mediterranean (based
 2159 on Østerhus et al. 2019).

2160

Branch and abbreviation	Period yyyy/mm-yyyy/mm	months	Gaps Months	Transport Sv	Sd(Sv)
Inflows					
Denmarks Strait, DS-inflow	1994/10-2015/12	250	5	0.9 ± 0.1	0.3
Iceland-Faroe, IF-inflow	1993/01-2015/12	276	0	3.8 ± 0.5	0.6
Faroe-Shetland, FS inflow	1993/01-2015/12	276	0	2.7 ± 0.5	1.1
European shelf, ES-inflow	1993/01-2015/12	276	0	0.6 ± 0.2	0.3
Bering Strait, BS-inflow	1997/08-2013/12	197	0	0.9 ± 0.1	0.4
Overflows					
Denmark Strait, DS-overflow	1996/05-2015/12	218	18	3.2 ± 0.5	0.4
Iceland-Faroe, IF-overflow	NA			0.4 ± 0.3	
Faroe Bank, FB-overflow	1995/12-2015/12	206	35	2.0 ± 0.3	0.3
Wyville Thomson, WT-overflow	2006/05-2013/05	61	24	0.2 ± 0.1	0.1
Surface outflows					
Can.A.Arch., CA-outflow	2004/100-2010/09	72	0	1.7 ± 0.2	0.7
Denmark Strat, DS-outflow	2011/09-2012/07	11	0	2.0 ± 0.5	0.5
Runoff and precipitation					
Freshwater input, freshwater	NA			0.2	

2161

2162 However, what do not balance are the freshwater transports. Haine et al. (2015)
 2163 estimated the freshwater storage in the Arctic Mediterranean in two periods, between 1980 and
 2164 2000 and between 2000 and 2010 (Table 2) and discussed the reason for the changes. What is clear,
 2165 is that the adjustment time for the baroclinic pressure field is much longer than that for the
 2166 barotropic pressure field. Perhaps it will never really be in balance.



2167

2168 Tabell 2: Storage of liquid freshwater and sea ice in the Arctic Ocean and transports of liquid
 2169 freshwater and sea ice through the main gateways of the Arctic Ocean (adapted from Haine et al.
 2170 2015).

2171

Period	1980 – 2000	2000 – 2010
Freshwater reservoirs (km ³)		
Liquid freshwater	93000	101000
Beaufort Gyre	18500	23500
Average sea ice cover	17800	14300
Total freshwater volume	110800	115300
Freshwater fluxes (km ³ a ⁻¹ /mSv)		
Runoff	3900 ± 390 / 123.57 ± 12.36	4200 ± 420 / 133.08 ± 13.31
Bering Strait (liquid)	2400 ± 300 / 76,045 ± 9.51	2500 ± 100 / 79.21 ± 3.17
Bering Strait (sea ice)	140 ± 40 / 4.44 ± 1.27	140 ± 40 / 4.44 ± 1.27
P – E	2000 ± 200 / 63.37 ± 6.34	2200 ± 220 / 69.71 ± 6.97
Greenland flux	330 ± 20 / 10.46 ± 0.63	370 ± 25 / 11.72 ± 0.79
Davis Strait (liquid)	-3200 ± 320 / -101.39 ± 10.14	-2900 ± 190 / -91.89 ± 6.02
Davis Strait (sea ice)	-160 ± ? / -5.07 ± ?	-320 ± 45 / -10.14 ± 1.43
Fram Strait (liquid)	-2700 ± 530 / -85.55 ± 16.79	-2800 ± 420 / -88.72 ± 13.31
Fram Strait (sea ice)	-2300 ± 340 / -72.88 ± 10.77	-1900 ± 280 / -60.20 ± 8.87
Barents Sea Opening	-90 ± 90 / -2.85 ± 2.85	-90 ± 90 / -2.85 ± 2.85
Fury and Hecla straits	-200 ± ? / -6.34 ± +	-200 ± ? / -6.34 ± ?
Total fluxes (km ³ a ⁻¹ /mSv)		
Inflow sources	8800 ± 530 / 278.83 ± 16.79	9400 ± 490 / 297.85 ± 15.53
Outflow sinks	-8700 ± 700 / -275.67 ± 22.18	-8250 ± 550 / -261.41 ± 17.43
Residual	100 ± 900 / 3.17 ± 28.52	1200 ± 730 / 38.02 ± 23.13

2172

2173 Of the Atlantic water about 6 Sv are transformed to dense overflow water while
 2174 slightly more than 2 Sv become less dense water that together with the Pacific water make up the
 2175 outflow waters (Østerhus et al, 2019). The overflow water sinks into the deep and eventually joins
 2176 the southward moving deep western boundary, but the outflow circulates in the upper part of the
 2177 subpolar gyre and will influence the upstream conditions of the inflows to the Arctic Mediterranean.

2178 The most conspicuous northern input to the subpolar gyre was the “Great Salinity
 2179 Anomaly” observed in the late 1960s and early 1970s (Dickson et al., 1988). The outflow of low
 2180 salinity water and ice through Denmark Strait strongly reduced the salinity in the gyre and the

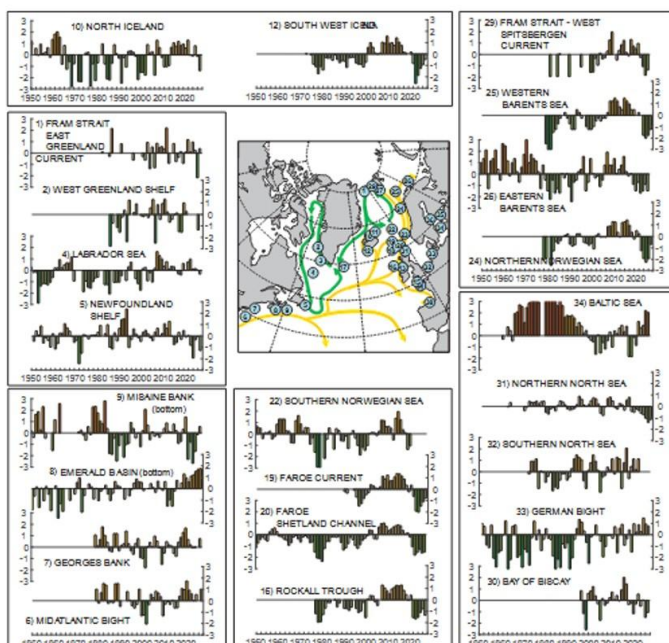
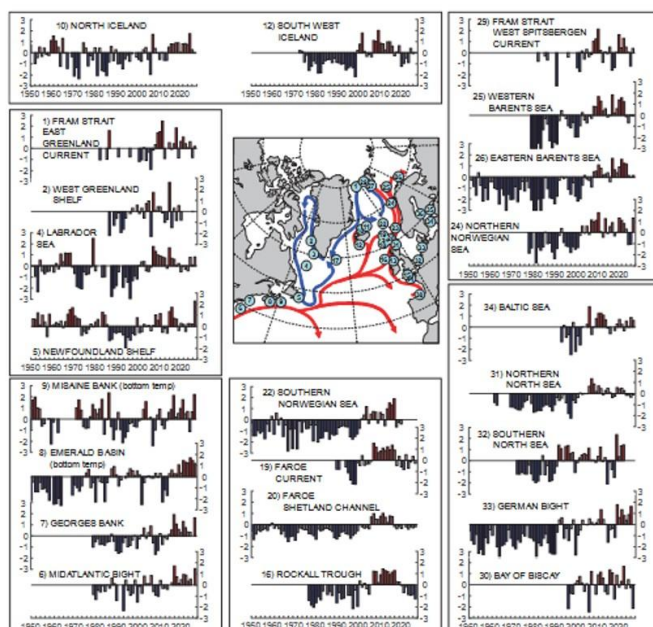


2181 anomaly could be traced around the subpolar gyre and the into the Nordic Seas at least as far as
2182 Fram Strait (Dickson et al.,1988).

2183 Up to the mid-1990s the surface waters in the subpolar gyre were colder and less
2184 saline than their average temperature and the same conditions prevailed in the Nordic Seas and the
2185 Barents Sea (Figure 25). In the late 1980s to the mid-1990s the North Atlantic Oscillation (NAO) index
2186 (the air pressure difference between the Azores and Iceland) was high and positive, and the cold
2187 continental air that dominated over the Labrador Sea led to a strong and deep convection and the
2188 created Labrador Sea water was exceptionally cold and fresh (Lazier et al., 2002). The cooling of the
2189 Labrador Sea increased the circulation of the subpolar gyre, which extended far to the east and partly
2190 prevented warmer water from the subtropical gyre to enter the Nordic Seas. The high NAO index was
2191 also manifested in the changes in the Barents Sea and in the Arctic Ocean, where the river runoff was
2192 diverted farther to the east, from the Amundsen Basin to the Makarov Basin.

2193 As the NAO index eventually became lower the subpolar gyre relaxed and retreated,
2194 leaving a freer passage for the waters of the North Atlantic Drift to reach the Greenland-Scotland
2195 Ridge and enter the Nordic Sea (Hátún et al, 2005; Häkkinen et al., 2008). After this a period of
2196 almost 15 year of warm, saline surface water was observed in the subpolar gyre and in the Nordic
2197 Seas and the Barents Sea (Fig. 25).

2198



2199

2200 Figure 25. Positions of the ICES Report of Ocean Climate (IROC) standard surface temperature
 2201 anomaly and salinity anomaly time series, and some selected temperature and salinity time series.
 2202 The anomalies are from the long term mean temperature and salinity at the location (from González-
 2203 Pola et al., 2023).



2204

2205 The North Atlantic drift splits as it approaches the European continent and one part
2206 turns south and remains in the subtropical gyre. The simpleminded picture would be that it is the
2207 southernmost branch that turns south, but observations from floats launched in the upper 15 m
2208 indicated that most of the floats turned south and instead the deeper layers, around 300 m and
2209 deeper, enter the subpolar gyre (Brambilla and Talley, 2006; Burkholder and Lozier, 2011). On its
2210 path towards the Nordic Seas the water from the subtropical gyre is also cooled and freshened by
2211 mixing with the low salinity upper layers of the subpolar gyre flowing eastward from the Labrador
2212 Sea (Burkholder and Lozier, 2011).

2213 In 2009 the RAPID Array at 26 °N showed an increase of 2.5 Sv in the southward
2214 recirculation of the North Atlantic Drift (Smeed et al., 2014). This would reduce the warm water
2215 inflow to the subpolar gyre and less warm water would enter the Norwegian Sea. This change
2216 probably ended or at least contributed to the end of the 20 years period of warm surface water in
2217 the subpolar gyre (Fig. 25).

2218 In 2012 a strong freshening of the subpolar gyre was observed, the strongest on in 120
2219 years (Holliday et al., 2020). This freshening appears to be different from the one associated with the
2220 Great Salinity Anomaly in that it originated in a rerouting of the circulation of the low salinity
2221 Labrador Current. Instead of moving south around Newfoundland, it was detached from the
2222 continental slope and joined the subpolar gyre circulation eastward. This low salinity signal has
2223 continued northward, into the Barents Sea and to Fram Strait (Fig. 25). If this freshening, taking place
2224 at least in the surface water, will imply a stronger stability of the Arctic Ocean water column and
2225 perhaps limit the vertical mixing in the Arctic Ocean and possibly affect the ice-ocean interactions,
2226 remains to be seen.

2227 The atmospheric circulation patterns and the wind fields thus strongly influence the
2228 circulation into and out of the Arctic Mediterranean Sea, but are they also the main causes for the
2229 overturning circulation? The overturning requires that the northward flowing water becomes denser



2230 and sinks into the deep. Moreover, it also appears to require a sill that allows the convection to build
2231 up a reservoir of dense water and also create a density difference between the deep waters on the
2232 two sides of the ridge. As the dense water crosses the ridge, the density difference allows it to
2233 accelerate and entrain ambient water, practically doubling its volume. This is different from the deep
2234 convection in the Labrador Sea that increases its depth and its density only gradually and marginally
2235 relative to the underlying waters. This might be the main reason for the small contribution from the
2236 Labrador Sea to the overturning circulation.

2237 The formation of dense water in the Arctic Mediterranean also provides a constant,
2238 but perhaps weaker and often less obvious forcing than the wind driven circulation. The dense
2239 outflowing water has to be replaced, when the sea level starts to become lower, if not before. The
2240 outstanding question is: Can the processes in the Arctic Mediterranean produce enough dense, and
2241 dense enough, water in the future? If the convection does not reach to the bottom, it will create
2242 stagnant conditions in the deep basins, but as long as intermediate waters are formed, still denser
2243 than the waters in the subpolar gyre, and the pressure head at the sill is present, the overturning
2244 circulation should be maintained. A large input of freshwater to the Greenland Sea, either from the
2245 Arctic Ocean or from ice melting on Greenland, could strongly affect the convection in the Greenland
2246 Sea (Stigebrandt, 1985). Only the cooling of the Atlantic water in the Norwegian Sea and the
2247 unknown rate of deep water formation in the Arctic Ocean would then remain as sources of dense
2248 overflow water, but that might be sufficient, as it has been assumed before.
2249



2250 References:

- 2251 Aaboe, S. and Nøst, A.: A diagnostic model of the Nordic Seas and the Arctic Ocean Circulation:
2252 Quantifying the effects of a variable bottom density along a sloping topography,
2253 Journal of Physical Oceanography, 38, 2685-2703, doi:10.1175/2008JPO3862.1, 2008
- 2254 Aagaard, K.: On the deep circulation in the Arctic Ocean. Deep Sea Research, 27, 251-268, 1980
- 2255 Aagaard, K., Coachman, L.K., Carmack, E.C.: On the halocline of the Arctic Ocean. Deep-Sea Research
2256 28, 529-545, 1981.
- 2257 Aagaard, K., Swift, J.H., Carmack, E.C.: Thermohaline circulation in the Arctic Mediterranean Seas.
2258 Journal of Geophysical Research 90, 4833-4846, 1985.
- 2259 Anderson, L.G., Björk, G., Holby, O., Jones, E.P., Kattner, G., Koltermann, K.-P., Liljeblad, B., Lindegren,
2260 R., Rudels, B., Swift, J.H.: Water masses and circulation in the Eurasian Basin: Results
2261 from the Oden 91 Expedition, Journal of Geophysical Research 99, 3273-3283, 1994.
- 2262 Bailey, W. B.: On the origin of Baffin Bay Deep Water, J.Fish. Res. Board Can, 13(3), 303–308, 1956.
- 2263 Baines, W. D. and Turner, J.S.: Turbulent buoyant convection from a source in a confined region. J.
2264 Fluid Mech. 37, 289-306, 1969.
- 2265 Bent, S.: Upon the Thermal paths to the Pole, St. Louis Mercantile Library Association, St Louis, 1872.
- 2266 Bjerknes, V.F.K.: Über die Bildung von Cirkulationsbewegungen und Wirbeln in reibungslosen
2267 Flüssigkeiten, Videnskabselskabets Skrifter I. Matematisk – Naturvidenskabelig Klasse
2268 No.5, 29 pp, 1898a
- 2269 Bjerknes, V.F.K.: Über einen hydrodynamischen Fundamentalsatz und seine Anwendung besonders
2270 auf die Mechanik der Atmosphäre und des Weltmeeres. Kungliga Svenska Vetenskaps-
2271 Akademiens Handlingar 31 (4), 35 pp, 1898b.
- 2272 Bjerknes, V.F.K. 1901.: Circulation relative zu der Erde. Öfversigt af Kungliga Vetenskaps-Akademiens
2273 Förhandlingar 58 (10), 739-757, 1901.
- 2274 Björk, G., Winsor, P.: The deep waters of the Eurasian Basin, Arctic Ocean: geothermal heat flow,
2275 mixing and renewal, Deep-Sea Res. I 53, 1253-1271, doi:10.1016/j.dsr.2006.05.006,
2276 2006.
- 2277 Björk, G., Anderson, L.G., Jakobsson, M., Antony, D., Eriksson, B., Eriksson, P., Hell, B., Hjalmarsson,
2278 S., Janzen, T., Jutterström, S., Linders, J., Löwemark, L., Marcussen, C., Olsson, K.A.,
2279 Rudels, B., Sellén, E., Sølvsten, M.: Flow of Canadian Basin Deep Water in the Western
2280 Eurasian Basin of the Arctic Ocean, Deep Sea Res. I, 57, 577-586,
2281 doi:10.1016/j.dsr.2010.01.006, 2010.
- 2282 Björk, G., Jakobsson, M., Rudels, B., Swift, J.H., Anderson, L.G. Darby, D.A. Backman, J., Coakley, B.,
2283 Winsor, P., Polyak, L., Edwards, M.: Bathymetry and deep-water exchange across the
2284 central Lomonosov Ridge at 88°-89°N. Deep Sea Research I, 54, 1197-1208
2285 doi:10.1016/j.dsr.2007.05.010, 2007.
- 2286 Bourke, R.H. and Paquette, R.G.: Formation of Baffin Bay bottom and deep waters, in Chu, P.C. and
2287 Gascard, J.-C. (eds.), Deep convection and deep water formation in the oceans. Pp.
2288 135–155. Amsterdam: Elsevier, 1991.
- 2289 Brambilla, E., Talley, L.D. : Surface drifter exchange between the North Atlantic subtropical and
2290 subpolar gyres, Journal of Geophysical Research 111, C07026,
2291 doi:10.1029/2005JC003146, 2006.



- 2292 Bryden, H.L., Johns, W.E., King, B.A., McCarthy, G., McDonagh, E.L., Moat, B.I., Smeed, D.A.:
2293 Reduction in ocean heat transport at 26°N since 2008 cools the eastern subpolar gyre
2294 of the North Atlantic Ocean, *J. Clim.*, **33**, 1677–1689, (doi:10.1175/JCLI-D-19-0323.1),
2295 2020.
- 2296 Burkholder, K.C., Lozier, M.S.: Mid-depth Lagrangean pathways in the North Atlantic and their impact
2297 on the salinity of the eastern subpolar gyre, *Deep-Sea Research I*, 58 (12), 1196-1204,
2298 doi:10.1016/j.dsr.2011.08.007, 2011
- 2299 Budéus, G., Schneider, W., Krause, G.: Winter convection events and bottom water warming in the
2300 Greenland Sea, *Journal of Geophysical Research*, 103, 18513-18527, 1998.
- 2301 Budéus, G. and Ronski, S.: An integral view of the hydrographic development in the Greenland Sea
2302 over a decade, *The Open Oceanography Journal*, 3, 8-39, 2009.
- 2303 Carmack, E.C. and Aagaard, K.: On the deep water of the Greenland Sea, *Deep-Sea Research*, 20, 687-
2304 715, 1973.
- 2305 Carmack, E.C., Williams, W.J., Zimmermann, S.L.: The Arctic Ocean warms from below. *Geophysical
2306 Research Letters* 39, L07604, 2012.
- 2307 Carpenter, W.B.: On the Gibraltar Current, the Gulf Stream, and the general oceanic circulation,
2308 *Proceedings of the Royal Geographical Society*, 15, 54-88, 1871.
- 2309 Coachman, L.K. and Aagaard, K.: Physical oceanography of the arctic and subarctic seas, In: Herman,
2310 Y. (Ed), *Marine geology and oceanography of the arctic seas*, Springer Verlag, New
2311 York, pp. 1-72, 1974.
- 2312 Coachman, L.K., Aagaard, K., Tripp, R.: Bering Strait: The regional physical oceanography, Univ. of
2313 Washington Press, Seattle, 172 pp., 1975.
- 2314 Croll, J.: Climate and time in their geological relations: A theory of secular changes of the earth's
2315 climate, Appleton, New York, XVI + 577 pp., 1875.
- 2316 Curry, B., Lee, C.M., Petrie, B.: Volume, freshwater, and heat fluxes through Davis Strait, 2004-2005,
2317 *Journal of Physical Oceanography* 41, 429-436, doi:10.1175/2010JPO4536.1, 2011.
- 2318 Curry, B., Lee, C.M., Petrie, B., Moritz, R.E., Kwok, R.: Multi-year volume, freshwater and heat
2319 transports through Davis Strait 2004-2010, *Journal of Physical Oceanography*. 44,
2320 1244-1266, 2014.
- 2321 De Jong, M.F., Sjøiland, H., Bower, A.S., Furey, H.H.: The subsurface circulation of the Iceland Sea
2322 observed with RAFOS floats, *Deep-Sea Research I*, 141, 1-10,
2323 <https://doi.org/10.1016/j.dsr.2018.07.008>, 2017.
- 2324 De Steur, L., Hansen, E., Gerdes, R., Karcher, M., Fahrback, E. Holfort, J.: Freshwater fluxes in the East
2325 Greenland Current: a decade of observation, *Geophysical Research Letters*, 36 (23),
2326 L23611, <http://dx.doi.org/10.1029/2009GL041278>, 2009.
- 2327 De Steur, L., Pickart, R.S., Macrander, A., Våge, K., Harden, B., Jónsson, S., Østerhus, S., Valdimarsson,
2328 H.: Liquid freshwater transport estimates from the East Greenland Current based on
2329 continuous measurements north of Denmark Strait, *Journal of Geophysical Research:
2330 Oceans*, 122, doi:10.1002/2016JC012106, 2016.
- 2331 Dickson, R.R., Meincke, J., Malmberg, S.-A. Lee, A.J.: The "great salinity anomaly" in the northern
2332 North Atlantic, 1968-1982, *Progress in Oceanography*, 20, 103-151, 1988.



- 2333 Dickson, R.R., Rudels, B., Dye, S., Karcher, M., Meincke, J., Yashayaev, I.: Current estimates of
2334 freshwater flux through the Arctic and Subarctic seas, *Prog. Oceanogr.*, 73, 210-230,
2335 doi:10.1016/j.pocean.2006.12003, 2007.
- 2336 Dickson, R.R., Meincke, J., Rhines, P. (Eds). Arctic, Sub-arctic Ocean fluxes: Defining the role of the
2337 Northern Seas in Climate, Springer, 736 pp., 2008.
- 2338 Dmitrenko, I.A., Rudels, B., Kirillov, S.A., Aksenov, Y.O., Lien, V.S., Ivanov, V.V., Schauer, U., Polyakov,
2339 I.V., Coward, A., Barber, D.G.: Atlantic water flow into the Arctic Ocean through the St.
2340 Anna Trough in the northern Kara Sea, *Journal of Geophysical Research: Oceans*, 120
2341 (7), 5158-5178, 2015.
- 2342 Doddridge, E.W., Meneghello, G., Marshall, J., Scott, J., Lique, C.: A three-way balance of the Beaufort
2343 Gyre: The ice-governor, wind stress, and eddy diffusivity, *Journal of Geophysical
2344 Research: Oceans*, 124 (5), 3107-3124, 2019.
- 2345 Ekman, V.W.: On the influence of earth's rotation on ocean currents, *Arkiv för matematik, astronomi
2346 och fysik*, 2(11), 53 pp., 1905.
- 2347 Gascard J.-C., Richez C., Roault C.: New insights on large-scale oceanography in Fram Strait: the
2348 West Spitsbergen Current, In Smith Jr, W.O., Grebmeier, J.M. (eds), Arctic
2349 Oceanography, marginal ice zones and continental shelves, AGU 49, Washington DC,
2350 pp 131-182, 1995.
- 2351 Gascard, J.-C., Watson, A.J., Messias, M.-J., Olsson, K.A., Johannessen, T., Simonsen, K.: Long-lived
2352 vortices as a mode of deep ventilation in the Greenland Sea, *Nature*, 416, 525-527,
2353 2002.
- 2354 González-Pola, C, Larsen, K.M.H., Fratantoni, P., Beszczynska-Möller, A. (eds): ICES Report on Ocean
2355 Climate, ICES Cooperative Research Reports, Vol. 358, 123 pp.,
2356 <https://doi.org/10.17895/ices.pub.24755574>, 2023.
- 2357 Gordon, A.: Deep Antarctic convection west of Maud Rise. *Journal of Physical Oceanography*, 8, 600-
2358 612, 1978.
- 2359 Haine, T.W.N., Curry, B., Gerdes, R., Hansen, E., Karcher, M., Lee, C., Rudels, B., Spreen, G., de Steur,
2360 L., Stewart, K.D., Woodgate, R.: Arctic freshwater export: Status, mechanisms, and
2361 prospects, *Global and Planetary Change*, 125, 13-35, 2015.
- 2362 Häkli, E (1992) Adolf Erik Nordenskiöld och Kartläggningen av de Arktiska områdena, in Häkli, E.,
2363 Nurminen, J., Raurala, N.-E. (eds), Nordostpassagen, Helsingfors Universitets förlag,
2364 John Nurminens Stiftelse, Helsingfors, 50-88, 1992.
- 2365 Hátún, H, Sandø, A.B., Drange, H., Hansen, B., Valdimarsson, H.: Influence of the Atlantic subpolar
2366 gyre on the thermohaline circulation, *Science* 309, 1841-1844, 2005.
- 2367 Helland-Hansen, B.: Report on hydrographical investigations in the Faroe-Shetland Channel and the
2368 northern part of the North Sea in the year 1902, Fishery Board for Scotland, Report of
2369 the North Sea Fishery Investigation Committee (Northern Area) 1902-03, British
2370 Sessional Paper, Vol 14 (1), 1-49, 1905.
- 2371 Helland-Hansen, B.: Physical Oceanography, in J Murray and J Hjort (eds), The depth of the ocean,
2372 Macmillan, London, 210-306, 1912.
- 2373 Helland-Hansen, B., Nansen, F.: The Norwegian Sea. Its physical oceanography based upon the
2374 Norwegian researches 1900-1904, Rep. on Norw. Fishery and Marine Investigations, II
2375 (1), Kristiania, 390pp, 1909.



- 2376 Holliday, N.P., Bersch, M. Berx, B., Chafik, L., Cunningham, S., Florindo-López, C. Hátún, H., Jlohns, W.,
2377 Josey, S.A., Larsen, K.M.-H., Mulet, S., Oltmanns, M., Reverdin, G., Rossby, T. Thierry,
2378 V., Valdimarsson, H., Yashayaev, I.: Ocean circulation causes the largest freshening
2379 event for 120 years in the eastern subpolar North Atlantic, *Nature Communications*,
2380 11, 585, <https://doi.org/10.1038/s41467-020-14474-y>, 2020.
- 2381 Howard, L.N.: Convection at high Rayleigh number, in *Proc. eleventh Congress Applied Mech.*,
2382 München, H. Görtler (ed), Springer Verlag, Berlin, 1109-1115, 1967.
- 2383 Jackson, J.M., Carmack, E.C., McLaughlin, F.A., Allen, S.E. Ingram R.G.: Identification, characterization
2384 and change of the near-surface temperature maximum in the Canada Basin, 1993-
2385 2008, *Journal of Geophysical research*, 115, C05021, Doi:10.1029/2009JC005265,
2386 2010.
- 2387 Jones, E.P., Anderson, L.G.: On the Origin of the Chemical Properties of the Arctic Ocean Halocline,
2388 *Journal of Geophysical Research*, 91, 10759-10767, 1986.
- 2389 Jones, E.P., Rudels, B., Anderson, L.G.: Deep Waters of the Arctic Ocean: Origins and Circulation,
2390 *Deep-Sea Res.*, 42, 737-760, 1995.
- 2391 Jónsson, S., and Valdimarsson, H.: A new path for the Denmark Strait overflow water from the
2392 Iceland Sea to Denmark Strait, *Geophysical Research Letters*, 31, L03305,
2393 doi:10.1029/2003GL019214, 2004.
- 2394 Kalnay, E., Anderson, D.L.T., Bennett, A.F., Busalacchi, A.J., Cohn, S.E., Courtier, P., Derber, J., Lorenc,
2395 A.C., Parrish, D., Purser, J., Sato, N., Schlatter, T.: Data assimilation in the ocean and in
2396 the atmosphere: What should be next?, *Journal of the Meteorological Society of*
2397 *Japan*, 75 (1b), 489-496, 1997.
- 2398 Kalnay, E., Kanamitsu, M., Kistler, R., Collins, W., Deavem, D., Gandin, L., Iredell, M., Saha, S., White,
2399 G., Wollen, J., Zhu, Y., Chelliah, M., Ebisuzaki, W., Higgins, W., Janowiak, J., Mo, K.C.,
2400 Ropelewski, C., Wang, J., Leetma, A., Reynolds, R., Jenne, R., Joseph, D.: The
2401 NCEP/NCAR 40-Year Reanalysis Project, *Bulletin of American Meteorological Society*,
2402 77 (3), 437-472, 1996.
- 2403 Knipovitch, N.: Hydrologische Untersuchungen im Europäischen Eismeer, *Annalen der Hydrographie*
2404 *and Maritimen Meteorologie*, Sonderabdruck, 62 pp., 1905.
- 2405 Killworth, P.D.: On “chimney” formations in the oceans, *Journal of Physical Oceanography*, 7, 531-
2406 554, 1979.
- 2407 Killworth, P.D.: Deep convection in the world ocean, *Reviews of Geophysics*, 21 (1), 1-26, 1983.
- 2408 Knudsen, M.: *Hydrography, Danish Ingolf -Expedition, Bd I, (2)*, Kopenhagen, 1899.
- 2409 Kraus, E.B. and Turner, J.S.: A one-dimensional model of the seasonal thermocline II The general
2410 theory and its consequences, *Tellus*, 19, 98-106, 1967.
- 2411 Latarius, K. and Quadfasel, D.: Water mass transformation in the deep basins of the Nordic Seas:
2412 Analysis of the heat and freshwater budgets, *Deep-Sea Research I*, 114, 23-42, 2016.
- 2413 Lazier, J., Hendry, R., Clarke, A., Yashayaev, I., Rhines, P.: Convection and restratification in the
2414 Labrador Sea, 1990-2000. *Deep-Sea Res. I*, 49, 1819-1835, doi:10.1016/S0967-
2415 0637(02)00064-X, 2002.
- 2416 Lewis, E.L., Jones, E.P., Lemke, P., Prowse, T.D., Wadhams, P.: (eds), *The Freshwater Budget of the*
2417 *Arctic Ocean*, Kluwer Academic Publishers, Dordrecht, 623pp, 2000.



- 2418 Lien, V.S. and Trofimov, A.G.: Formation of Barents Sea Branch Water in the north-eastern Barents
2419 Sea, *Polar Research* 32, 1.12, 18905, <http://dx.doi.org/10.3402/polar.v32i0.18905>,
2420 2013.
- 2421 Lind, S. and Ingvaldsen, R.: Variability and impacts of Atlantic water entering the Barents Sea from
2422 the north, *Deep-Sea Research I*, 62, 70-88, 2012.
- 2423 Lind, S., Ingvaldsen, R., Furevik, T.: Arctic warming hotspots in the northern Barents Sea linked to
2424 declining sea-ice import, *Nature climate change*, 8, 634-639, 2018.
- 2425 Lozier, M.S., Li, F., Bacon, S., Bahr, F., Bower, A.S., Cunningham, S.A., de Jong, M.F., de Steur, L.,
2426 DeYoung, B., Fischer, J., et al.: A sea change in our view of the overturning in the
2427 subpolar North Atlantic, *Science*, 363, (6426), 516-521, 2019.
- 2428 Manucharyan, G.E., and Spall, M.A.: Wind-driven freshwater buildup and release in the Beaufort
2429 Gyre constrained by mesoscale eddies, *Geophysical Research Letters*, 43, 273-282,
2430 doi:10.1002/2015GL065957, 2016.
- 2431 Manucharyan, G.E., Spall, M.A., Thompson, A.F.: A theory of the wind-driven Beaufort Gyre
2432 variability, *Journal of Physical Oceanography*, 46, 3263-3278. <https://10.1175/JPO-D-16-0091.1>, 2016.
- 2434 Marnela, M., Rudels, B., Goszczko, I., Besczynska-Möller, A., Schauer, U.: Fram Strait and Greenland
2435 Sea transports, water masses and water mass transformations 1999-2010 (and
2436 beyond). *Journal of Geophysical Research: Oceans*, 121, 2314-2346,
2437 doi:10.1002/2015JC011312, 2016.
- 2438 Marshall, J. and Schott, F.: Open-Ocean convection: observations, theory, and models, *Reviews of*
2439 *Geophysics*, 37 (1), 1-64. 1999.
- 2440 Marsigli, L.F.: Osservazioni Intorno al Bosforo Tracio Overo Canale di Constantinopli Rappresentate in
2441 Lettera alla Sacra Real Maesta di Cristina Regina di Svezia, Roma, (Reprinted 1935,
2442 *Bolletina di Pesca, Piscicoltura e Idrobiologia*, 11, 734-758, 1681.
- 2443 Maslowski, W., Newton, B., Schlosser, P., Semtner, A., Martinson, D.: Modelling recent climate
2444 variability in the Arctic Ocean, *Geophysical research Letters*, 27, 3743-3746,
2445 doi:10.1029/1999GL011227, 2000.
- 2446 Mauritzen C.: Production of dense overflow waters feeding the North Atlantic across the Greenland
2447 Sea-Scotland Ridge. Part 1: Evidence for a revised circulation scheme, *Deep-Sea*
2448 *Research*, 43, 769-806, 1996a.
- 2449 Mauritzen C.: Production of dense overflow waters feeding the North Atlantic across the Greenland
2450 Sea-Scotland Ridge. Part 2: An inverse model, *Deep-Sea Research*, 43, 807-835, 1996b.
- 2451 McCartney, M.S.: Subantarctic Mode Water, in Angel, M. (ed.), *A Voyage of Discovery*, Pergamon
2452 Press, Oxford, 103-119, 1977.
- 2453 McCartney, M.S. and Talley, L.D.: The Subpolar Mode water of the North Atlantic Ocean, *Journal of*
2454 *Physical Oceanography*, 12, 1169-1188, 1982.
- 2455 McDougall, T.J.: Greenland Sea bottom water formation: a balance between advection and double
2456 diffusion, *Deep-Sea Research*, 30, 1109-1117, 1983.
- 2457 Meincke, J., Rudels, B., Friedrich, H.: The Arctic Ocean -Nordic Seas Thermohaline System, *ICES*
2458 *Journal of Marine Science*, 54, 283-299, 1997.



- 2459 Melling, H., Agnew, T.A.; Falkner, K.K., Greenberg, D.A., Craig, M.L., Münchow, A., Petrie, B.,
2460 Prinsenberg, S.J., Samelson, R.M., Woodgate, R.A.: Freshwater fluxes via Pacific and
2461 Arctic outflows across the Canadian Polar shelf, In Dickson, R.R., Meincke, J., Rhines, P.
2462 (eds), Arctic-Subarctic Ocean Fluxes, Springer, Dordrecht, pp., 193-247, 2008.
- 2463 Meneghello, G., Marshall, J., Campin, J.-M., Doddridge, E., Timmermans, M.-L.: The ice-ocean
2464 governor: Ice-ocean stress feedback limits Beaufort Gyre spin-up, *Geophysical*
2465 *Research Letters*, 45, 11293-11299, <https://doi.org/10.1029/2018GL080171>, 2018.
- 2466 Merz, A. 1922.: Temperaturschichtung und Vertikalzirkulation in Südatlantischen Ozean nach den
2467 *Challenger* und *Gazelle*-Beobachtungen, *Zeitschrift der Gesellschaft für Erdkunde zu*
2468 *Berlin*, 7, (10), 288-300, 1922.
- 2469 Merz, A., and Wüst G.: Die Atlantische Vertikalzirkulation, *Zeitschrift der Gesellschaft für Erdkunde zu*
2470 *Berlin*, 1-2, 1-35, 1922.
- 2471 Metcalf, W.F.: On the formation of bottom water in the Norwegian Basin, *Eos*, 36 (4), 596-600, 1955.
- 2472 Mills, E.L. The fluid envelope of our planet, University of Toronto Press, Toronto, XII + 434 pp., 2009.
- 2473 Mohn, H.: 1880. Die Norwegischen Nordmeer Expedition: Resultate der Lothungen und
2474 Tiefseetemperatur-Beobachtungen, *Petermanns Geographische Mitteilungen*,
2475 *Ergänzungsband XIV*, 63, 1-24, 1880.
- 2476 Mohn, H.: The North Ocean: Its depth, temperature and circulation, *The Norwegian North Atlantic*
2477 *Expedition 1876-1878 II (2)*, Grøndahl and Søn, Christiania, 212 pp., 1887.
- 2478 Morison J.H., Steele M., Anderson R.: Hydrography of the upper Arctic Ocean measured from the
2479 nuclear submarine USS Pargo, *Deep-Sea Res I*, 45, 5-38, 1998.
- 2480 Morison, J., Kwok, R., Peralta-Ferriz, C., Alkire, M., Rigor, I., Andersen, R., Steele, M.: Changing Arctic
2481 Ocean freshwater pathways, *Nature*, 481, 66-70, doi:10.1038/nature10705, 2012.
- 2482 Mortin, J., Svensson, G., Graverson, R.G., Kapsch, M.-L., Stroeve, J.C., Boisvert, L.N.: Melt onset over
2483 Arctic sea ice controlled by atmospheric moisture transport, *Geophysical Research*
2484 *Letters*, 43, 6636-6642, doi:10.1002/2016GL069330, 2018.
- 2485 Münchow, A., Melling, H.: Ocean current observations from Nares Strait to the west of Greenland:
2486 Interannual to tidal variability and forcing, *Journal of Marine Research*, 66(6), 801-833,
2487 2008.
- 2488 Nansen, F.: Oceanography of the North Polar Basin, *The Norwegian North Polar Expedition 1893-*
2489 *1896, Scientific Results III (9)*, Jakob Dybwad, Christiania, 427pp., 1902.
- 2490 Nansen, F. 1906.: Northern Waters, Captain Roald Amundsen's oceanographic observations in the
2491 Arctic Seas in 1901, *Videnskabs-Selskabets Skrifter*, 1 Matematisk-Naturvidenskabelig
2492 Klasse 1, Kristiania, 1-145, 1906.
- 2493 Nansen, F.: Das Bodenwasser und die Abkühlung des Meeres, *Internationale Revue des Gesamten*
2494 *Hydrobiologie und Hydrographie*, 5, 42 pp., 1912.
- 2495 Nansen, F.: The waters of the North-eastern North Atlantic, *Internationale Revue der gesamten*
2496 *Hydrobiologie und Hydrographie*, Werner Klinkhardt, Leipzig, 139 pp., 1913.
- 2497 Nansen, F.: 1915. Spitsbergen Waters, *Videnskabs-selskabets skrifter I. Matematisk-*
2498 *Naturvidenskabelig klasse I (3)*, 145 pp., 1915.
- 2499 Newton, J.L., Sotirin, B.J.: Boundary undercurrent and water mass exchanges in the Lincoln Sea, *J*
2500 *Geophys Res.*, 102:3393-3403, 1997.



- 2501 Niiler, P.P. and Kraus, E.B.: One-dimensional models of the upper ocean, in Kraus, E.B. (ed). Modelling
2502 and prediction of the upper layers of the Ocean, Pergamon Press, Oxford, 143-179.
2503 1977.
- 2504 Nøst, A., and Isachsen, P.E.: The large-scale time-mean ocean circulation in the Nordic Seas and the
2505 Arctic Ocean estimated from simplified dynamics, *Journal of Marine Research*, 61, 175-
2506 210, 2003.
- 2507 Nøst, A., Nilsson, J., Nycander, J.: On the asymmetry between cyclonic and anticyclonic flow in basins
2508 with sloping boundaries, *Journal of Physical Oceanography* 38, 771-787, 2008.
- 2509 Østerhus, S. and Gammelsrød, T.: The abyss of the Nordic Seas is warming, *Journal of Climate*, 12,
2510 3297-3304, 1999.
- 2511 Østerhus, S., Woodgate, R.A., Valdimarsson, H., Turrell, B., de Steur, L., Quadfasel, D., Olsen, S.M.,
2512 Moritz, M., Lee, C.M., Larsen, K.M.H., Jónsson, S., Johnson, C., Jochumsen, K., Hansen,
2513 B., Curry, B., Cunningham, S. Berx, B.: Arctic Mediterranean exchanges: a consistent
2514 budget and trends in transports from two decades of measurements, *Ocean Science*,
2515 15, 379-399, <https://doi.org/10.5194/os-15-379-2019>, 2019.
- 2516 Petermann, A.: Der Nordpol und Südpol, die Wichtigkeit ihrer Erforschung in geographischer und
2517 kulturhistorischer Beziehung, Mit Bemerkungen über die Strömungen der Polar-
2518 Meere, *Pet. Mitt.*, Gotha, 146-160, 1865.
- 2519 Peterson, I., Hamilton, J., Prinsenberg, S., Pettipas, R.: Wind-forcing of volume transports through
2520 Lancaster Sound, *Journal of Geophysical Research*, 117, C11018, 2012.
- 2521 Pickart, R.S., Torres, D.J., Frantantoni, P.S.: The East Greenland Spill Jet, *Journal of Physical*
2522 *Oceanography*, 35, 1037-1053, 2005.
- 2523 Polyakov, I.V., Beszczynska-Möller, A., Carmack, E., Dmitrenko, I., Fahrbach, E., Frolov, I., Gerdes, R.,
2524 Hansen, E., Holfort, J., Ivanov, V., Johnson, M., Karcher, M., Kauker, F., Morison, J.,
2525 Orvik, K., Schauer, U., Simmons, H., Skagseth, Ø., Sokolov, V., Steele, M., Timokhov, L.,
2526 Walsh, D., Walsh, J.: One more step towards a warmer Arctic, *Geophysical Research*
2527 *Letters*, 32, L17605, doi:10.10292005GL023740, 2005.
- 2528 Polyakov, I. V., Alekseev, V. A., Ashik, I. M., Bacon, S., Beszczynska-Möller, A., Dmitrenko, I., Fortier,
2529 L., Gascard, J.-C., Hansen, E., Hölemann, J., Ivanov, V. V., Kikuchi, T., Krillov, S., Lenn, Y.-
2530 D., Piechura, J., Repina, I., Timokhov, L. A., Walczowski, W., Woodgate, R.: Fate of the
2531 early-2000s Arctic warm pulse, *Bulletin of American Meteorological Society*, 92, 561-
2532 566, 2011.
- 2533 Polyakov, I.V., Pnyushkov, A.V., Rember, R., Ivanov, V.I., Lenn, Y.-D., Padman, L., Carmack, E.C.:
2534 Mooring-Based Observations of Double-Diffusive Staircases over the Laptev Sea Slope,
2535 *J. Phys. Oceanogr.*, 42, 95-109, doi10.1175/2011JPO4606, 2012.
- 2536 Polyakov, V.I., Pnyushklov, A.V., Alkire, M.B., Ashik, I.M., Baumann, T.M., Carmack, E.C., Goszczko, I.,
2537 Guthrie, J., Ivanov, V.V., Kanzow, T., Krishfield, R., Kwok, R., Sundfjord, A., Morison, J.,
2538 Rember, R., Yulin, A.: Greater role for Atlantic inflows on sea-ice loss in the Eurasian
2539 Basin of the Arctic Ocean, *Science*, 356, 285-291, 2017.
- 2540 Quadfasel, D. and Rudels, B. Some new observational evidence for salt induced convection in the
2541 Greenland Sea, *Inst. für Meereskunde, Hamburg, Tech. Rep.* 4-90., 30 pp, 1990.
- 2542 Quadfasel, D., Rudels, B., Kurz, K.: Outflow of dense water from a Svalbard fjord into the Fram Strait,
2543 *Deep-Sea Res.*, 35, 1143-1150, 1988.



- 2544 Quadfasel, D., Rudels, B., Selchow, S.: The Central Bank vortex in the Barents Sea: water mass
2545 transformation and circulation, ICES Mar. Sci. Symp., 195, 40-51, 1992.
- 2546 Quadfasel, D., Sy, A., Wells, D., Tunik,: Warming of the Arctic, Nature, 350, 385, 1991.
- 2547 Rennell, J.: Investigations of the currents of the Atlantic Ocean and of those which prevail between
2548 the Indian Ocean and the Atlantic, J.G. and FD Rivington, London, 350 pp., 1832.
- 2549 Riis-Carstensen, E.: The *Godthaab* expedition 1928. The hydrographic work and material, Meddelser
2550 om Grönland 78(3), 101 pp., 1936.
- 2551 Rothrock, D.A., Yu, Y., Maykut, G.A.: Thinning of the Arctic Sea-Ice Cover, Geophys Res Letters, 26,
2552 3469-3472, 1999.
- 2553 Rudels, B.: The ΘS relations in the northern seas: Implications for the deep circulation, Polar
2554 Research, 4 n.s., 133-159, 1986a.
- 2555 Rudels, B.: The outflow of Polar Water through the Arctic Archipelago and the oceanographic
2556 conditions in Baffin Bay, Polar Research, 4 n.s., 161-180, 1986b.
- 2557 Rudels, B.: The formation of Polar Surface Water, the ice export and the exchanges through the Fram
2558 Strait, Progress in Oceanography, 22, 205 – 248, 1989.
- 2559 Rudels, B.: The thermohaline circulation of the Arctic Ocean and the Greenland Sea, Phil Trans R Soc
2560 Lond, A 352, 287-299, 1995.
- 2561 Rudels, B.: Constraints on exchanges in the Arctic Mediterranean – Do they exist and can they be of
2562 use?, Tellus, 62A, 109-122, 2010.
- 2563 Rudels, B. Volume and freshwater transports through the Canadian Arctic Archipelago – Baffin Bay
2564 system, J. Geophys. Res., 116, C00D10, doi:10.1029/2011JC007019, 2011.
- 2565 Rudels, B.: Arctic Ocean circulation, processes and water masses: a review of observations and ideas
2566 with focus on the period prior to the International Polar Year 2007-2009, Progress in
2567 Oceanography, 132, 22-67, <http://dx.doi.org/10.1016/j.pocean.2013.11.006>, 2015.
- 2568 Rudels, B.: Arctic Ocean Circulation, in Cochran, J.K., Bokuniewicz, J.H., Yager, L.P. (Eds.),
2569 Encyclopedia of Ocean Sciences, 3rd Edition, vol. 3, Elsevier, ISBN 978-0-12-813081-0,
2570 262-277, 2019.
- 2571 Rudels, B.: The Physical Oceanography of the Arctic Mediterranean Sea: Explorations, Observations,
2572 Interpretations, Elsevier, Amsterdam, XV + 520 pp., 2021.
- 2573 Rudels, B. and Carmack, E.: Arctic Ocean water mass structure and circulation, Oceanography, 35(3-
2574 4), 52-65, <https://doi.org/10.5670/oceanogr.2022.116>, 2022.
- 2575 Rudels, B. and Quadfasel, D.: Convection and deep water formation in the Arctic Ocean - Greenland
2576 Sea system, J. of Marine Systems, 2, 435-450, 1991.
- 2577 Rudels, B., Anderson, L.G., Jones, E.P.: Formation and evolution of the surface mixed layer and the
2578 halocline of the Arctic Ocean, Journal of Geophysical Research, 101, 8807-8821, 1996.
- 2579 Rudels, B., Eriksson, P., Grönvall, H., Hietala, R. Launiainen, J.: Hydrographic Observations in Denmark
2580 Strait in fall 1997, and their Implications for the Entrainment into the Overflow Plume,
2581 Geophys. Res. Letters, 26, 1325-1328, 1999c.
- 2582 Rudels, B., Friedrich, H.J., Quadfasel, D.: The Arctic Circumpolar Boundary Current, Deep-Sea Res. II,
2583 46, 1023-1062, 1999b.



- 2584 Rudels, B., Friedrich, H.J., Hainbucher, D., Lohmann, G.: On the parameterisation of oceanic sensible
2585 heat loss to the atmosphere and to ice in an ice-covered mixed layer in winter, Deep-
2586 Sea Research Part II, 46, 1385-1425, 1999a.
- 2587 Rudels, B., Jones, E.P., Anderson, L.G., Kattner, G.: On the intermediate depth waters of the Arctic
2588 Ocean, in The role of the Polar Oceans in Shaping the Global Climate, Johannessen,
2589 O.M., Muench, R.D., Overland, J.E. (eds), American Geophysical Union, Washington
2590 D.C., 33-46, 1994.
- 2591 Rudels, B., Jones, E.P., Schauer, U., Eriksson, P.: Atlantic Sources of the Arctic Ocean surface and
2592 halocline waters, Polar Research, 23, 181-208, 2004.
- 2593 Rudels, B., Korhonen, M., Schauer, U., Pisarev, S., Rabe, B., Wisotzki, A.: Circulation and
2594 transformation of Atlantic water in the Eurasian Basin and the contribution of the
2595 Fram Strait inflow branch to the Arctic Ocean heat budget, Progress in Oceanography,
2596 132, 128-152, <http://dx.doi.org/10.1016/j.pocean.2014.04.003>, 2015.
- 2597 Rudels, B., Marnela, M., Eriksson, P.: Constraints on estimating mass, heat and freshwater transports
2598 in the Arctic Ocean: An exercise, In Arctic-Subarctic Ocean Fluxes, Dickson, R.R.,
2599 Meincke, J., Rhines, P. (eds.), Springer, Dordrecht, 315-341, 2008.
- 2600 Ryder, C.: Tidligere Ekspeditioner til Grønlands Østkyst nord for 66°, Nr. Br., Geogr. Tids., Bd. 11,
2601 København, pp. 62-107, 1891-1892.
- 2602 Sandström, J.W.: Dynamische Versuche mit Meerwasser, Annalen der Hydrographie und maritimen
2603 Meteorologie, XXXVI Jahrgang, 6-23, 1908.
- 2604 Sandström, J.W. and Helland Hansen, B.: Über die Berechnungen von Meereströmungen, Report on
2605 Norwegian Fishery and Marine Investigations, 2 (4), 1-43, 1903.
- 2606 Schauer, U., Muench, R.D., Rudels, B., Timokhov, L.: Impact of eastern Arctic shelf water on the
2607 Nansen Basin intermediate layers, J. Geophys. Res., 102, 3371-3382, 1997.
- 2608 Schauer, U., Loeng, H., Rudels, B., Ozhigin, V.K., Dieck, W.: Atlantic Water flow through the Barents
2609 and Kara Seas, Deep-Sea Research I, 49, 2281-2298, 2002.
- 2610 Segtnan, O.H., Furevik, T., Jenkins, A.D.: Heat and freshwater budgets of the Nordic seas computed
2611 from atmospheric reanalysis and ocean observations, Journal of Geophysical Research
2612 116, C11003, doi:10.1029/2011JC006939, 2011.
- 2613 Smeed, D.A., McCarthy, G.D., Cunningham, S.A., Frajka-Williams, E., Rayner, D., Johns, W., Meinen,
2614 C., Baringer, M.O., Moat, B., Duchez, A., et al.: Observed decline of the Atlantic
2615 Meridional Overturning Circulation 2004-2012, Ocean Science 10, 29-38, 2014.
- 2616 Somavilla, R., Schauer, U., Budéus, G.: Increasing amount of Arctic Ocean deep water in the
2617 Greenland Sea, Geophysical Research Letters, 40, 4361-4366., doi:10.1002/grl.50775,
2618 2013.
- 2619 Spreen, G., Kern, S., Stammer, D., Hansen, E.: Fram Strait sea ice volume export estimated between
2620 2003 and 2008 from satellite data, Geophysical Research Letters, 36, L19502, 2009.
- 2621 Stern, M.E.: Lateral mixing of water masses, Deep-Sea Res., 14, 747-753, 1967.
- 2622 Stigebrandt, A.: A model for the thickness and salinity of the upper layers of the Arctic Ocean and the
2623 relation between the ice thickness and some external parameters, Journal of Physical
2624 Oceanography, 11, 14507-1422, 1981.



- 2625 Stigebrandt, A.: The North Pacific: A global-scale estuary, *Journal of Physical Oceanography*, 14, 464-
2626 470, 1984.
- 2627 Stigebrandt, A.: On the hydrographic and ice conditions in the northern North Atlantic during
2628 different phases of a glaciation cycle, *Palaeogeography, Palaeoclimatology,*
2629 *Palaeoecology*, 50, 303-321, 1985.
- 2630 Sutherland, D.A. and Pickart, R.S.: The East Greenland Current: Structure, variability and forcing,
2631 *Progress in Oceanography*, 78 (1), 55-78. <http://doi.org/10.1016/j.pocean.2007.09.006>,
2632 2008.
- 2633 Sverdrup, H.U. and Soule, F.M.: *Scientific Results of the Nautilus Expedition 1931, Papers in Physical*
2634 *Oceanography and Meteorology*, Massachusetts Institute of Technology and Woods
2635 Hole Oceanographic Institution, Cambridge, Massachusetts, 76 pp., 1933.
- 2636 Sverdrup, H.U., Johnson, M.W., Fleming, R.H.: *The Oceans: Their Physics, Chemistry and General*
2637 *Biology*, Prentice-Hall, New York, 1042 pp, 1942.
- 2638 Swift, J.H., Aagaard, K., Malmberg, S.-A.: The contribution of the Denmark Strait overflow to the deep
2639 North Atlantic, *Deep-Sea Research*, 27, 29-42, 1980.
- 2640 Swift, J.H. and Aagaard, K.: Seasonal transitions and water mass formation in the Icelandic and
2641 Greenland Seas, *Deep-Sea Research*, 28, 1107-1129, 1981.
- 2642 Tait, J.B., Lee, A.J., Stefánsson, U., Herman, F.: Temperature and salinity distributions and water-
2643 masses of the region, *Rapp. P.-v. Cons. Explor. Mer.*, 157, 38- 63, 1967.
- 2644 Timmermans, M.-L., Garrett, C., Carmack, E.: The thermohaline structure and evolution of the deep
2645 waters in the Canada Basin, Arctic Ocean, *Deep-Sea Res. I*, 50, 1305-1321,
2646 doi:10.1016/S0967(03)00125-0, 2003.
- 2647 Timmermans, M.-L., Toole, J., Krishfield, R. Winsor, P.: Ice-Tethered Profiler observations of the
2648 double-diffusive staircase in the Canada Basin thermocline, *Journal of Geophysical*
2649 *Research*, 113, C00A02, 2008.
- 2650 Timmermans, M.-L., Marshall, J.: Understanding Arctic Ocean Circulation: A review of Ocean
2651 Dynamics in a Changing Climate, *Journal of Geophysical Research: Oceans*, 120,
2652 2018JC014378, 2020.
- 2653 Toole, J.M. and Georgi, D.T.: On the dynamics and effects of double-diffusively driven intrusions,
2654 *Prog. in Oceanogr.*, 10, 121-145, 1981.
- 2655 Turner, J. S.: *Buoyancy Effects in Fluids*, Cambridge Univ. Press, Cambridge, 367pp, 1973.
- 2656 Våge, K., Pickart, R.P., Spall, M.A. Valdimarson. H., Jónsson, S., Torres, D.J., Østerhus, S., Eldevik, T.:
2657 Significant role of the North Icelandic Jet in the formation of Denmark Strait overflow
2658 water, *Nature, Geoscience*, 4 (10), 723-727, <http://dx.doi.org/10.1038/ngeo1234>,
2659 2011.
- 2660 Våge, K., Pickart, R.S., Spall, M.A., Moore, G.W.K., Valdimarson, H., Torres, D.J., Erofeeva, S.Y., Nilsen
2661 J.E.Ø.: Revised circulation scheme north of the Denmark Strait, *Deep Sea Res. I*, 79,
2662 20–39, DOI:[10.1016/j.dsr.2013.05.007](https://doi.org/10.1016/j.dsr.2013.05.007), 2013
- 2663 Våge, K., Moore, G.K.W., Jónsson. S., Valdimarson, H.: Water mass transformation in the Iceland Sea.
2664 *Deep-Sea Research I* 101, 98-109. <http://ds.doi.org/10.1016/j.dsr.2015.04.001>, 2015.



- 2665 Von Lenz, E.: Bemerkungen über die Temperatur des Weltmeeres in verschiedene Tiefen, Bulletin de
2666 la Classe physico-mathématique de l'Académie impériale des sciences de St.
2667 Petersbourg, 5, 65-74, 1845.
- 2668 Von Waitz, J.S.: Undersökning om orsaken, hvarföre vattnet i Atlantiska hafvet alltid strömar in uti
2669 Medelhafvet, genom Sundet vid Gibraltar, Kongliga Svenska Vetenskaps-Akademiens
2670 Handlingar, 16, 27-50, 1755
- 2671 Wadhams, P., Holfort, J., Hansen, E., Wilkinson, J.P.: A deep convective chimney in the winter
2672 Greenland Sea, Geophys Res Letter, 29, doi:0.1029/2001GL014306, 2002.
- 2673 Watson A.J., Messias, M.-J., Fogelqvist, E., Van Scoy, K.A., Johannessen, T., Oliver, K.I.C., Stevens,
2674 D.P., Tanhua, T., Olsson, K.A., Carse, F., Simonsen, K., Ledwell, J.R., Jansen, J., Cooper,
2675 D.J., Kruepke, J.A., Guilyardi, E.: Mixing and convection in the Greenland Sea from a
2676 tracer release experiment, Nature, 401, 902-904, 1999.
- 2677 Werenskiöld, W.: Coastal Currents, Geofysiske Publikasjoner, 10 (13), Oslo, 1935.
- 2678 Werenskiöld, W.: Henrik Mohn og Oseanografien, Norsk Geografisk Tidsskrift, vol VI (6), Oslo, 293-
2679 302, 1937.
- 2680 Wettlaufer, J.S., Worster, M.G., Huppert, H.E.: Natural convection during solidification of an alloy
2681 from above with application to the evolution of sea ice, Journal of Fluid Mechanics,
2682 344, 291-316, 1997.
- 2683 Weyl, P.K.: The role of the oceans in climate change, Meteorological Monographs, 8, 37-62, 1968.
- 2684 Worthington, L.V.: Oceanographic results of Project Skijump I and II, Trans Am Geophys Union, 34(4),
2685 543-551, 1953.
- 2686 Worthington, L.V.: The Norwegian Sea as a mediterranean basin, Deep-Sea Res., 17, 77-84, 1970.
- 2687 Worthington L.V.: On the North Atlantic Circulation, Johns Hopkins Oceanographic Studies, No. 6, The
2688 Hopkins University Press, 110 pp., 1976.
- 2689 Wüst, G.: Relief und Bodenwasser im Nordpolarbecken, Zeitschrift der Gesellschaft für Erdkunde zu
2690 Berlin 5/6, 163-180, 1941.
- 2691 Zacharov, V.F.: Cooling of the Arctic and the ice cover of the Arctic Seas, Arctic and Antarctic
2692 Research Institute, Leningrad, Trudy, 337, 1-96, 1976.
- 2693
- 2694